AGENT-BASED NETWORK MODELING FOR THE 2008 FINANCIAL CRISIS

AND THE SLUGGISH RECOVERY

by

Young Joon Oh

APPROVED BY SUPERVISORY COMMITTEE:

Dr. Euel Elliott, Chair

Dr. L. Douglas Kiel

Dr. Clint Peinhardt

Dr. John R. McCaskill

To my wife Seung-Hee and my daughter Hara

AGENT-BASED NETWORK MODELING FOR THE 2008 FINANCIAL CRISIS

AND THE SLUGGISH RECOVERY

by

YOUNG JOON OH, BA, MA

DISSERTATION

Presented to the Faculty of

The University of Texas at Dallas

in Partial Fulfillment

of the Requirements

for the Degree of

DOCTOR OF PHILOSOPHY IN

PUBLIC POLICY AND POLITICAL ECONOMY

THE UNIVERSITY OF TEXAS AT DALLAS

August 2015

ACKNOWLEDGMENTS

It is a long journey to write a dissertation, and I want to express my gratitude to people who made this journey possible.

First of all, I want to thank my advisor Dr. Euel Elliott. Without his encouragement, help and patience, I could not complete this journey. I would also like to thank my committee members: Dr. L. Douglas Kiel, Dr. Clint Peinhardt, and Dr. John R. McCaskill. I appreciate the comments and contribution.

I am grateful to Dr. Maximilian Schich, who guided me in Complex Networks, and introduced Dr. Dirk Helbing, who made helpful comments on my model in his workshop.

Also, I want to thank my teachers in Korea, who provided me with motivation. Dr. Su-ik Hwang and Dr. Hoon Jaung.

I am thankful for great helps from many people. Dr. Brandon Seitzler, Katy Seitzler, their family, Dr. Heja Kim, Dr. Yongwan Chun, Monghyeon Lee, Kwang Soo Kim, Dr. Kwang Bin Bae, Hyeongmo Koo, Soojin Min, Dr. Minwook Ha, Dr. Gwang Ho Ha, and Hee Do Park. Finally, I would like to thank my wife and my family in Korea.

June 2015

AGENT-BASED NETWORK MODELING FOR THE 2008 FINANCIAL CRISIS

AND THE SLUGGISH RECOVERY

Publication No. ____________________

Young Joon Oh, PhD
The University of Texas at Dallas, 2015

Supervising Professor: Dr. Euel Elliott

The 2008 financial crisis was a very unpredictable event. To analyze this event, we use Agent-based network models. Our models suggest crises are very-rare-but-extremely-dangerous events, which are called "Dragon kings". Due to insufficient information, policies for a resilient system have limitations. Paradoxically, the safer a system is, the more likely it can face the Dragon king. Furthermore, our multiple networks model proposes that once systemic risks spread in interdependent networks, the risk patterns are more unpredictable, because the risks hiddenly spread. As a result, the high level of complexity of the multiple networks produces the pop-corn effect of the 2008 crisis. We also investigate the slow recovery after the financial crisis. Our evolutionary prisoner's dilemma game model shows cooperation strategy outperforms defection in a small-world network. But, when the small-world network becomes a random network, defection is new dominant strategy. Thus, under high level of randomness, cooperators are exploited by defectors. In the real world, governmental policies and investments of other agents are also exploited under high uncertainty. It leads to the slow recovery.

TABLE OF CONTENTS

LIST OF FIGURES

LIST OF TABLES

CHAPTER 1

INTRODUCTION

The U.S. financial crisis that began in 2007-2008 turned into the Great Recession. Bubbles in the housing market burst and the impact of this risk sent shock waves through the financial system. Ultimately, it spread economic ruin far beyond the financial market, causing one of the worst economic downturns since the Great Depression. Since the 2008 financial crisis, the most critical mission for governments has been to establish a resilient financial system and economic recovery.

The financial crisis inevitably led to calls for reform and additional regulation of the financial system. Policy makers tried to introduce more regulations into the financial system. However, it is doubtful whether more regulations can fix what is broken. Generally, financial regulations are involved with the health of an individual bank. One may think the health of individual banks leads to stability of an entire financial system. It may be true, but not always. We need to consider "the fallacy of composition." The whole is not always the sum of its parts. Regulations to reduce risks to individual banks may not create a stable financial system (Lim and Lim, 2010). There can be a trade-off between individual bank health and systemic safety. This is called "the regulator's dilemma" (Beale et al., 2011). The safest allocation between assets for individual banks is to equally distribute the assets. It refers to "uniform diversification." However, as for an entire system, the safest option is to avoid uniform diversification, because uniform diversification increases homogeneity of the system. This leads to a high probability of total system failure, meaning simultaneous bank failures. Thus, to minimize this probability, an individual bank needs to avoid uniform diversification, but, paradoxically, the bank cannot minimize the probability of its own risk. This dilemma indicates that a solution for safety of individual banks may not be appropriate to tackle risks at a systemic level. In the efforts to be safe, banks can expose the entire system to risks. As this instance illustrates, policy-making for a safe financial system is much more complex than we expect. Hence, we will examine this complexity.

First of all, we need to look at the entire story of the financial crisis. After 2000, securitization made more credit available for mortgages. The sharp increase in house prices resulted from the growth of credit (Kindleberger and Aliber, 2011). Thus, financial innovations made it possible to distribute the loans in question to different economic agents, and banks could share their risks with other financial institutions. This financial system was thought to be a very safe system. However, as house prices stopped rising, many financial institutions began to suffer from losses and potential losses due to the subprime loans. To minimize the losses from bank failures, banks froze interbank markets, and the lack of banks' liquidity made the whole financial system worse. After the financial crisis, the adverse impact on the real economy was huge. Even though the government introduced various policies to eliminate the impact of the financial crisis, the recovery was slow and the adverse impact lasted longer than we expected. Even after the economy had begun to recover, the unemployment rate continued to rise and stay high. This unemployment rate pattern was not typical, compared to other recessions since World War II (Dwyer and Lothian, 2011).

Two questions are raised. High interconnectedness of banks was considered to produce a resilient financial system by sharing risks. In fact, it worked well before the financial crisis. Thus, it was hard to predict massive bank failures. However, we experienced one of the worst crisis. What led to the unpredictable financial crisis in 2008? Another question is what explains the atypical recovery pattern after the 2008 financial crisis. In other words, why was the recovery so slow?

We address these questions using the perspective of complex adaptive systems. The story of the financial crisis concerns contagion, networks, interaction, and interdependence between the real economy and the financial economy. They are the main components of complex adaptive systems (Miller and Page, 2009). Therefore, the first step for our crisis analysis is understanding complex adaptive systems.

The former European Central Bank (ECB) President Jean-Claude Trichet argued that in terms of the crisis, the existing economic and financial models have serious limitations, and we need to develop complementary tools. He suggested the Agent-Based Model as a tool which can capture complex interactions between financial agents (Trichet, 2010). Agent-based models (ABM) offer the possibility of a new paradigm for examining complex adaptive systems. It can capture non-linear behavioral patterns, heterogeneous agents, adaptation and their interconnectedness, which are main properties of complex adaptive systems. ABM is bottom-up modeling rather than top-down modeling. While top-down modeling imposes strong assumptions, such as seeking equilibrium and rationality, bottom-up modeling examines emergent properties by individuals' interactions and adaptation without any dominant assumption (Miller and Page, 2009). ABM has been applied to many fields in social sciences. It has contributed to studies about how the emergence of the features at a system level is originated from interactions of agents at an individual level. In particular, ABM can play a critical role in policy analysis studies, because it allows policy makers to examine how a policy measure works among heterogeneous individuals (Dawid and Neugart, 2011). Therefore, we use ABM as a main tool to deal with the complexity of the crisis.

Network theory is another tool needed in this dissertation. A network is a structure, capturing interactions and interdependence in complex adaptive systems. Since the financial crisis was based on interbank networks, ABM and network theory can be a good combination to analyze and diagnose the financial crisis and the sluggish recovery.

In addition, as a programming language, we use Netlogo to model the financial crisis and the sluggish recovery (Wilensky, 1999).

CHAPTER 2

AGENT-BASED MODEL

2.1 Agent-Based Model

Agent-based modeling can be defined as a computational approach to modeling complex systems composed of heterogeneous, autonomous, interacting and goal-oriented agents within an environment and a given rule set. This approach is based on the object-oriented model in which entities are elementary units, rather than variables (Cioffi-Revilla, 2013). The origin of this methodology is von Neumann's work on self-reproducing automata (Von Neumann, 1951). It is difficult to call von Neumann's model an agent-based model, but his study is a pioneer for construction and modeling artificial life. The roots of ABM can be found in Thomas Schelling's research about segregation (Schelling, 1971). His simple dynamic model provided insights into the relationship between micromotives at an individual level and macrobehaviors at a system level (Schelling, 2006). Since the studies of von Neumann and Schelling, ABM has been applied to various studies about social phenomena. In this section, we introduce the main features of ABM.

ABM is a tool to explain complex adaptive systems or complex systems. A complex system is an outcome of agents' collective actions. Autonomous agents have their own properties, but when they cooperate, the collective properties can be different from individual properties. Interactions of the agents can make new properties at a system level. This phenomenon is called "emergence". Therefore, to understand complex systems, we need to examine not only the properties of the systems, but also agents' behaviors and their interactions (Mitchell, 2009). Complex systems are different from complicated systems. While "complicatedness" comes from entwined independent elements, complexity arises from entwined dependencies of elements. A change in an element may not cause a fundamental change in a complicated system, but the same change can induce a huge difference in a complex system. Since all elements are connected to each other, a small change leads to a domino effect in complex systems (Miller and Page, 2009). Many phenomena in our society can be considered complex systems, such as trades in a market, transmission of culture or public opinion, voting behavior, spreading epidemic disease, and cooperation (Laver and Sergenti, 2011; Epstein, 2006; Epstein and Axtell, 1996).

To clarify the terms, we present the definitions of complex system and ABM.

> Complex system: "A system in which large networks of components with no central and simple rules of operation give rise to complex collective behavior, sophisticated information processing, and adaptation via learning or evolution" (Mitchell, 2009).
>
> Agent-based model: "A computational method that enables a researcher to create, analyze, and experiment with models composed of agents that interact within an environment" (Gilbert, 2008).

From these definitions, we propose the building blocks for ABM. They are as follows (Cioffi-Revilla, 2013; Gilbert, 2008; Miller and Page, 2009).

- Bottom-up approach : an emergent system arises out of individual entities at the lower level.
- An agent is autonomous and heterogeneous.
- An agent follows a given behavior rule set to achieve a goal.
- They interact each other within environments.

There are two categories in ABMs (Lengnick, 2011). The first category models try to produce a replica of the real world. The EURACE model belongs to this category (Dawid et al., 2012). The EURACE project develops an agent-based model for economic system. It constructs a software platform to perform very large scale agent-based simulations on high performance computers. Thus, this project tries to reproduce the economic events of the real world. This category can provide credible results about the real world, but the outcome is as complex as the real world. Thus, it can be hard to obtain a clear and simple explanation for the outcome due to the complexity. The second category seeks much simpler models, compared to the first category models. The models in this category are abstracted from the real world. Most agent-based models belong to this second category. It does not attempt to create a replica, but it tries to create a minimal and simple world. Thus, unlike the former category, the second category models have only several types of agents and behavioral rules (Lengnick, 2011). Our models are included in this second category.

2.1.1 Agent-based model vs. Equation-based model

ABM competes with other modeling methods. The most common model form is the equation-based model (EBM) or the variable-based model. EBM is "a set of equations, and execution consists of evaluating behaviors" (Parunak et al., 1998). EBM is different from ABM in many ways. First of all, while ABM is a tool for bottom-up approach, EBM is a method for top-down approach. EBM assumes that agents are homogeneous in the model, unlike ABM. Fundamentally, the aim of ABM is emulating agents' behaviors, whereas EBM seeks to evaluate them (Parunak et al., 1998; Cioffi-Revilla, 2013). Thus, EBM examines characteristics of interest by the evaluation of the equations in the model. EBM is the dominant modeling method in the various fields. The most distinct advantage is that EBM can clearly show the dynamics of the system of interest. A social system can be abstracted as a set of equations, and social entities are also represented by equations and variables (Cioffi-Revilla, 2013). Some argue that the biggest advantage of EBM is fewer free parameters, compared to ABM. A free parameter means that a variable is determined by the modeler. Thus, many free parameters can lead to the certain result desired by the modeler (Wilensky and Rand, 2015). In spite of some advantages of EBM, ABM has some benefits over EBM. First of all, ABM is based on a realistic assumption, which is heterogeneity. Secondly, ABM does not require knowledge of the aggregate phenomena. It just needs simple rules for the agents. Furthermore, ABM can offer that more detailed information about both individual and system level. In terms of the free parameter issue, we cannot agree that ABM has more free parameter than EBM. This is because EBM tends to hide its free parameters. When EBM cannot incorporate the free parameters in the variables of the equations, the free parameters are implicit and hidden (Wilensky and Rand, 2015). Although ABM competes with EBM, they can be complementary, because each method has the different stochastic aspect. While ABM is a good tool to capture stochastic fluctuations, EBM can provide a good description of the statistics of the fluctuations (Cecconi et al., 2010).

2.2 Verification and Validation

ABM stimulates social or economic events, and a question of the accuracy of the simulated events is always raised. Thus, once an agent-based model is created, the model needs to be verified and validated. The verified and validated model means that its outcome is accurate and relevant. Verification and validation can be defined as follows:

> Verification is "ensuring that the computer program of the computerized model and its implementation are correct" (Sargent, 2004).
>
> Validation is "substantiation that a computerized model within its domain of applicability possesses a satisfactory range of accuracy consistent with the intended application of the model" (Schlesinger, 1979).

Simply speaking, verification or internal validity is the process of determining if the model is doing what the modeler intends. Validation is the process of determining if the model corresponds to the target phenomena.

2.2.1 Verification

The verification process involves debugging. To eliminate bugs in the code of a simulation model, the modeler rechecks every single line of code to ensure that the model is properly working. In addition, the modeler needs to observe whether functions in the code generate the outputs in the expected way. Finally, it is important to test if the model can reproduce the expected outputs within the certain range of parameters. Importantly, we should not expect the binary result of this process. The extent of verification exists along a continuum rather than either verified or unverified model (Wilensky and Rand, 2015; Gilbert, 2008; Cioffi-Revilla, 2013).

2.2.2 Validation

The validation process involves pattern matching between the model outputs and the target social phenomena. The initial step is calibration or ex-ante validation. It is the process of selecting good parameter values to allow the model to reproduce the patterns of the real system (Railsback and Grimm, 2011). After calibration and model implementation, the model creator needs to carry out validation or ex-post validation. There are many means of validation, and we introduce some of them. Animation and operational graphics are methods to show patterns of the values or behaviors graphically. Event validity is the process for comparing event occurrences between the simulation model and the real system. Face validation is the process concerning comparison between properties of the model and those of the real world. Multi-stage validation consists of three steps. The first step is developing the model's assumptions. Second, the modeler validates the assumptions with the empirical data. The final step is comparing the pattern of the model to the real system. There is not a single best validation method. Thus, several validations can be exploited to check if the model is accurate (Sargent, 2004; Wilensky and Rand, 2015; Cioffi-Revilla, 2013; Cirillo and Gallegati, 2012).

If a simulation model is not aimed at empirical description, the validation process needs to check whether the patterns of the model are interpretable, and whether the model is based on plausible behavior rules of the agents. More importantly, the model needs to be able to develop into the more specific model which can be validated with empirical data (Gilbert, 2008). As for validation, we want to emphasize that models cannot produce the same pattern as the real world, because models simplify the real world. What the modeler can do is incorporating a certain number of important aspects of the real system (Wilensky and Rand, 2015).

2.3 Models

ABM is applied to many fields of social science. In this section, we briefly describe some examples.

2.3.1 Segregation Model

Thomas Schelling made the first attempt to apply ABM to social science. His interest is racial segregation in the U.S. His model is an abstract model, which is not aimed at empirical description. The model has a chessboard, having square grid cells. They indicate households in an urban area. The agents consist of pennies and dimes, which are two different groups. In every round, an agent calculates the fraction of neighbors. If the number of the other group neighbors is greater than the given tolerance threshold, the household will be unhappy and decide to move out. Consequently, the model generates clusterings for each group even when the tolerance threshold is large (Schelling, 1971).

2.3.2 Sugarscape

The Sugarscape model is considered the first generation ABM. Like Schelling's model, the agents in this model are inhabitants, and the environment is a two dimensional grid, containing sugar in each cell. Sugar is energy for agents, and agents collect and consume sugar which is randomly distributed in the cells. Agents have two behavior rules. First, they need to find the closest cell, having the greatest amount of sugar, and move to the cell and harvest the sugar. Second, if an agent has no energy, the agent dies and a new agent is born. The Sugarscape model can be applied to many social issues. For example, if sugar is replaced by wealth, wealth distribution is the target phenomenon of the Sugarscape model (Epstein and Axtell, 1996).

2.3.3 Anasazi

ABM helps archaeology studies overcome their experimental limitations. The Anasazi model explains settlement patterns of Anasazi farmers who lived in Long House Valley in Arizona from A.D. 800 to 1300. The agents store and spend maize, and decide to stay or move to another residence location by changes in agricultural conditions. With simple agent behavior rules, modelers search proper parameters to reproduce the historical clustering settlement of Anasazi farmers. According to the model result, the main reason why Long House Valley was abandoned was not degraded agricultural environments but sociocultural push or pull factors which induced Anasazi farmers to join the exodus from Long House Valley (Axtell et al., 2002).

2.3.4 Prisoner's Dilemma Game

Axelord's model shows the winner is the Tit-for-Tat strategy in the tournament of the prisoner's dilemma strategies (Axelrod and Hamilton, 1981). Then, he applies ABM to the tournament which is much more complicated. In the model, each agent is a player of a typical prisoner's dilemma game, which produces a 2×2 outcome table. A player can remember three previous game outcomes. Thus each player knows 4^3 strategy histories of the game, and Axelord adds six hypothetical strategy movements. Now, each play has the string of seventy strategy genes $(64 + 6)$. In this case, the number of strategies is 2^{70}. To find good strategies from a large number of strategies, Axelord exploits the genetic algorithm in his agent-based model. By the genetic algorithm, successful strategies are inherited to the next generation with some mutation. The result identifies that Tit-for-Tat is the best strategy in the tournament of the prisoner's dilemma game (Axelrod, 1997).

CHAPTER 3

NETWORK THEORY

3.1 Network Theory

Complex interconnectedness is one of the main properties of modern systems, such as the Internet, a transportation system, the electrical power grids, citations, the food web, and markets. These interconnected systems can be characterized as networks. The definition of a network is that it is "a collection of points joined together in pairs by lines" (Newman, 2010). In complex theory, a network tends to be called a complex network. When a network has a large number of interconnected nodes and it is hard to understand the overall behavior of the network, it is called a complex network (Van Steen, 2010). In a network, points are called nodes or vertices, and lines are referred to as links or edges (Newman, 2010). In this section, we briefly introduce basic network terminology and network models. In addition, we explain the relation between ABM and network theory.

3.1.1 Network Terminology (Newman, 2010)

Adjacency matrix:

$$A = \begin{pmatrix} 0 & 1 & \cdots & 0 \\ 1 & 1 & \cdots & 0 \\ \vdots & \vdots & \ddots & \vdots \\ 0 & 0 & \cdots & 0 \end{pmatrix}$$

Figure 3.1. Adjacency Matrix

Assume a network with n nodes. A link between nodes i and j is denoted as (i,j). From nodes and links, we can get a link list, for example (1,2), (2,1), and (2,2). This list is mathematically represented by a matrix. It is called an adjacency matrix. The matrix of a simple network consists of 0 and 1. 1 indicates that there is a link between two nodes, and 0 means two nodes has no link (see Figure 3.1).

Direction:

A link can have a direction, pointing from one node to another. A network which has directed links is referred to as a directed network. In this case, 1 in the adjacency matrix,A_{ij}, means that there is a link from i to j. Thus, the adjacency matrix for a directed network is asymmetric. An undirected network can be considered a type of direct network. In this case, one undirected link needs to be replaced with two directed links.

Degrees:

The degree of a node is the number of links which the node has. The degree of a node i for an undirected network is denoted by k_i:

$$k_i = \sum_{j=1}^{n} A_{ij}$$
$$m = \frac{1}{2}\sum_{i=1}^{n} k_i$$

If a undirected network has m links, the number of link ends of the network is $2m$. Thus, the sum of the degree of all nodes is equal to $2m$.

Average Path Length:

A path is a sequence of nodes, connected by a link. The length of a path is the number of links traversed along the path. Links can be traversed more than one time. The shortest path is referred to as the path, having the shortest distance between two nodes. Average path length is the mean distance from a node to others. This is used for a measure for centrality of a network. The average path length (l_i) is can be written as:

$$l_i = \frac{1}{n} \sum_j d_{ij}$$
$$s.t. \quad d_{ij} \text{ is the length of the shortest path from i to j.}$$

Clustering Coefficient:

This is a measure for transitivity. If three nodes are connected by a link, it implies that they are transitive. Simply speaking, it means that "the friend of my friend is also my friend". The clustering coefficient is quantified by the fraction of node triples. The closed triple means transitive nodes. The clustering coefficient (C) is represented as:

$$C = \frac{\text{number of closed triples}}{\text{number of connected triples of nodes}}$$

If C = 1, it means perfect transitivity. When C = 0, it implies no closed triples. A tree network tends to show C = 0.

Eigenvector Centrality:

Eigenvector centrality measures the level of importance of a node's neighbors, which means its connected nodes. If neighbor nodes of a node are connected to many other nodes or a node has many neighbors, the node has the high eigenvector centrality. The eigenvector centrality (x_i) can be written as:

$$x_i = \kappa_1^{-1} \sum_j A_{ij} x_j$$
$$s.t. \quad \kappa \text{ is an eigenvalue.}$$

3.1.2 Network Models

Erdos-Renyi model (Erdős and Rényi, 1959) (ER network):

The Erdos and Renyi model is called a random network or a Poisson random network. Erdos and Renyi propose a simple network model, which has n nodes with connection probability p. The model is represented by $G_{n,p}$. It means that each node can be connected with another node with the probability p. If nodes have equal probability and the network has m links, the network can be written as $G_{n,m}$. The distinct property of the ER network is that the average degree distribution follows the Poisson distribution. This is why this model is called the Poisson random network.

$$p_k = \binom{n}{k} p^k (1-p)^{n-k} \simeq \frac{z^k e^{-z}}{k!}$$
$$s.t. \;\; k \text{ is a degree.}$$

According to the Poisson distribution, the degree of a node can vary from 0 to n. Although the ER network tries to reproduce a real system with randomness, it does not capture the properties of the real system. First of all, the real world is not based on randomness. Furthermore, the ER network underestimates the number of high degree nodes and wide dispersion of the degree distribution of the real networks (Barabasi, 2015).

Small-world network (Watts and Strogatz, 1998):

Watts and Strogatz's small-world model is motivated by the small-world effect, observed in the real world. If we randomly choose any two individuals from any place, we can find that they are connected through ,at most, six hops in the acquaintance network. It is called six degrees of separation. Today, the distance between two individuals who are randomly chosen is smaller due to technology developments (Backstrom et al., 2012). The small-world model has paradoxical two properties: a high clustering coefficient and a low average path length.

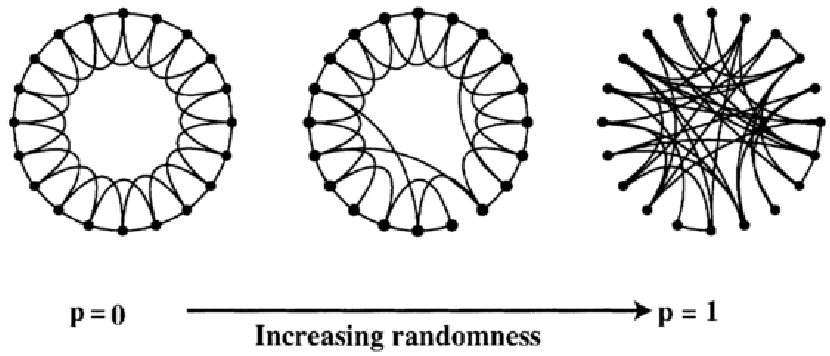

Figure 3.2. Regular, Small-world, Random Networks. Reprinted with permission from (Watts, 2004)

Watts and Strogatz propose an algorithm to create a small-world network. The algorithm rewires some links of a circle network or a regular network. Figure 3.2 illustrates the process. There are three types of networks. The left side network is the regular network. The middle network is the small-world model. Based upon the algorithm, some links are rewired to other nodes which are randomly chosen. The right side one is a random network, which all links are rewired. As the number of rewired links increases, the regular network becomes the small-world network, and then it finally becomes the random network.

Barabasi-Albert model (Barabási and Albert, 1999) (BA network):

In the real network, degree distributions tend to have a long tail. For example, we can easily find a hub website in the Internet networks. A few web pages have a considerably large number of links, but most web pages have a small number or links (Albert et al., 1999). Thus the distribution can have a fat tail or a long tail. The fat-tailed distribution is graphically represented as Figure 3.3. The left side plot is for a Poisson distribution, and the middle plot shows a fat-tailed distribution or a scale-free distribution. The fat-tailed distribution illustrates most nodes have a very small number of links while a few nodes have the majority of links. The right side plot is the fat-tailed distribution with log-log scale. As you can see,

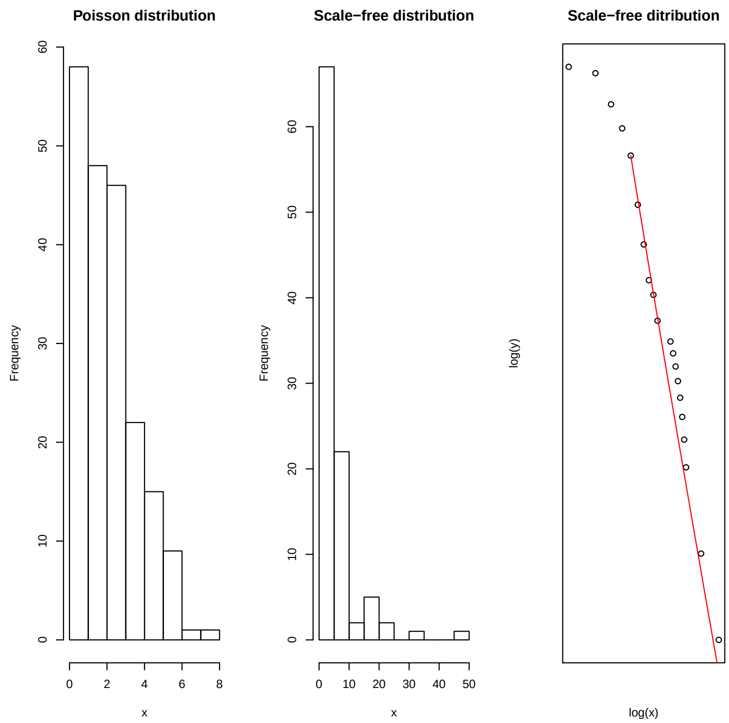

Figure 3.3. Poisson and Scale-free Distributions

the fat-tailed distribution can be represented by a line in the log-log scale plot. A fat-tailed distribution can be written as:

$$P(j) \approx j^{-\gamma}$$

$s.t.$ $P(j)$ is a probability function for j and γ is a scale-free exponent.

Due to this expression, it is also called a scale-free distribution or a power-law distribution. Barabasi and Albert suggest an algorithm to create a scale-free network. This process is called "preferential attachment". It means the larger a node's degree, the greater the probability which the node can have new links. Simply speaking, "the rich get richer". Thus, as the size of hubs increases, the tail of the degree distribution is longer. This network is a realistic form to analyze bank networks. Assume there are a few initial banks. New banks will make a interbanking connection with the initial banks. If the bank network has a hub bank, the new bank will want to make a connection with the hub bank. Thus we can expect the bank network will follow a scale-free distribution over time. Furthermore, the real bank networks follow the fat-tailed distribution (Kim et al., 2002; Boss et al., 2004; Krause and Giansante, 2012).

3.2 Network and Agent-Based Model

When we model complex systems in the social science field, we need to consider individual behaviors and their interactions. When an individual makes a decision about an event, his decision is influenced by the other individuals around him. Thus, the outcome from an individual's decision can be thought as an output of interactions. However, the interactions are not totally random events. In fact, interactions are organized (Kirman, 2010). Our decision will be influenced by people who we already know, rather than strangers. An organization of these interactions is a network. We can think that we are embedded in networks or social contexts (Granovetter, 1985). Our preferences, expectations, and decisions can be conditioned by our networks. Therefore, a model creator needs to consider structures of networks in which the individuals are embedded (Alexander, 2007).

As noted, environments are a main element of ABM. In agent-based modeling for the social sciences, the environment can be thought as networks. Thus, networks can provide ABM with structures for interactions. On the other hand, ABM can help with network modeling. In modeling a network, a big obstacle is capturing emergent behaviors of complex networks. ABM can provide a network model with a tool to capture the emergent phenomena (Jackson et al., 2008).

Consequently, we propose to combine these two models for making a better model. We believe that the agent-based network model will be a good combination to analyze complex social systems.

CHAPTER 4

FINANCIAL CRISIS AND AGENT-BASED MODEL

4.1 The 2008 Financial Crisis

When did the 2008 financial crisis begin? There may be a couple of explanations for it. But we indicate August 9, 2007 as the starting date. On August 9, 2007, the investment bank BNP Paribas became insolvent because of losses from sub-prime mortgages. The impact of insolvency and fear of failures started to spread to the entire economic system beyond the financial market.

However, governments and financial authorities could not stop the contagion of risk and fear. On September 15, 2008, a new page of U.S financial history was written. The fourth-largest investment bank, Lehman Brothers, filed for bankruptcy and it was the biggest bankruptcy filing in the U.S. history. The impact immediately spread to all kinds of markets, and hundreds of banks collapsed. The failures caused chain reactions for another failures. Furthermore, the monetary policies and fiscal policies could not stimulate the economy. On August 2009, FRB chair Ben Bernanke said that economy was recovering, but the unemployment rate rose again in the next month (See Table 4.1). The impact of the crisis widely spread and the recovery needed much more time .

In this chapter, we explain limitations of conventional models in analyzing the financial crisis, and the possibility of ABM in crisis studies.

Table 4.1. Financial Crisis Time line(Guillén, 2009; Kingsley, 2012)

August 9, 2007	Investment bank BNP Paribas froze three funds because of "complete evaporation of liquidity". They acknowledged the risk of sub-prime mortgage markets.
September 14, 2007	British bank Northern Rock faced a liquidity crisis. Depositors withdrew their savings. It was the biggest run on a British bank for 150 years.
October 1, 2007	Swiss bank UBS announced \$3.4bn losses from sub-prime related investment. Citigroup also announced \$3.1bn losses
January 21, 2008	Stock prices slumped. It was the biggest fall since 11 September 2011.
January 24, 2008	The largest 1-year drop in US house sales was announced
February 17, 2008	British government nationalized Northern Rock.
March 16, 2008	J.P. Morgan Chase announced purchase of Bear Stearns
April 30, 2008	US house prices showed the first annual fall for 12 years.
July 14, 2008	US financial authorities began to help Fannie Mae and Freddie Mac.
August 30, 2008	British Chancellor Alistair Darling warned that economies were entering the worst crisis for 60 years.
September 7, 2008	Fannie Mae and Freddie Mac were bailed out by the US government.
September 15, 2008	Lehman Brothers filed for bankruptcy. This is the biggest bankruptcy filing in the U.S. history. Bank of America purchased Merrill Lynch.
September 16, 2008	Global stock market suffered worldwide slumps
September 18, 2008	Russian stock market trading was suspended for two days
September 21, 2008	Morgan Stanley and Goldman Sachs gave up their investment bank status. They became commercial banks.
September 25, 2008	Big Banks collapsed : Washington Mutual. Later, Wachovia.
September 28, 2008	The British government nationalized Bradford& Bingley.
October 3, 2008	The U.S. Congress passed the \$ 700 bn asset relief program which was rejected four days ago.
October 7, 2008	In Iceland, the three biggest commercial banks collapsed. Bank stock prices fell sharply.

Table 4.1 continued

October 13, 2008	The British government announced to bail out several banks, including the Royal Bank of Scotland and Lloyds TSB.
October 14, 2008	The US treasury injected capital into 9 large banks
October 15, 2008	J.P.Morgan and Wells Fargo announced big profit falls.
October 28, 2008	US consumer confidence showed the lowest record since 1967.
November 10, 2008	The US treasury invested $40 bn for AIG to restructure its loan.
November 14, 2008	The G20's leaders agreed to cooperate with respect to the global financial crisis. Then, they agreed on the $ 5tn global stimulus package(April 2, 2009)
November 20, 2008	US stock market suffered a sharp decline. In particular, Citigroup showed a 23% drop on the previous day, and another 26% drop.
November 23, 2008	Citigroup was bailed out by total $326 bn asset-relied package.
December 1, 2008	The National Bureau of Economic Research officially acknowledged the recession.
December 20, 2008	S&P downgraded eleven of the world's largest banks.
January 10, 2009	The unemployment rate in the U.S rose to 7.2%.
February 13, 2009	Thirteen banks collapsed in Nebraska, Florida, Illinois and Oregon. Congress passed a $787bn economic stimulus package.
March 2, 2009	AIG showed the largest corporate loss in the US history, with a deficit of $61.7bn.
March 6, 2009	The unemployment rate in the U.S rose to 8.1%.
March 10, 2009	US Federal Reserve chief Ben Bernanke said that this financial crisis was the worst one since the Great Depression.
June 1, 2009	General Motors filed for bankruptcy protection.
June 19, 2009	The number of bank failures was 40 so far this year.
August 24, 2009	Federal Reserve Chair Bernanke said the US economy was recovering
September 4, 2009	The unemployment rate in the U.S rose to 9.7%.
September 7, 2009	Joseph Stiglitz warned of a double-dip recession
October 24, 2009	The number of bank failures was more than 100 so far this year.
October 29, 2009	The official data showed the US economy began to grow, but analysts warned a sluggish recovery.
November 6, 2009	The unemployment rate in the U.S rose to 10.2%.
December 14, 2010	The Federal Reserve warned that the economic recovery was still too slow to reduce high unemployment rate

4.2 Conventional Models

In spite of the quantitative success of economic theories, the 2008 financial crisis has given rise to dissatisfaction with the economic models. Most models failed to predict this huge crisis. In this section, we briefly introduce the conventional models and their limitations.

In macroeconomic theories, the dominant models are based on the Dynamic Stochastic General Equilibrium (DSGE). DSGE models have four major assumptions. (1) perfect competition, (2) optimizing utility, (3) market clearing, and (4) rational expectations (Arrow and Debreu, 1954). Under these assumptions, an agent seeks unique and stable equilibrium, which is Pareto efficient. The models perform well in normal economic situations. However, it is doubtful if the models work well for rare events like crises. This is because the strong assumptions of the conventional models tend to supersede empirical observations (Bouchaud, 2008). Furthermore, the models are based on the past empirical data, but rare events are less important in the models because the models rely on the Gaussian distributions. The models can successfully forecast economic events within a certain range, but they can provide wrong insights in the face of outliers. This is a fatal flaw of the conventional models (Farmer and Foley, 2009). In reality, however, economic shocks follow the fat-tailed or the power-law distribution. Large-scale shocks are rare, but very dangerous (Fagiolo et al., 2012; Sornette, 2009).

Assumptions similar to those of DSGE have influenced the financial studies. The efficient market hypothesis (EMH) notes that prices totally incorporate all available information in financial markets. EMH rests on three major assumptions (Shleifer, 2003). First, investors are rational. Second, some investors are not rational. However, since their trades are random, the effects on prices will be canceled out. Third, irrational traders' influences on prices can be eliminated by rational arbitrageurs in the financial market. Thus, investors can use information "correctly and immediately" in the efficient market (Blinder, 2013). In theory, investors cannot exploit informational advantages to obtain profits, because such profits are already reflected in prices (Fama, 1970). Therefore, the possibility of bubbles is ruled out in EMH, because a price equilibrium already captures all information.

Both DSGE and EMH represent orthodox beliefs of economists, whereby economic phenomena are based on equilibria of rational and efficient markets. However, the assumptions of DSGE and EMH restrict flexibility of models to explain the rare and dangerous changes in the real world. Due to these beliefs, economists underestimate the empirical observations, which are economic crises. Hence, the conventional models have serious limitations to deal with crises.

The financial crisis has different properties, compared to normal economic events. Thus we need a new tool for it. In the second part of this chapter, we examine the different properties of the bank failures and recent studies which are not based on the conventional models. We believe the alternative models can provide a solution to overcome limitations of DSGE and EMH.

4.3 Contagion and Systemic Risk

In 2008, insolvency of banks was transmitted to other banks and the entire system, like disease contagion. To explain a large-scale breakdown, we will focus on this contagion or systemic risk (Elsinger et al., 2006). Systemic risk can be defined as "the contagion, inducing threats to the financial system as a whole, due to the default of one (or more) of its component institutions" (Hurd and Gleeson, 2011). The systemic risk tends to cause a cascading failure. This effect is triggered by an infinitesimal shock, but the effect spreads to the entire network. When nodes in the network are highly connected, the impact of the cascade failure will be extreme and more unpredictable (Watts, 2002; Hurd and Gleeson, 2013). In addition, a cascading failure pattern tends to have a steep slope pattern (Nedic et al., 2006; Crucitti et al., 2004).

The spread of bank failures was similar to the contagion of disease (Anderson and May, 1991; Newman, 2002; Meyers, 2007). Like a contagious disease outbreak, when a bank crisis happens in one region, it spreads to other banks in the adjacent regions. As the definition shows, systemic risk is a contagious phenomenon in the financial market. However, there is a big difference between the diseases contagion and the bank failure spread. High interconnectedness is likely to cause spread of risk or disease in both cases, but in the financial market, the interbank linkages have a role as an insurance against risk contagion (Gai, 2013; Allen and Gale, 2000; Leitner, 2005; Brusco and Castiglionesi, 2007). This insurance makes the entire system resilient. Actually, the financial system seemed resilient before the 2008 financial crisis. But, suddenly, the robustness broke down and risks spread. Before the financial crisis, the interconnected banks had shared their risks, and lowered the potential for contagion. However, once the contagion began, the high connectivity made the nodes highly exposed to the default risks (Gai and Kapadia, 2010). What changed the character of the financial system in 2008? First, we may need to explore the market structure, because the risk contagion depends on market conditions. In the complete market, the impact of the liquidity shock can be absorbed by all other banks. The interconnected banking system creates insurance against risks. As banking linkages increase, the banks obtain safer mutual insurances (Leitner, 2005). Due to this property, there is no risk contagion. However, this status may be fragile. In the incomplete market, a few banks are exposed to the shock. Then, the risk begins to spread to the neighboring banks rather than being absorbed. Thus, the possibility of contagion relies on the market structure (Allen and Gale, 2000). The mutual insurances help the banking system to avoid the adverse impact of shocks. But, without unexpected shock, risks can be contagious in the interconnected banking system. As banks have high connectivity, their behaviors show more risk-taking propensity, that is, imprudent investments. This is because the higher connectivity can provide them with greater mutual insurances. This offers the banks motivation for moral hazard. Thus, additional bank linkages can increase the probability of risk contagion (Brusco and Castiglionesi, 2007).

The asset structure and information can play an important role in causing systemic risk. If a bank has a large proportion of short-term finance, it will be very vulnerable to adverse information on the bank's future solvency. After the spread of adverse information, if investors stop rolling over the debt for the bank, the default probability of the bank will sharply increase. Then the impact will transmit insolvency to other banks by interbank linkages (Allen et al., 2012).

Financial connections reduce depositors' uncertainty about banks. Depositors may worry about denial of withdrawal at a particular location. This need makes interregional financial connections. Highly interconnected financial linkages allow depositors to withdraw money when they want. However, if depositors believe that their claims can be denied, they will begin to withdraw the capital. When the belief about denial spreads, the domino effect of bank failures is triggered through interregional banking networks (Freixas et al., 2000). Similarly, assortativity of edges and links is also an important factor in the interbank network system, because it can cause systemic risks and the cascading failures (Hurd and Gleeson, 2011). Assortativity is a network property. It means a node with a high degree has a relatively high tendency to be connected to another high-degree node (Newman, 2010). As the assortativity increases, the probability of systemic risk becomes higher. In other words, the sizes of the hub nodes in the financial network can make the entire system more vulnerable to systemic risk.

There are many causes to trigger a crisis. But many studies about the financial networks have common features. These are connectivity and concentration. They amplify systemic risks. As the financial institutions are more connected and concentrated, the contagious insolvency is transmitted more quickly to other nodes in the network. This phenomenon is induced by the externality which the network structure creates. No agent wants contagious insolvency, but the contagion emerges from agents' behaviors in the networks (Gai et al., 2011; Gai, 2013).

4.4 Agent-based Models as Alternative Models

As noted in the previous chapters, ABM is flexible and reflects properties of the real world. The agents are heterogeneous and their rationality is bounded. More importantly, it is based on interactions of agents, not on equilibria (Farmer and Foley, 2009). Due to these features, the number of policy studies using ABM is increasing in social science (Dawid and Neugart, 2011). In the first part of this section, we show ABMs dealing with macroeconomic issues. Then, we examine ABM studies about the financial crisis.

4.4.1 Macroeconomic Models

ABM is often used for analyzing economic topics in normal times. Especially when it is difficult to obtain actual data, ABM can be a good analysis tool. In this subsection, we introduce the agent-based models, dealing with the economic topics which have limited data.

The government has two scenarios for redistribution of tax revenues. The first option is to exploit the revenues as unemployment benefits. The second one is using them as cash incentives for investments in R&D. But, it is hard to directly compare these two options. A simulation model enables us to do it. The simulation model shows that the first policy has adverse effects on growth. On the contrary, the second option has a positive effect on growth (Russo et al., 2007).

Innovation is considered a rare event, but its positive effect is huge. Schumpeterian economics considers innovations as the main engine for economic growth, whereas Keynesian economics argues fiscal policy can lead to economic growth (Kirman, 2010). But, it is also difficult to make a direct comparison between them. ABM provides a tool for the comparison. ABM experiments for Schumpeterian and Keynesian policies illustrate that only Schumpeterian policies cannot maintain high economic growth. These policies can work well when Keynesian policies are working. Therefore, it can be wrong to believe that technology innovations are related to long-run growth, and demand-related policies are for short-run growth (Dosi et al., 2010). The model can be used to compare fiscal policy and monetary policy. The model indicates that redistributive fiscal policies that reduce inequality are more critical for long-run growth. In contrast, monetary policies cannot obtain effective results in economic growth under high inequality (Dosi et al., 2013).

The EURACE is an artificial economy model. The EURACE model is designed for making a replica of the real economic system. Thus, this model can deal with more complicated economic issues. For example, the model compares the quantitative easing policy (QE) to the fiscal tightening (FT). The results show the QE is more effective to stabilize the economy, but the effect of the FT is better than that of QE in the long run. It shows the extended use of the QE can cause the adverse effect on the economy (Cincotti et al., 2010).

The relation between the monetary policy and employment is also a difficult problem. In the real world, changing monetary policy can influence many parts of economy. Thus, it is hard to distinguish the effect on the employment from other effects of monetary policy. To find the effect on the employment, the simulation model of Raberto et al.(2008) creates a random interest rate policy to compare with the tighter monetary policy. The model shows that the tighter monetary policy outperforms the random policy rule in inflation and workers' utility (Raberto et al., 2008).

4.4.2 Financial Crisis Models : Systemic risks and Bubbles

Since the 2008 financial crisis, ABM has been used as an alternative methodology to analyze issues about the financial crisis. In the second part of this section, we introduce various applications of ABM for the issues.

The systemic risk studies we introduced above exploit the ideas of ABM, because interconnectedness, interactions, and contagion are the main targets of ABM. Thus, ABM is one of the common tools for contagious events in networks. Information contagion was an important factor in the spread of fear in the 2008 financial crisis. The initial sub-prime mortgage shock was relatively small. However, the shock led to the Great Recession. This is because uncertainty rose significantly. Under high uncertainty, the agents begin to withdraw their capital from small banks. It makes the situation even worse. Insolvency of small banks affects their neighbors, which have healthy financial conditions. This pattern exacerbates the financial network's distress. As a result, a relatively small shock can cause serious systemic risks (Caballero and Simsek, 2009).

The starting point of the systemic risk in the financial network was bubbles in the real economy. Blinder defines bubbles as "a large and long-lasting deviation of the price of some asset from fundamental value" (Blinder, 2013). How can the prices keep soaring? Leverage is the key (Thurner, 2011). If one buys a \$50 asset by putting \$10 down and receiving a \$40 loan, it can be said that it is leveraged 5 to 1. It is not a problem itself. But, when the asset price becomes \$70, his loan is still \$40, but his wealth becomes \$30. With the same leverage condition, he can buy a \$150 asset. This is the beginning of the bubble creation. However, suppose the asset price does not rise at all and then decreases by \$30. Now, his wealth is zero. If the price keeps decreasing, the bubble implodes ferociously. Losses will spread beyond borrowers to banks which provided the leverage (Blinder, 2013).

Thurner(2011) emphasizes the role of leverage in creating bubbles and systemic risk. His model has uninformed and informed investors. Uninformed investors randomly buy and sell the assets, which leads to underpriced assets. However informed investors have information about the true values of the assets. Thus, they make profits from the underpriced assets. For higher profits, the informed investors can use leverage from banks. Thurner's model shows that high leverage makes the asset market more volatile. As explained, even small fluctuations can cause big losses under high leverage condition. Although the informed investors have information, the market can be more unpredictable due to the high leverage, leading to vulnerability of the financial system (Thurner, 2011).

Inflation can also bring about bubbles in the real economy. Which one is the primary cause of bubble creation? The model by Geanakoplos et al. (2012) simulates a housing market for a period of 1997 to 2009 based on individual data of Washington DC. Their model shows that when interest rates are held constant, and leverage changes, the bubble and burst are observed. But, when leverage is frozen, the bubble is significantly weakened and there is no burst (Geanakoplos et al., 2012). Therefore, excessive leverage is the primary cause of generating bubbles in the housing market.

4.4.3 Financial Crisis Models : Regulation

After the financial crisis, bank regulations became an important issue to diagnose the huge bank failures. The model of Westerhoff(2008) simulates volatility of a market to examine the impact of regulatory policies. The model illustrates why central bank intervention is often unsuccessful. For successful central bank intervention, the intervention should be performed before agents' adaptations for it. However, as the profit opportunity system changes, agents quickly modify their strategies for the new situation. Thus, the impact of central bank intervention decreases (Westerhoff, 2008).

In many cases, the bank regulations are created in normal times. Regulating risky banks in normal times can cause an unexpected result in bad times. This is because the criteria of the regulations can suppress the lending activity of banks. A decrease in lending activity leads to insolvency of other banks (Ashraf et al., 2011). Less strict regulations refer to higher leverage which firms can exploit. This leads to more investments. However, as firms use excessive leverage, the possibility of insolvency and bankruptcies also increases (Raberto et al., 2011). Therefore, without considering this non-linear relationship, it would be difficult to make proper bank regulation for the safe financial system.

Table 4.2. Agent-based Models for Policy Research

Policy Research	Researcher	Main Topics
Social Policy	Schelling (1978)	Patterns of residential segregation.
	Epstein and Axtell (1996)	Emergence of cultural segregation(Sugarscape model)
Systemic Risk and Bubble	Thurner (2011)	Leverage, vulnerability, systemic crash, synchronization effect
	Geanakoplos et al.(2012)	Housing market bubble and burst by leverage
	Gai et al.(2011)	Network resilience, strict prudential liquidity regulation
	Caballero and Simsek (2009)	Information contagion, Bank failures
Fiscal Policy	Russo et al.(2007)	Tax rate and growth, Redistributive policy
	Dosi et al.(2010)	Keynesian and Schumpeterian policies
	Dosi et al.(2013)	Income distribution and growth
Monetary Policy	Dosi et al.(2013)	Inequality and growth
	Cinocotti et al.(2010)	Quantitative easing (QE) and Fiscal tightening (FT), EURACE
	Raberto et al.(2008)	Tight monetary policy, controlling inflation
Bank Regulation	Ashraf et al.(2011)	Banks as financial stabilizers, less strict prudential bank regulation
	Roberto et al.(2011)	Effect of leverage on economic performance or business cycle, EURACE

CHAPTER 5

HIDDEN SPREAD OF SYSTEMIC RISK IN MULTIPLE NETWORKS

In a network system, systemic risk spreads to the entire network through links. As the complexity of the network increases, the spread pattern of the systemic risk becomes more unpredictable. Thus, although the policy-makers may create their best policy for the resilient system, based on the past data and studies, it is difficult to say if the policy can deal with the complexity. Since we use only partial information, we may fail to figure out the implicit mechanism of the underlying system. The best thing we can do is to focus on not only phenomena of the macro-level, but also behaviors at the micro-level. The main advantage of our tool is that it can capture both levels. Hence, we believe that we can provide an alternative perspective on the hidden mechanism of the financial crisis.

What our models explain is straightforward. First, systemic risk is unpredictable in the complex systems. Second, one may predict a cascading avalanche failures in a system, due to the systemic risk. But we think even this prediction can be wrong in the real world. One may explain the Black swan as a rare event with existing models and data. But sometimes we need to consider a "Dragon king" which is a very rare, but extremely dangerous event. In this case, the distribution for the Dragon king can be beyond a fat-tailed distribution which outliers follow (Sornette, 2009). Theoretically, the probability of this rare event may be ignorable, but empirically, it is not, such as the Great Depression, the 1997 financial crisis, the 2008 financial crisis and South Korea MERS outbreak. Thus, we need a different point of view to analyze these events. We seek the alternative view from ABM. ABM focuses on the complexity itself. Especially, financial systems have high level of complexity, because they are highly interconnected and concentrated. One believed that the modern financial system was a very safe system, because the risks could be shared by other institutions, but this belief was wrong. We propose a possible explanation for the wrong belief with our models about systemic risk which is rare but extremely dangerous.

5.1 Basic Model (Gai, 2013)

To model the financial crisis, we assume a bank network with nodes and links. The nodes refer to banks, and links mean interbank relations. Thus, a balance sheet of a bank is associated with interbank links. In other words, banks are exposed to an attack from a default. Thus, the system can be vulnerable to systemic risk. The real bank network has direct links for claims and obligations, but we use indirect links for the simplicity of the model. However, the links can work like direct links through parameters in the model.

Table 5.1. Stylized Balance Sheet (Gai, 2013)

Fixed Assets(A^F)	Retail Deposit(L^D)
Collateral Assets(A^C)	
Reverse Repo(A^{RR})	Repo(L^R)
Unsecured Interbank Assets(A^{IB})	Unsecured Interbank Liabilities(L^{IB})
Liquid Assets(A^L)	Capital(K)

For the first model, Gai (2013)'s model is used as a reference model (Gai, 2013). The main component of Gai's model is a balance sheet of an individual bank. Table 5.1 illustrates the simple balance sheet. The liabilities of each bank are comprised of unsecured interbank liabilities (L_i^{IB}), repo liabilities (L_i^R), retail deposits (L_i^D) and capital (K_i). For simplicity, Gai assumes the total unsecured interbank liability portion of every bank is evenly distributed for each outgoing link. Repo means repurchase agreements. For example, Bank A sells a security to Bank B at a certain price and both banks agree that Bank A will repurchase it in the near future. In the transaction, the security is collateral. Reverse repo is the opposite transaction to the repo. Bank A buys a security and agrees to sell it in the near future. We can think that the security seller is a borrower and the buyer is a lender. Thus, the repo can be regarded as a short-term collateralized loan. When a bank needs to use repo funding using A^C, the aggregate haircut(h) will be required to obtain it. This haircut will protect the lender against the security prices fall below the collateral value. Thus, the repo rate reflects the underlying probability of default on the securities, used as the collateral. The model considers an additional individual bank haircut,h_i. Therefore, the maximum amount of repo funding is (1-h-h_i)A_i^C. It can be interpreted to mean that even if a bank provides identical collateral to another bank, the lender will ask an additional haircut as extra protection when the lender thinks that the borrower has relatively high default probability. Reverse repo is also secured with collateral that has the same h in the model. In Reverse repo transaction, the amount of collateral can be calculated as (A_i^{RR} / (1-h)). Finally, the maximum amount of repo funding for the reverse repo is $\frac{(1-h-h_i)}{1-h} \cdot A_i^{RR}$.

As for assets, since every interbank liability is another bank's interbank assets, unsecured interbank assets (A_i^{IB}) are endogenously determined by network links in the model. In addition to unsecured interbank assets, banks have four other assets : 1) fixed assets (A_i^F) which are completely illiquid and cannot be used as collateral, 2) assets for only repo transactions (A_i^C), 3) reverse repo assets (A_i^{RR}), and 4) unencumbered fully liquid assets (A_i^L).

With assets and liabilities, we can create a condition for liquidity. For the simple model, Gai precludes retail deposits and new external funding, and the intervention of the central bank. These assumptions seem unrealistic, but they can be plausible under some conditions. First of all, it was difficult to obtain new assets during the crisis time. In addition, the intervention of the central banks cannot be immediate. So, we can use these strong assumptions to simplify our model. With these assumptions, we modify the condition of Gai's model for our purpose. The modified condition for liquidity is as follows.

$$A_i^F + A_i^L + (1-h-h_i)A_i^C + \frac{(1-h-h_i)}{(1-h)}A_i^{RR} + A_i^{IB} - L_i^{IB} - L_i^R - L_i^D + e_i > 0$$

In this condition, e_i indicates idiosyncratic risk of an individual bank. When a bank cannot satisfy this condition, it implies that the bank is insolvent. From the condition, we can see that diverse shocks have the potential to trigger a liquidity crisis at bank i if the bank is unable to have sufficient amounts of assets. For example, additional haircuts have the potential to trigger widespread liquidity stress. Also, if a bank has trouble meeting the condition, counter party banks need to take defensive actions to avoid default. One of the options is hoarding liquidity. For this, counter party banks will refuse to roll over unsecured interbank lending. It directly influences L_i^{IB}.

Now, let's develop the liquidity condition. From the liquidity condition, a bank can be illiquid in the three circumstances : 1) an increase in additional repo rates, 2) hoarding liquidity, and 3) a decrease in A^F by macroeconomic shocks. These circumstances have the potential to trigger liquidity shortage. To capture these circumstances, we suggest the more practical liquidity condition which is the main behavior rule in our model. It is as follows:

$$q \cdot A_i^F + A_i^L - \alpha \cdot loss_i + (1-h-h_i)A_i^C + \frac{(1-h-h_i)}{(1-h)}A_i^{RR} - L_i^R - L_i^D + e_i > 0$$

In the condition, q means a weight for losses of A_i^F. When an individual bank has losses from illiquid assets, such as a mortgage loan loss, q will decrease. $loss_i$ indicates aggregate losses from interbank liabilities (L^{IB}). It can be interpreted as losses by hoarding liquidity. When one of the counter party banks stops the rollover for loan, $loss_i$ will decrease. But as L^{IB} is based on the number of counter party banks, if a bank has more links than others, the decrease rate of $loss_i$ is smaller than that of others. α means a weight for $loss_i$. According to the given balance sheet, if a bank is solvent, it needs to satisfy at least one of the following conditions:

$$q \cdot A_i^F > L_i^D$$

$$A_i^L > \alpha \cdot loss_i$$

$$(1 - h - h_i)A_i^C + \frac{(1-h-h_i)}{(1-h)} A_i^{RR} > L_i^R.$$

5.2 Failure Pattern of the 2008 Financial Crisis

Now, let's move to the 2008 Financial crisis. As showed in Table 4.1, it began from 2007, and lasted until 2010 or even later. Since our focus is the systemic risk in the bank network, we need to look at the pattern of bank failures during that time.

In Figure 5.1, the top plot shows the interpolated pattern line, based on the daily data of the bank failures. The bottom plot illustrates the pattern for the bank failures, based on monthly data. For our model, we use the monthly data for validation process. As Figure 5.1 shows, even though there were systemic risk in the financial system, the failure pattern does not follow a typical cascading failure pattern which has a very steep slope. The dynamics resemble popping corns[1]. To understand this pop-corn effect, we try to reproduce this empirical pattern with our model, and explain what caused this pattern.

5.3 Systemic Risks in the Network

Before examining results of our model, we need to check initial values of parameters (See Table 5.2) and network statistics. Parameter values for the balance sheet are calibrated by Gai's model. Parameter *outlink* is the maximum outgoing links which a node can have. When a network generates, each node can make a diverse number of outgoing links, but the maximum number is given. This *outlink* is the main independent variable of our simulation experiments. Our model generates 100 different cases of ER and BA networks in every experiment scenario. Each ER network and BA network which our models generate has its

[1]Watch Frank Schweitzer's US Bank Failure video : `https://www.youtube.com/watch?v=o2Budc5N4Eo&ab_channel=futurict`

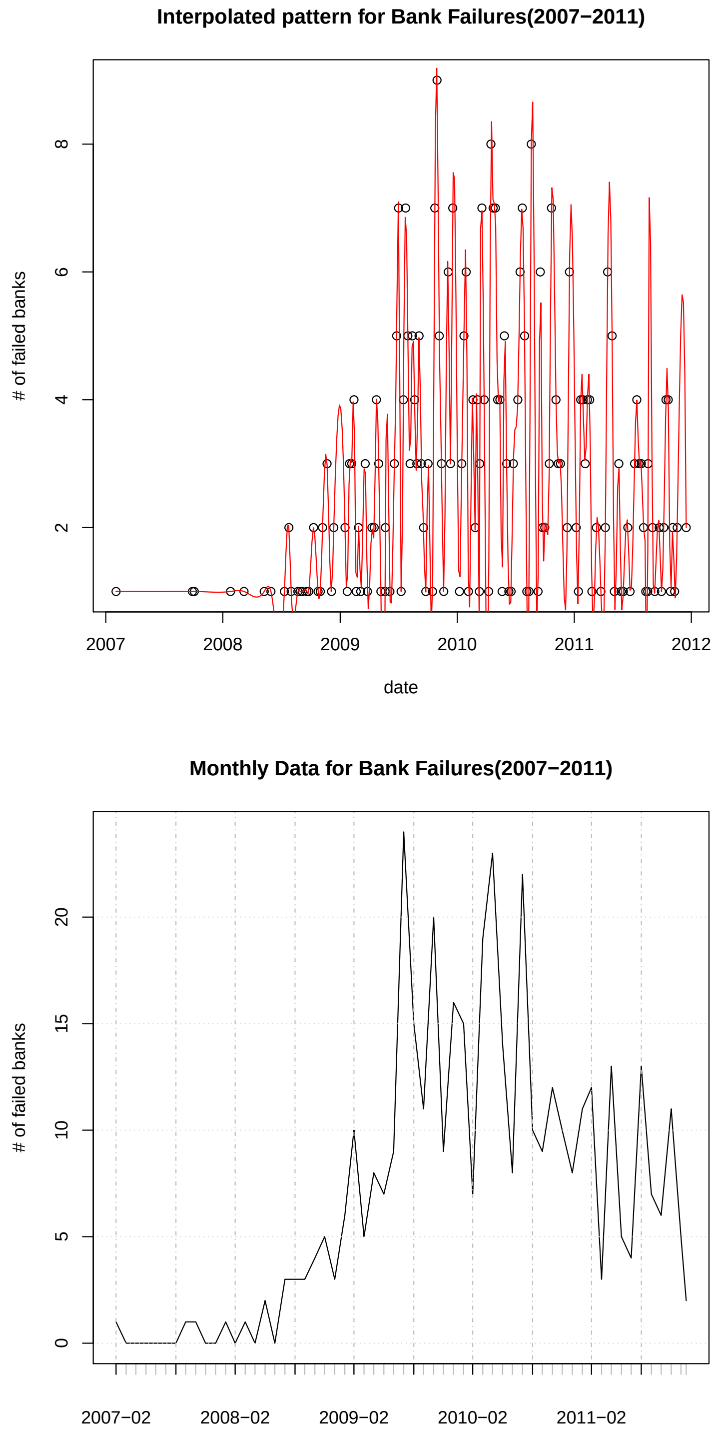

Figure 5.1. Bank Failures (2007-2011). Source: FDIC

Table 5.2. Parameter Values for Model 1

Parameter	value	Description
$nbanks$	500	Number of banks
$outlink$	varies	Maximum number of outgoing links
$network - structure$	BA or ER network	BA network or ER network
A^F	62	Fixed assets
q	1	Weight for A^F
L^D	61	Retail deposit
A^L	2	Fully liquid assets
α	0.15	Weight for $loss$
h	0.1	Aggregate haircut for repo collateral
h_i	0.05	Maximum value of additional haircut
A^{RR}	11	Reverse repo assets
L^R	20	Repo liabilities

own network statistics. In the Appendix A and B, we can check the statistics. In the network statistics, $Maxlink$ means the maximum value of the degree in a network. $Avglink$ refers to the average degree in a network. *Slope* is a line slope of degree distribution in the log-log scale. CC means the clustering coefficient of a network. *Path_length* is the average path length in a network. Hub means the number of hubs in a network. In our model, if a node has seven times more degrees than the average degree, we call it a hub. *Eigenvector* refers to average value for the eigenvector centrality of the hubs. Finally, $Kurtosis$ is the kurtosis value for the degree distribution of a network.

Thus, when each experiment scenario is conducted, our model produces outputs for 100 cases. For example, if our scenarios are from *outlink* 1 to 10 in an experiment, the sample size of the experiment is 1,000.

5.3.1 ER Network

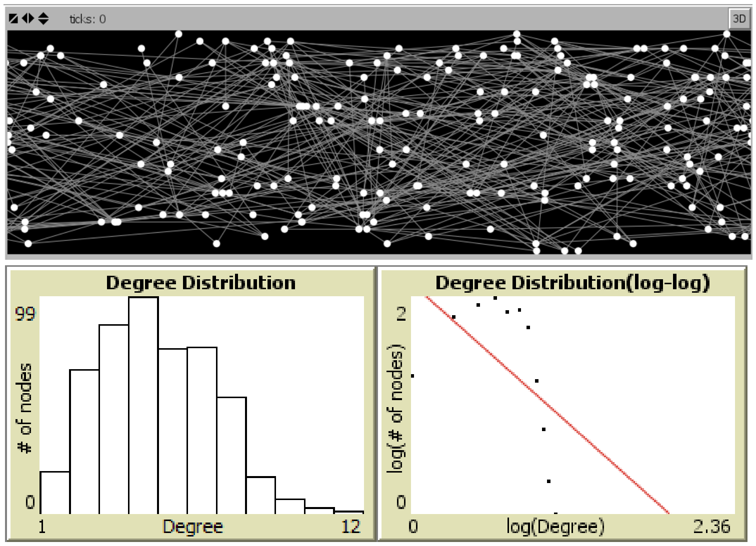

Figure 5.2. ER Network

Let's create a simple financial network in our model (see Figure 5.2). Nodes and links stand for banks and interbank linkages respectively, and the nodes are randomly connected in this model. As explained before, this random network is called an ER network. Thus, the degree distribution of this network follows the Poisson distribution. In Figure 5.2, the bottom panel plots shows the degree distribution. We can identify that it follows the Poisson distribution, and it is not linearly fitted in the log-log scale plot.

To test resilience of the network, our model randomly chooses one bank, and make it insolvent. Then, this failure triggers hoarding liquidity of counter party banks and an increase of repo rate. Thus, the risk spreads to neighboring nodes. This process is called "percolation" (Newman, 2010). We conduct the percolation experiments with different *outlink*s [2].

Figure 5.3 shows the systems of the random networks are very safe. If *outlink* is small, the number of interbank linkages which a bank can have is smaller than those of larger *outlink*

[2]Watch video clips for the model : `https://www.youtube.com/channel/UC8aCUQu3pE3x96QN2HjosHA`

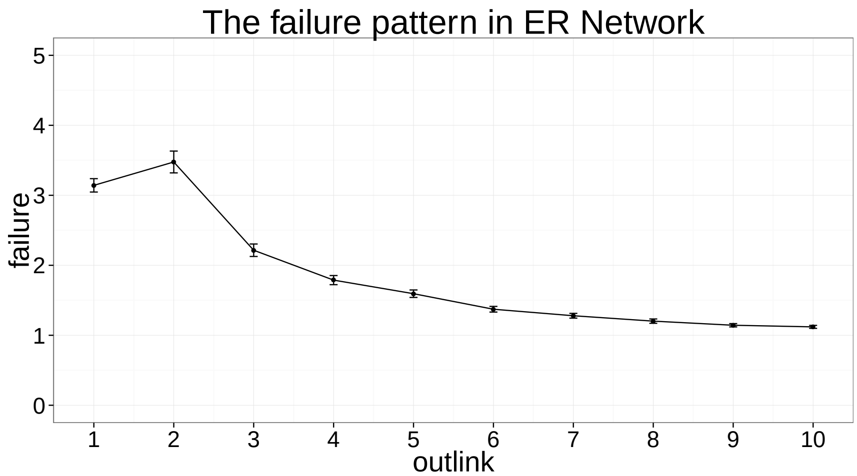

Figure 5.3. Failure pattern in the ER networks

scenarios, because the degrees of nodes heavily depend on *outlink*. If a node has more links, the node can be safer than others. As explained, the decrease rate of $loss_i$ is smaller, because risks are shared. In our model, even when an ER network has a small *outlink*, the risk cannot spread to the entire systems. Thus, the ER networks successfully play their roles as risk-sharing systems. While the ER networks are safe systems, they are not realistic systems. The ER networks are theoretical network models. We can use them as the reference cases. Now, we need to move to a more practical network form.

5.3.2 BA Network: very-rare-but-extremely-dangerous Event

The more practical network form is the BA network. As noted, the algorithm to create a BA network is the preferential attachment. Thus, the possibility of creating hub is very high.

Figure 5.4 illustrates a BA network. There are big blue nodes, which are hubs. A hub has seven times more links than the average degree. The bottom panel plots show the degree distribution of the BA network. We can find the fat-tailed or power-law distribution, and the pattern is linearly fitted, which is the typical property of a BA network.

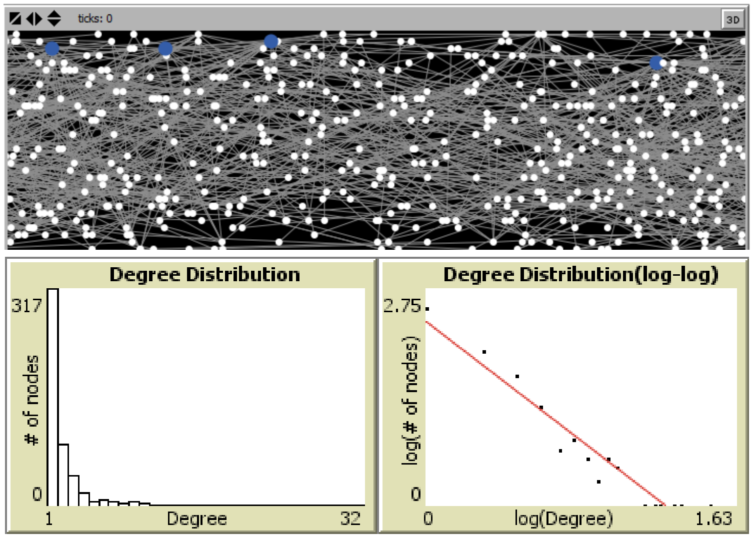

Figure 5.4. BA Network

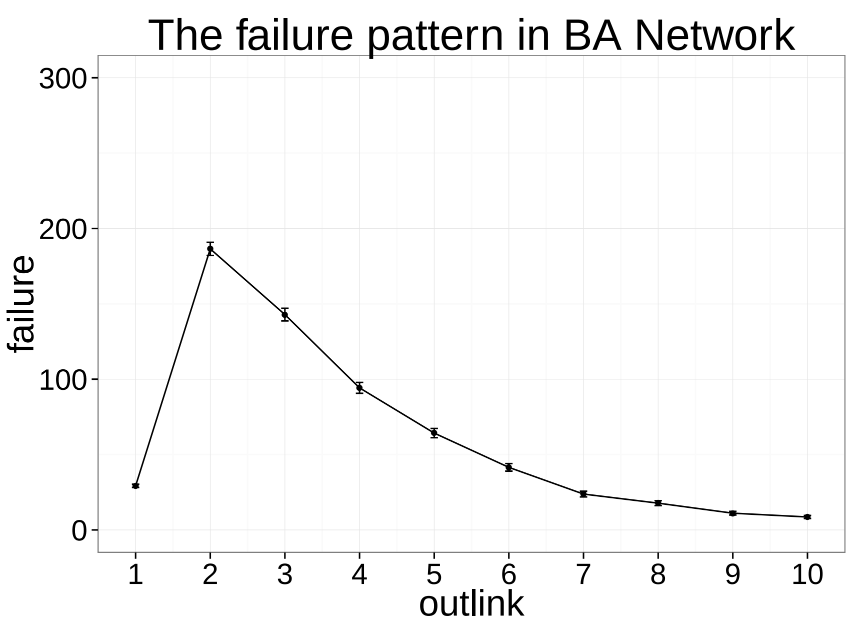

Figure 5.5. Failure Pattern in the BA networks

In the same percolation experiments[3], we find the different results from that of the ER networks (See Figure 5.5). The BA networks are more vulnerable than the ER networks. A single shock spreads to many other nodes. In the case of $outlink = 2$, the number of failure rises to almost 200. As *outlink* increases, the number of failure decreases. In terms of the pattern, the shape is very similar to that of the ER networks. Both are non-linear. But the pattern of the BA networks indicates that they are much more vulnerable when *outlink* is small.

To analyze in more detail, we examine histograms of different *outlink* scenarios. In Figure 5.6, when *outlink* is 1, the failure pattern shows the typical fat-tailed distribution. Mostly the failure sizes are not large, but the large-scale failures are rarely found. Importantly, we find a very different pattern from $outlink = 2$. It is hard to find the middle-scale failures. From $outlink = 2$, there seem to be two kinds of scales in the histograms, such as the large-scale failures and the small-scale failures. It is a typical percolation pattern of the BA networks (Albert et al., 2000; Newman, 2010). It is called a "robust and fragile" network.

More importantly, we want to emphasize the histograms of $outlink$= 7, 8, 9 and 10. In the histograms for those scenarios, there are only two distinct bars. Those systems are very safe, but there are very small possibilities of the extremely large-scale failures in those systems. We investigate the probabilities which over 99 percent of banks fail. The probabilities for *outlink* 1, 2, 3, 4, 5 and 6 are 0%. However, the *outlink* 7, 8, 9, and 10 show 0.01%, 0.08%, 0.05%, and 0.12%, respectively. Although the networks of *outlink* 7, 8, 9, and 10 are very safe, they can face the extremely dangerous events with the tiny probabilities. This can be beyond the typical property of the BA networks, which is "robust and fragile". In the networks of the high *outlink*s, the risks are very rare, allowing us to ignore the probabilities. However once the networks face the risks, the risks can be extremely dangerous, like Dragon kings (Sornette, 2009). This is a reason why existing models failed to predict the 2008 crisis.

[3]Watch video clips for the model : `https://www.youtube.com/channel/UC8aCUQu3pE3x96QN2HjosHA`

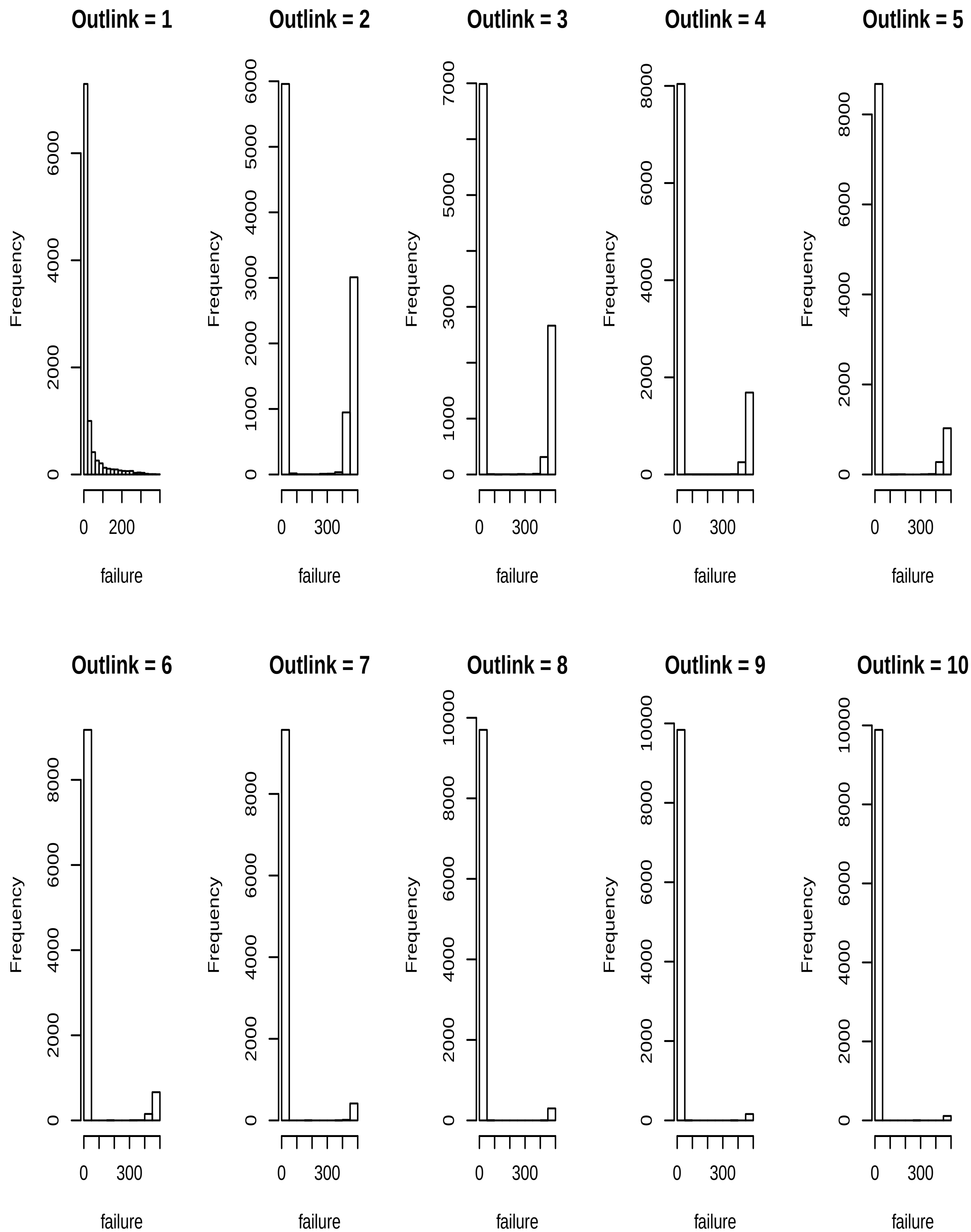

Figure 5.6. Histograms of Failures in the BA Networks

The safer a BA network is, the more likely it can face a very-rare-but-extremely-dangerous event. This paradoxical phenomenon makes a crisis unpredictable in the real world.

Therefore, there are two transition points for phase transitions in our model. The first point is *outlink* 2. After this point, the failures decrease on average, and the networks become "robust and fragile". The second one is *outlink* 7. When *outlink* is 7 or larger, the risks are the very-rare-but-extremely-dangerous events.

The results of the experiments imply that even if one believe that a system is resilient, it can be wrong. Previous data and studies can provide wrong information, because the available information about these rare events is limited. In spite of the small probabilities, the very-rare-but-extremely-dangerous events have been observed in the real world, such as the Great Depression, the 1997 financial crisis, the 2008 financial crisis, and the South Korea MERS outbreak. Therefore, our results suggest the policies which were made in normal times will have a limitation to defend the system against possible attacks of these events.

In the second part of this section, we examine more details of the systemic risks in the BA networks.

5.3.3 Systemic risk and Network Statistics

When nodes are exposed to a default risk, the vulnerability largely depends on a value of *outlink* or the degree. High degrees tend to guarantee to avoid being vulnerable.

Now, we take a look at network statistics of the BA networks in the model.

Figure 5.7 shows correlations between values of the network statistics. All correlation coefficients are significant. As explained, the degrees in the networks heavily depend on *outlink*. Most correlation coefficients show strong relationships between parameters.

To understand relationship between the failure patterns and the network statistics, we create regression models. The regression models have two dependent variables : the number of failures and the probability which over 90 percent of nodes fail. The models are as follows.

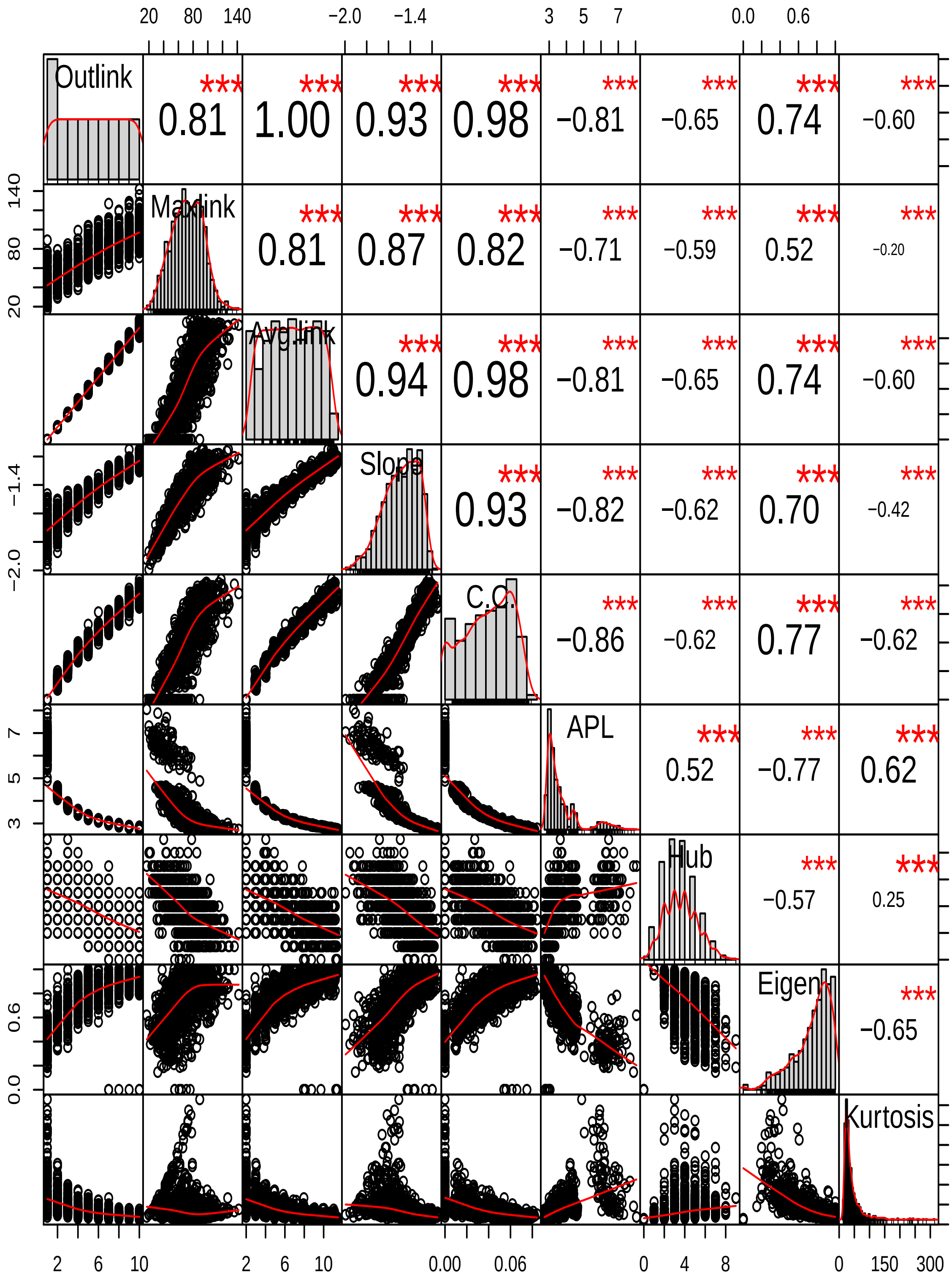

Figure 5.7. Correlations for Network statistics of the BA Networks

1. failed_bank $= \beta_0 + \beta_1 outlink + \beta_2 maxlink + \beta_3 avglink + \beta_4 slope + \beta_5 CC + \beta_6 path\_length + \beta_7 hub + \beta_8 eigenvector + \beta_9 kurtosis$

2. failed_bank $= \beta_0 + \beta_1 CC + \beta_2 path\_length + \beta_3 hub + \beta_4 eigenvector + \beta_5 kurtosis$

3. failed_bank $= \beta_0 + \beta_1^* CC + \beta_2^* path\_length + \beta_3^* hub + \beta_4^* eigenvector + \beta_5^* kurtosis$

4. probability $= \beta_0 + \beta_1 outlink + \beta_2 maxlink + \beta_3 avglink + \beta_4 slope + \beta_5 CC + \beta_6 path\_length + \beta_7 hub + \beta_8 eigenvector + \beta_9 kurtosis$

5. probability $= \beta_0 + \beta_1 CC + \beta_2 path\_length + \beta_3 hub + \beta_4 eigenvector + \beta_5 kurtosis$

6. probability $= \beta_0 + \beta_1^* CC + \beta_2^* path\_length + \beta_3^* hub + \beta_4^* eigenvector + \beta_5^* kurtosis$

The regression models 1 and 4 have all network statistics of our model as the independent variables. However, as Figure 5.7 shows, the models have multicollinearity problems. Thus, we run the regression models with the selected independent variables (Model 2 and 5). The β^*s in Model 3 and 6 refer to the standardized coefficients. Table 5.3 provides the results of the regression models.

From the results of the Model 3 and 6, *outlink*, the clustering coefficients (CC), the average path length (*path_length* or APL), and *hub* are significant for the both dependent variables at 95% confidence interval. Among them, CC and APL have stronger effects on the dependent variables, compared to the other independent variables except *outlink*. Since we want to investigate the failure patterns by the structures of networks, we focus more on CC and APL. From the regression results, we can conclude that as CC and APL are larger, the system is more resilient. To identify this conclusion, we examine all cases of failures. The boxplots (See Appendix C) of the BA networks illustrate the patterns of failures in different cases. Case 54 (Appendix C.3) shows greater resilience, compared to others. In the boxplot for the Case 54, we cannot find any distinct bar which means frequency of failures. Thus, the

Table 5.3. Regression Results

	Dependent variable:					
	failed_bank		*failed_bank*	probability		*probability*
	(1)	(2)	(3)	(4)	(5)	(6)
out_link	−15.440***	−15.718***		−2.543***	−2.622***	
	(0.486)	(0.468)		(0.097)	(0.094)	
maxlink	−0.062			0.008		
	(0.128)			(0.026)		
avglink	−4.790*			−1.348**		
	(2.819)			(0.565)		
slope	−103.621***			−20.346***		
	(26.873)			(5.390)		
C.C.	−795.624**	−2, 131.880***		−118.134*	−412.461***	
	(335.145)	(109.028)		(67.222)	(21.921)	
path_length	−65.385***	−64.024***		−12.248***	−12.225***	
	(2.731)	(2.270)		(0.548)	(0.456)	
hub	2.983***	3.730***		0.453**	0.636***	
	(1.029)	(0.971)		(0.206)	(0.195)	
eigenvector	8.579	6.602		1.786	1.124	
	(10.361)	(10.254)		(2.078)	(2.062)	
kurtosis	0.064	−0.089*		−0.026*	−0.050***	
	(0.067)	(0.046)		(0.013)	(0.009)	
out_link			−0.705***			−0.636***
			(0.021)			(0.023)
C.C.			−0.777***			−0.813***
			(0.040)			(0.043)
path_length			−1.046***			−1.081***
			(0.037)			(0.040)
hub			0.092***			0.085***
			(0.024)			(0.026)
eigenvector			0.021			0.019
			(0.032)			(0.035)
kurtosis			−0.049*			−0.148***
			(0.025)			(0.027)
Constant	279.762***	452.474***	−0.000	49.559***	84.447***	−0.000
	(51.055)	(17.290)	(0.017)	(10.240)	(3.476)	(0.019)
Observations	1,000	1,000	1,000	1,000	1,000	1,000
R^2	0.706	0.696	0.696	0.653	0.640	0.640
Adjusted R^2	0.703	0.694	0.694	0.650	0.638	0.638
Residual Std. Error	34.937 (df = 990)	35.469 (df = 993)	0.553 (df = 993)	7.008 (df = 990)	7.131 (df = 993)	0.602 (df = 993)
F Statistic	263.765*** (df = 9; 990)	378.472*** (df = 6; 993)	378.472*** (df = 6; 993)	207.388*** (df = 9; 990)	294.220*** (df = 6; 993)	294.220*** (df = 6; 993)
Note:						*p<0.1; **p<0.05; ***p<0.01

network of the Case 54 is safer than others on average. But as many outliers shows, it cannot avoid the Dragon kings. Specifically, most cases ordinarily show a large number of failures in the scenarios of $outlink = 2$ and 3, except the Case 54. In terms of CC and APL, the Case 54 has the largest CC and APL in the scenario of $outlink = 2$ (See Appendix B). As for the scenario of $outlink = 3$, only Case 24 has higher CC and APL than those of Case 54. As the boxplots in the Appendix C show, the Case 24 has safe status in the scenario of $outlink = 2$. Thus, we conclude that as a network has higher transitivity and centrality, the network is safer on average. It means that the networks have well connected clusters and efficient connections among nodes. In our model, the Case 54 is transitive and centralized in all scenarios.

5.4 Hidden Spread of Systemic Risk in Multiple Networks

In this section, we model systemic risks in the multiple networks. It is the second part of our models. We want to illustrate that once a resilient network system is exposed to risks of the other network which is interconnected to the former network, the resilience will be frequently threatened. This is because the multiple networks have higher complexity. More importantly, the complexity makes risk patterns more unpredictable. Hence, the systemic risks in the multiple networks will be more unpredictable and dangerous.

5.4.1 Housing Market Model

First of all, we need to model another network which is for the real economy. The other network in our model is the housing market network. This is because the housing market is considered to be one of the main causes of the 2008 financial crisis. We focus on investors in modeling the housing market. The real actors in the market are not houses, but investors.

To model the housing market, we use Thurner's model as the reference model (Thurner, 2011). The model has two main components. One is investors. They sell and buy houses.

The investors are roughly categorized by two groups. The first group are informed investors who are opinion leaders and have information about the true value of houses. Due to this information, they can use leverage from banks to buy more houses. In addition, 10 percent of informed investors are risk-seeking investors. This type of investor makes aggressive investments. The second group is uninformed investors. They do not have enough information. Although they exploit information about the current house price to make decisions, their decisions are partly based on a random factor due to insufficient information about the true value. Thus, they are called "noise investors". Among uninformed investors, some are called "followers". Each investor is a node in the social network of investors. These followers obtain information about other investors' decisions from the social network. After collecting information, they make their decisions by using the information. In every round, all investors have three options : selling, buying, and no-action which is the option when there is no house they want to buy. However, the informed investors can hold their houses until they can obtain profits from transactions. The other component is houses. Suppose all houses have the same true value which is '1'. However, market prices of houses vary.

Market Price Formation

To determine a market price, Thurner (2011) uses a market clearing mechanism, which prices are determined by the demand functions of investors. We modify it for our purpose. The modified equation is as follows :

$$D_{informed}(P_t) + D_{noise}(P_t) + D_{follower}(P_t) = N$$

$D(P_t)$ means the demand of investors, and N is the number of houses. Thus, the price(P_t) depends on this market clearing equation. If investors want to obtain more houses, the equation indicates prices will increase.

Table 5.4. Parameter Values for Model 2

Parameter	value	Description
#houses	150	Number of houses
ninvestors	150	Number of investors
informed(%)	10	Proportion of informed investors
noise(%)	60	Proportion of noise investors
leverage-ratio	varies	Maximum leverage
financial-cost	0.01	Cost for using leverage
discount-rate	0.27	Discount rate in making a margin call
volatility	0.3	Weight for the volatility random variable
ρ	0.99	Coefficient of AR(1)

Informed Investor

Assume the informed investors know the true price of houses. Thus, their demand depends on a mispricing signal(mp).

$$mp = V - P_t - \text{financial-cost}$$

V is the true price, and financial-cost refers to the cost for using leverage. If mp of a house is positive, it means that the house is under-priced. Since the informed investors believe the price will increase, they want to buy it. After the price increase to a certain price which is beyond the purchase price, the informed investor will sell it. On the other hand, when mp is negative, the informed investors do not buy the house. When informed investors find the houses which have positive mp, they want to buy as many houses as they can. For this, they will borrow money from banks, which is called “leverage”. Each informed investor can have three leverage providers in the model. If the investors are the risk-seeking type, they can use the maximum leverage to buy many houses. Others will use half maximum leverage. If an informed investor using leverage makes a loss in the housing market, the loss will directly affect the balance sheets of the leverage providers, that is, banks.

Noise Investor

Basically, this group makes its demand based on the current price. However, their decisions are partly based on a random distribution, because they do not know the true value of houses. In addition, since all uninformed investors cannot have sufficient information, they do not hold their houses for more than one round.

$$P_{i,t+1} = \rho \cdot P_t + volatility \cdot \chi_i + (1 - \rho)$$

This equation is for the expected price in period $t + 1$ for the noise investors. ρ and *volatility* are determined between 0 and 1. χ is a random variable, following $N(0, 1)$. Thus, this equation is an AR(1) model. Since ρ is determined below 1, this AR(1) model is stable. When P_t is the true value, we can also expect the true value in $t + 1$ on average. If P_{t+1} is higher than P_t, the noise investors want to buy the house, because they expect the prices will go up in $t + 1$.

Follower

This group has a simpler behavior rule. In the network of investors, the followers collect information about others' decisions and purchase prices. Then, they determine their purchase prices. A follower tries to buy a house if a majority of his friends buys houses. The follower's price for a house depends on the average price of the follower's friends in the social network which is a random network. In addition, their demands partly depend on a random factor because they are also uninformed investors. A follower's price function is as follows.

$$P_{follower_i} = average(P_j) + volatility \cdot \chi_i$$

Leverage

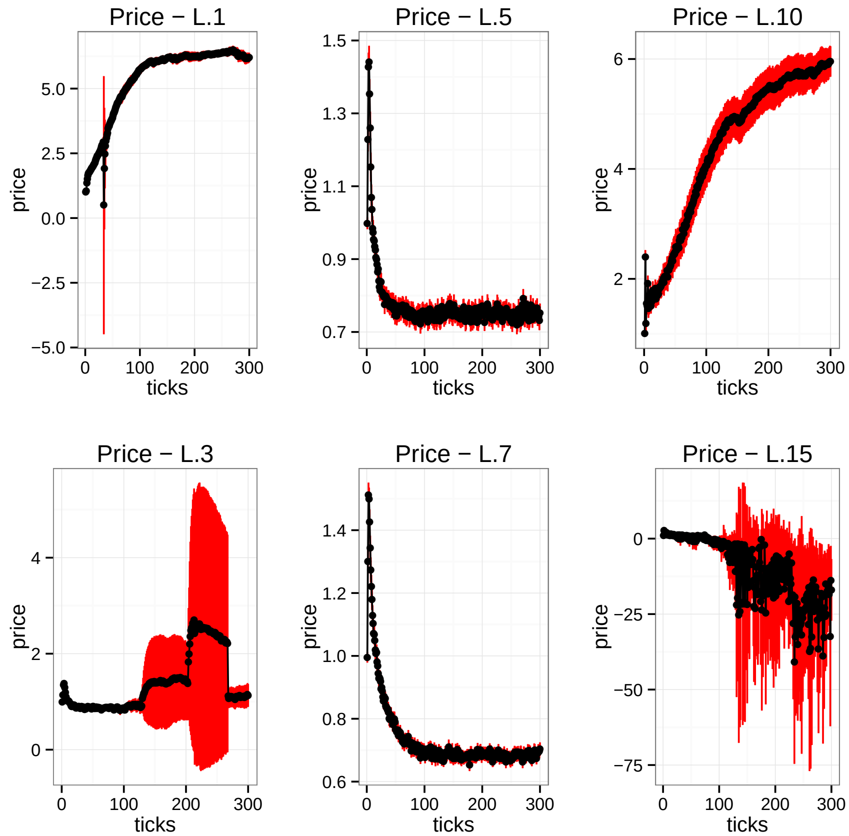

Figure 5.8. House price time series with different leverage

If an informed investor uses leverage 10, he or she can buy 10 times more houses than the number of houses an uninformed investor can buy in the model. Thus, demand increases and the purchase price also increases. We assume the number of houses each uninformed investor can buy is one. Thus, the informed investor can buy 10 houses in this example. The excessive leverage is considered as a major cause of volatility of housing market. This is because the excessive leverage allows investors to make speculative investments. These investments can generate bubbles in the housing market. We try to reproduce the volatile housing market in our model. As explained earlier, the risk-seeking informed investor can use maximum leverage. When they use the maximum leverage, if the prices of houses fall, they will make losses. The losses directly affect the balance sheets of the leverage providers. Then the leverage providers force the borrowers to sell their houses at cheap prices to repay the loans. It is called "making a margin call". In our model, a parameter 'discount-rate' is used to determine the house prices in this margin call process.

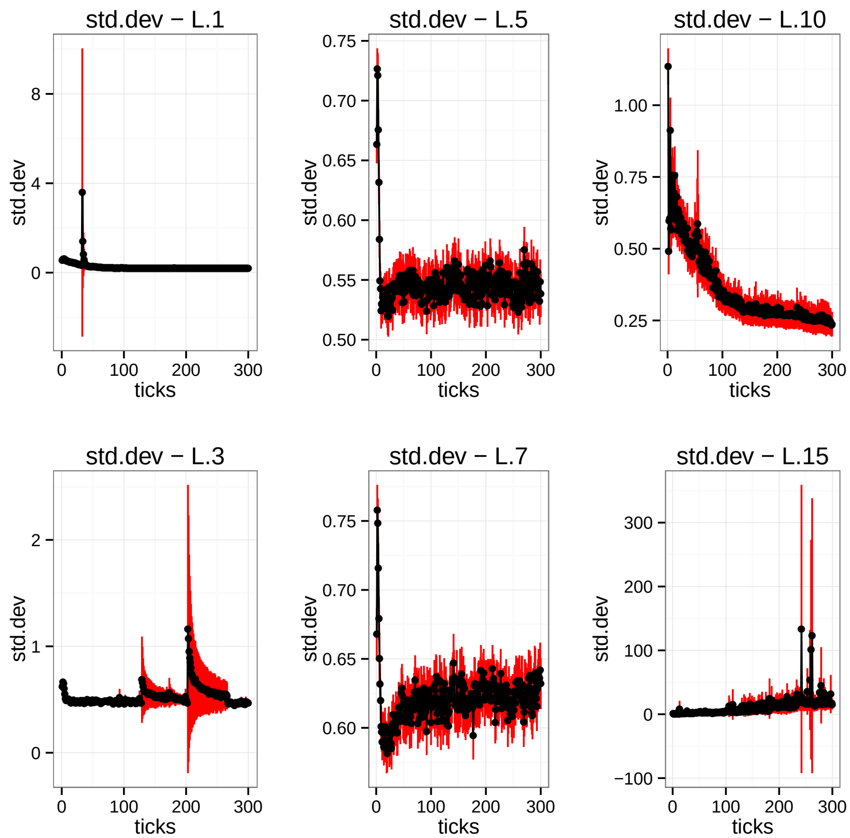

Figure 5.9. Standard deviation time series with different leverage

To construct the housing market model, we use parameters which are shown in the Table 5.4. The number of houses and that of investors are same, because we use the standard market clearing mechanism. Although the leverage is 1, all houses can be consumed. The discount-rate is calibrated by the empirical study (Shleifer and Vishny, 2010).

Figure 5.8 and 5.9 show the volatility of the housing market. We use six levels of leverage, such as 1, 3, 5, 7, 10 and 15. We assume that the level 15 is the excessive leverage. In the plots of prices, we can find the sharp fluctuation in leverage 15. The standard deviation of the house prices is the measure of volatility in the market. In Figure 5.9, when the leverage is 15, the standard deviation is much larger than others. It implies that the market is highly volatile.

To model the financial crisis, we use the highly volatile market status to reproduce the situation of the real housing market in the crisis period.

5.4.2 Multiple Networks

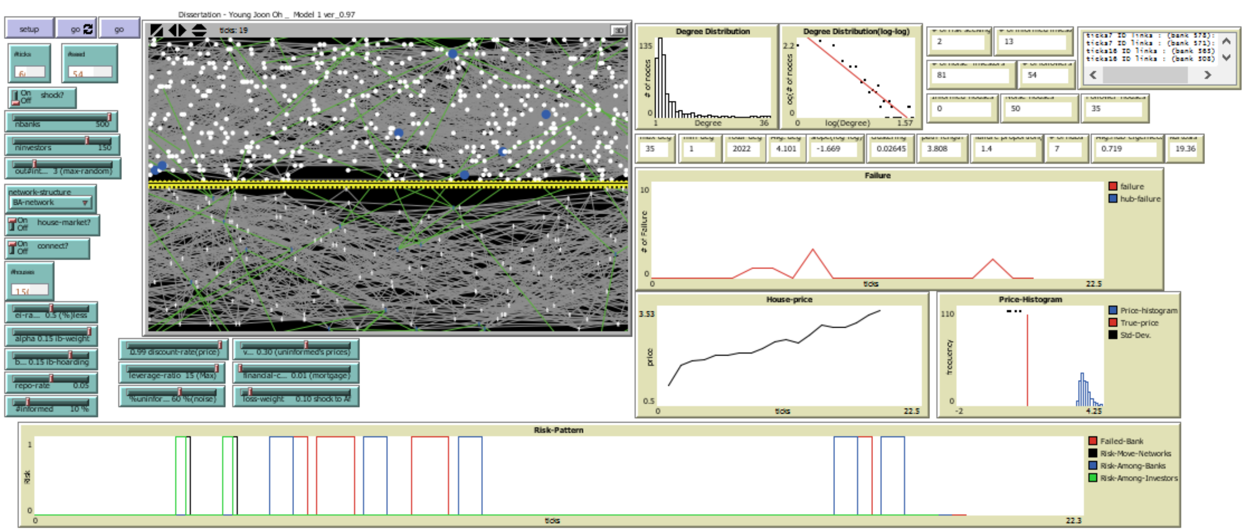

Figure 5.10. Hidden Spread of Systemic Risk Model

For the multiple networks model, we combine the two models : the BA network model and the housing market model. Since we assume that policy makers design a safe bank network, the multiple networks model uses the safest BA network (Case 54). As for the housing market, we use the most volatile housing market, using the leverage 15.

In the multiple networks model, if informed investors, using the maximum leverage make losses in the housing market, the losses affect illiquid assets (A^F) of the leverage providers. In other words, the parameter q decreases. Now, all leverage providers are exposed to the risks from the housing market. In addition, if a bank suffers losses from the housing market, the bank reduces amount of the leverage, which can cause a fall in house prices. If a bank reduces its leverage, the maximum leverage the users can exploit goes down, and the demands decrease. If all leverage providers of an informed investor fail, the investor should sell his houses at cheap prices. Thus, risks can move around the two networks. This feature of the multiple networks increases the complexity of the system.

Figure 5.10 is the multiple networks model, which is called the hidden spread of systemic risk model [4]. The main window is divided into two parts. The top window is the bank network, and the bottom window is the social network of investors. In the social network, informed investors tend to have relatively more degrees. The yellow line consists of houses. In fact, the model focuses on the interconnectedness between the bank network and housing market network. The investors are bridges between the two networks. The prices of houses are determined by investors, and the house prices and banks are interconnected by investors.

Figure 5.11 illustrates histograms of failures in the multiple networks. We can find greater vulnerability in the all scenarios of *outlink*, compared to the result of a single network. Now, the large-scale failures are the most frequent events in the results and we cannot find a consistent pattern. The network systems are not safe and the very-rare-but-extremely-dangerous events are not rare anymore. Thus, the high complexity of the multiple networks makes the network systems more vulnerable. In addition, the inconsistent pattern implies there are various phase transitions (Baxter et al., 2014). Once a multiple networks system is exposed to risks, it is hard to find a certain condition to keep it safe.

Figure 5.12 provides failure patterns over time. In the higher *outlink*, we can find a little bit steep slope in the patterns. But they show the similar patterns in general. The plots show their peaks at around 20 or 30 ticks. To analyze the actual data, we use these simulated time-series data.

[4]Watch video clips for the model : `https://www.youtube.com/channel/UC8aCUQu3pE3x96QN2HjosHA`

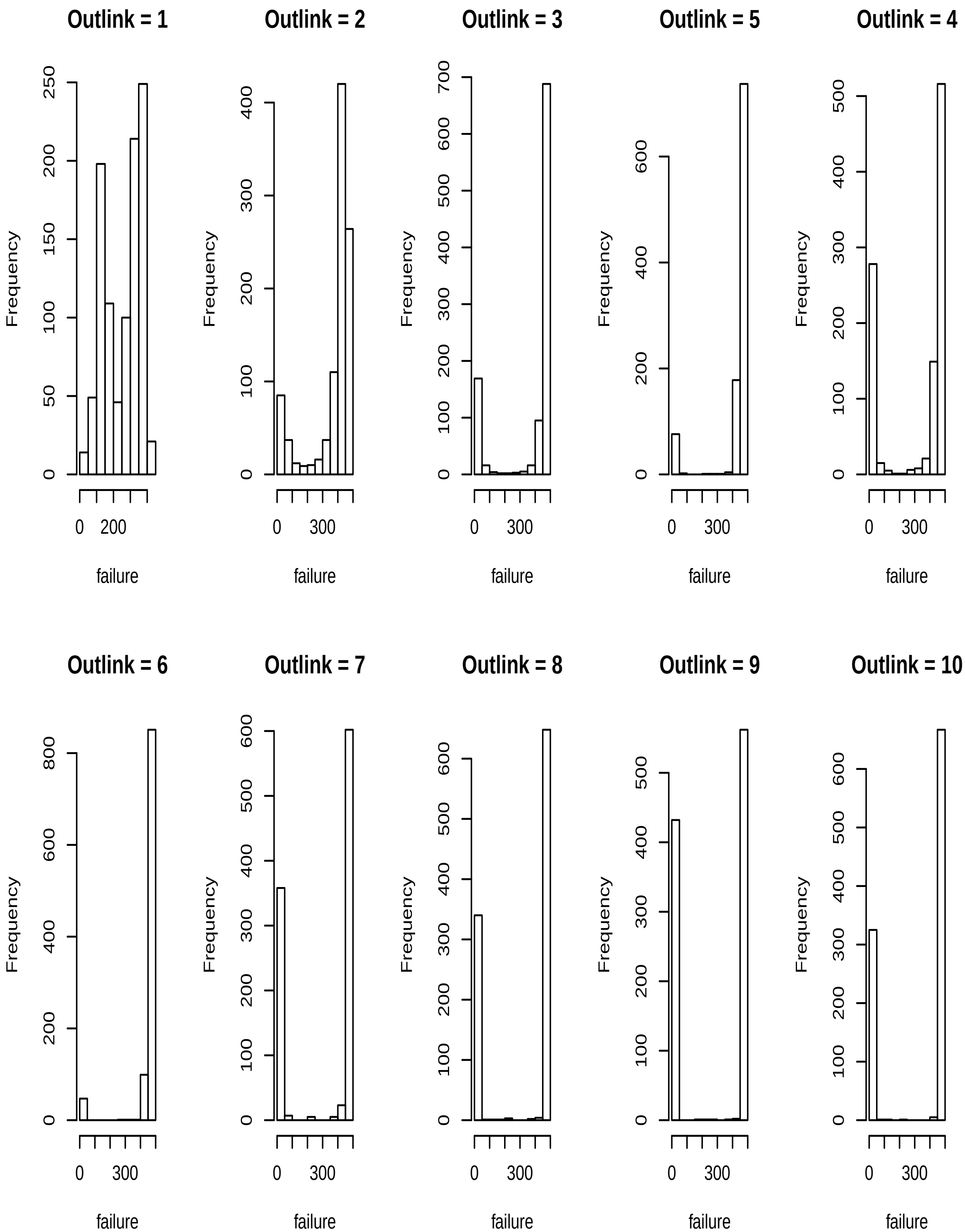

Figure 5.11. Histograms of Failures in the multiple networks

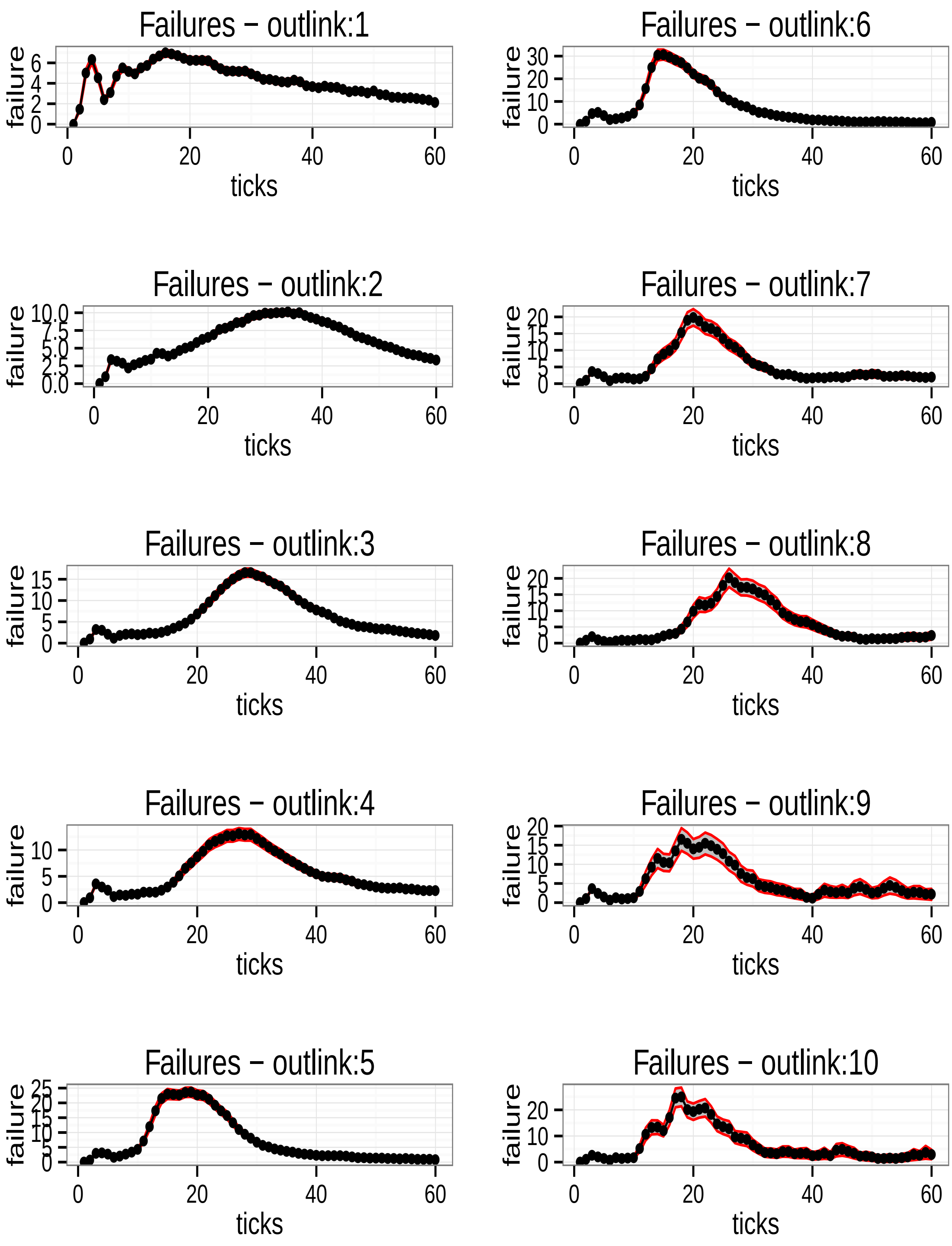

Figure 5.12. Failure patterns in the Multiple Networks

5.4.3 Empirical Validation

To validate the model, we use the Kolmogorov-Smirnov test. This test determines if the distributions of our simulated data are consistent with that of the actual data.

Table 5.5. Result of Kolmogorov-Smirnov test

outlink	D	p
1	0.47458	3.031e-06
2	0.28983	0.01351
3	0.23785	0.06906
4	0.23785	0.06906
5	0.2096	0.1464
6	0.2096	0.1464
7	0.31158	0.006202
8	0.26158	0.03412
9	0.2596	0.03628
10	0.2378	0.06906

In the Kolmogorov-Smirnov test, D is the test statistic. Since we want to find a scenario for which the two distributions are consistent, we need a p value which is larger than 0.05. From Table 5.5, *outlink* 3, 4, 5, 6 and 10 meet the criterion. Thus, the failure patterns of these scenarios are consistent with the actual data pattern. For more specific validation, we make the graphical comparisons.

In our model, one tick refers to one month of the real world. Figure 5.13 shows the failure patterns of actual data and those of the simulated data which pass the Kolmogorov-Smirnov test. The black dots are the monthly data for bank failures, and the black line stands for the fitted curve of the monthly data. As noted before, the scenarios with high *outlink* show

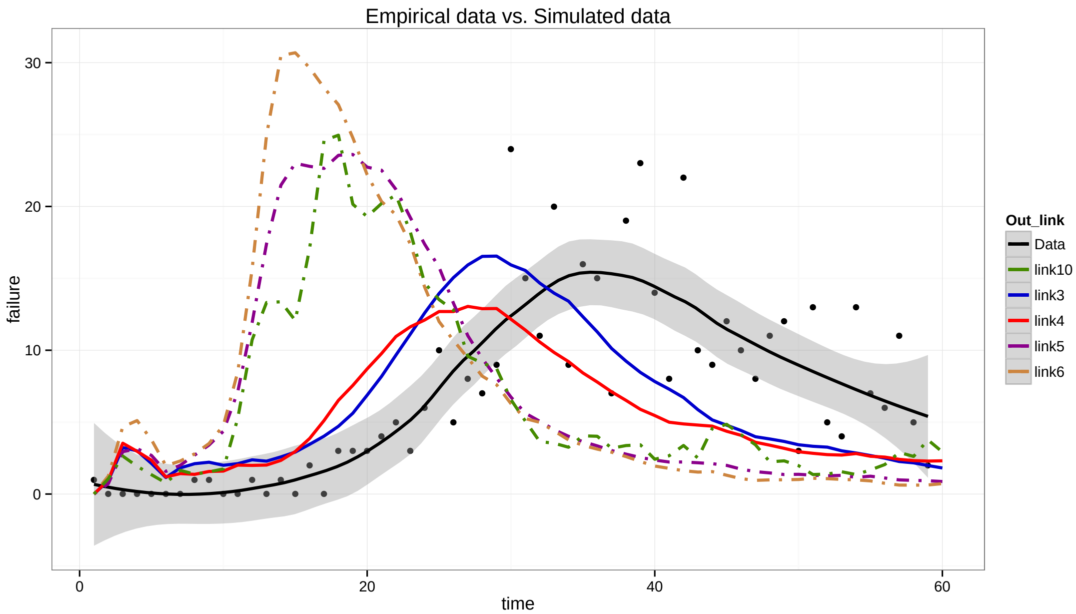

Figure 5.13. Validation

steeper slopes. The solid blue and red lines have very similar patterns to that of actual data. Among them, we choose the blue solid line which is for $outlink = 3$, because the blue line is more similar to the black line, compared to the red line. Now, the validated final model has three properties as follows : The BA network (Case 54), the housing market model with $leverage$ 15, and $outlink = 3$. In other words, the single bank network is relatively resilient and each node can have the maximum three outgoing links in the bank network, and the housing market is volatile.

Now, we investigate the failure pattern which the validated model produces. Figure 5.14 illustrates a result that the validated model produces. The red line illustrates the failures of banks. The figure also includes the result of the risk-pattern plot in the model. The wide grey lines mean the risk movements between the two networks. The blue lines refer to risk spread in the bank network. The green dashed lines mean that risk spread in the housing market. At first, a risk spreads in the real economy. Once the risk moves to the

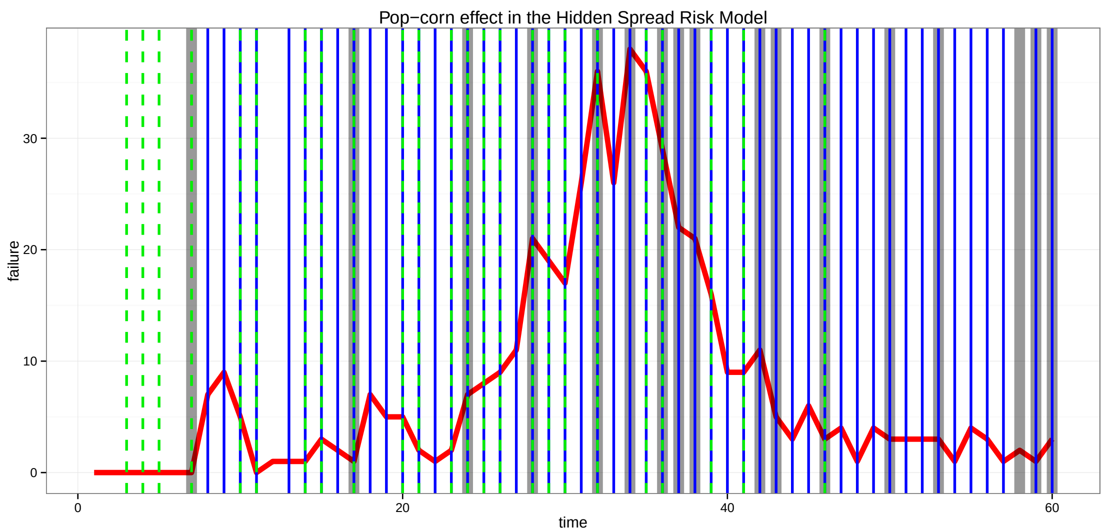

Figure 5.14. Risk Movements

bank network, the risk in the bank network begins to spread to other banks. But the first impact (the first grey line) of the shock from the housing market is not serious. While the risk is diffusing in the bank network, another risk also spreads in the real economy. It is not only because of volatility of the housing market, but because of a margin call by the leverage providers. After the second impact (the second grey line) of the shock, the risks in the bank network and those from the housing market make the failure pattern more complicated. The wide grey lines are located around peaks of the red line. When risk movements occur, the failure patterns change. As the frequency of the grey line increases, the number of failures also increases. Therefore, the frequency and the locations of the grey lines make a contribution to form this bank failure pattern. Since the pattern resembles the real data pattern, we can reach our conclusion with the result of our simulation model.

During the crisis, risk begins to spread in the housing market due to excessive leverage. Then, the risk moves to the bank network, and back to the housing market. At the same time, the risks are also transmitted to other agents in each network. The risk spread in each network causes another risk movement between networks. A node in one network can be attacked by a risk which is hidden in the other network. The attack creates other risk movements in the multiple networks, like ping pong.

Finally, the risk spread in each network and the risk movements between the networks create the pop-corn effect which we observed in the real world.

5.5 Implications

From our simulation models, we understand the underlying dynamics of a crisis. First of all, in the single BA network systems, there are two transition points. One is *outlink* 2. From this point, the BA networks show the typical percolation pattern, which is called "robust and fragile". The other one is *outlink* 7. After this point, we can find the very-rare-but-extremely-dangerous events. They are called "Dragon kings". The systems are very safe but they may face extremely dangerous events with small probabilities. Policy makers do not have sufficient information about these events. Even if the policy makers create a very resilient system with previous data, the resilience of the system may be threatened by an extremely dangerous event. The safer network systems are, the more likely they can face the Dragon kings.

Secondly, occurrence of the large-scale failure depends on network properties, such as transitivity and centrality. If a network is highly transitive and centralized, the network can be safe on average. Therefore, if policy makers create a network system with high transitivity and centrality, the system will be more resilient than others, although they may not avoid the Dragon kings.

Finally, if interdependent networks are exposed to risks, the system will be more vulnerable and the failure pattern will be more unpredictable. The large-scale failures are not rare in the multiple networks. One may predict a typical cascading failure due to systemic risks, but it can be wrong due to the high complexity. The risk movements between networks influence the risk pattern in complicated ways, and create diverse phase transitions. As our model shows, risks can spread in each individual network and they can move between networks. In this situation, the risk patterns are more unpredictable. We may not realize risks, because they are hidden in another network. But the hidden risks can attack a node in our network. These risk movements produce the pop-corn effect of the real world.

Consequently, the 2008 financial crisis is a Dragon king. It can be born only in a safe system. Its probability is so small that many economists fail to predict it, and it is extremely dangerous. Furthermore, high complexity can make the Dragon king real. Once the interdependent networks are exposed to risks, the system becomes much more vulnerable. Due to the high complexity of the multiple networks, the risk spread pattern shows the pop-corn effect, rather than the typical pattern of the cascading failures. In fact, the pop-corn effect in the real world illustrates how the risk pattern is unpredictable. It is difficult to predict which corn will pop, how many kernels will pop, and how long the popping process lasts. Therefore, we need to devote more effort to understand the Dragon kings in multiple networks.

CHAPTER 6

PRISONER'S DILEMMA OF THE SLUGGISH RECOVERY

The recovery following the 2008 financial crisis was disappointing. While the FRB announced that the economy was recovering in August 2009, the unemployment rate rose to 9.7% in the month following the announcement.

Table 6.1. Employment Growth After Recessions (Dwyer and Lothian, 2011). Source: U.S. Bureau of Labor Statistics, National Bureau of Economic Research

Recession		Duration	% change from peak employment				
Start	End	Months	1yr	2yrs	3yrs	3.5yrs	3.5+
Nov. 1948	Oct. 1949	11	-1.5	1.2	3.0	2.5	2.4
Jul. 1953	May 1954	10	-2.1	2.7	4.6	5.1	5.0
Aug. 1957	Apr. 1958	8	-2.8	0.7	2.1	1.9	1.4
Apr. 1960	Feb. 1961	10	-0.9	1.0	2.4	3.3	4.1
Dec. 1969	Nov. 1970	11	0.1	2.8	5.6	8.3	9.6
Nov. 1973	Mar. 1975	16	-0.3	0.3	3.9	6.4	7.7
Jan. 1980	Jul. 1980	6	0.2	-0.2	-0.9	1.6	3.0
Jul. 1981	Nov. 1982	16	-1.2	0.5	4.7	5.6	6.2
Jul. 1990	Mar. 1991	8	-1.1	-0.5	1.1	2.1	2.8
Mar. 2001	Nov. 2001	8	-1.2	-0.3	0.5	1.2	1.8
Dec. 2007	Jun. 2009	18	-1.7	-5.5	-5.2	-4.6	-4.5
Avg. without 2007-09		10.4	-1.1	0.8	2.7	3.8	4.4

Table 6.1 shows the employment growth after the start of recessions since World War II. The five columns in the right side indicate the percentage changes from the maximum

employment during recessions. The recovery after the 2008 financial crisis is the slowest one in the table. In other words, the period of recession is longer than others. Empirically, the recoveries tend to be slow after financial crises in many countries (Reinhart and Rogoff, 2009). Now, a natural question is raised. What caused the slow recovery? In this chapter, we propose a possible answer to it.

6.1 Uncertainty, Crisis, and Recovery

As Blanchard said that “crises feed uncertainty. And uncertainty affects behavior, which feeds the crisis” (Blanchard, 2009), crisis and uncertainty are closely associated. Although uncertainty is not a major cause for a crisis, once uncertainty increases, the uncertainty significantly affects crisis and recovery. An empirical study of Russia by Ananyev and Guriev(2015) shows how the financial crisis in Russia destroyed social capital, such as trust and norms and the restoration was very slow (Ananyev and Guriev, 2015). After the economic crisis in 2009, the income decline in Russia led to the significant destruction of trust and norms, which meant there was high uncertainty in the society and markets. Although the crisis was over, the destroyed trust was not restored at the pre-crisis level. Thus, once the uncertainty increases by a crisis, it can last longer than we expect. More importantly, high uncertainty in the society and markets can threaten stable economic growth. Many studies argue that the social capital or trust has a significant influence on economic growth (Woolcock, 1998; Bjørnskov, 2012; Knack, 2003; Algan and Cahuc, 2013). Thus, if the social capital is destroyed and uncertainty increases, this will adversely affect economic performance.

In the business cycle, there is a meaningful relationship between economic performance and uncertainty. Uncertainty is strongly countercyclical in all levels of economy. Especially, uncertainty is associated with slow recovery in the industry level. Under high uncertainty situation, firms tend to be cautious to make new investments, and this behavior leads to the low level of employment rate (Bloom, 2009; Bloom et al., 2012). In good times, economic agents in the markets can use a lot of information. But during a crisis, the economic agents suffer from scarce information. Thus, this circumstance makes agents' activities restricted and sluggish. The reactions to the governmental policies are also delayed. Consequently, economic activities heavily depend on the level of uncertainty (Veldkamp, 2005). Along the same line, an agent in a market is not only an information consumer, but a learner. In normal times, more production creates more information about the market. The agent can use precise information to make his decision, and he can engage in more economic activities. As a result, the more production, the more investments the agent can make. However, in bad times, noisy information is generated rather than precise information. Noisy information impedes agents' learning process in the market, and agents are reluctant to take risks of engaging in economic activities and investments. It leads to slow economic growth and recovery (Van Nieuwerburgh and Veldkamp, 2006). The noisy information can cause volatility of asset prices which is associated with countercyclical factors. Since agents' decisions cannot be based on precise information, a small change in the asset market can cause herd behavior of agents, and the asset market becomes more unstable (Bekaert and Wu, 2000). Thus, uncertainty shrinks economic activities.

Managerial risk aversion affects investment decisions of firms. When managers face high uncertainty of markets, they try to mitigate losses, and adopt a cautious stance to investments (Panousi and Papanikolaou, 2012). In particular, financial constraints strongly discourage investments. Under financial constraints, managers need to increase external finance costs to overcome the constraints. Hence, even risk-neutral managers tend to make risk-aversion decisions (Froot et al., 1993). Under high uncertainty, it is hard to expect that firms make aggressive investments and hire more employees.

The slow recovery can be attributed to high uncertainty about economic policy after the financial crisis. The index of economic policy uncertainty of Baker et al.(2012) shows that policy uncertainty tends to increase and then fall back down after a shock to the economy.

However, the high level of policy uncertainty lasted long after the 2008 financial crisis. When the fiscal stimulus packages and monetary policies were announced, the policy uncertainty increased even higher (Baker et al., 2012). After the financial crisis, economic agents began to worry about financial instability and additional regulations, sovereign debt, and currency issues. When the government announced policies for recovery, the policies escalated concern about interest rates and taxes, and the policy uncertainty stayed at high level. Thus, this policy uncertainty can discourage economic activities, even though the aim of policies is the encouragement of economic growth.

The studies we examine have one common factor. The policies for recovery cannot work well under high uncertainty. If the social capital is restored, we can expect better economic performance. However, once uncertainty increases dramatically, it is difficult to restore trust or norms (Ananyev and Guriev, 2015). Trust and norms are considered as the outcome of the cooperation of agents (Fehr and Fischbacher, 2004). Therefore, cooperation can be a key to reducing uncertainty. If economic agents cooperate with each other to increase employment and investments, rather than hoard money, the economy can be stimulated. In response to the investments, households increase their consumption. This behavior sequence reduces uncertainty about the markets, and it leads to economic recovery.

Most importantly, however, it is difficult to expect active cooperation after a financial crisis. This is the problem we try to solve in this chapter. In the next sections, we suggest our Prisoner's dilemma game model to answer our question : Why is it hard to promote cooperation which can stimulate the recovery?

6.2 Prisoner's Dilemma Game

To model cooperation under uncertainty, we use Prisoner's Dilemma game (PD game). The PD game has two players. They are suspects in a major crime. But the prosecutor does not have enough evidence to convict them. Each player has two strategies : cooperation and defection. Cooperation means that a subject keeps silent. When the two subjects choose cooperation, they will be convicted of the minor offense. Defection implies that a subject betrays the other one. When only one player chooses defection, the betrayer is freed, and the other subject will be convicted of the major crime. Obviously, cooperation is the best option for both players, but they choose defection. It is why this game is called Prisoner's Dilemma (Osborne, 2004). In a non-iterated PD game, we cannot expect cooperation from the two players. But the iterated PD game can produce a different outcome. In this case, a player can remember the other's strategies in the previous rounds, and exploit his memory. Thus, a betrayer can be punished. If we assume N players, rather than two players, the players can share and update their memories. Therefore, in an iterated N-person PD game, cooperation can be a dominant strategy (Beaufils et al., 1998; Harrington, 2009).

Furthermore, the PD game can be applied to players with bounded rationality. It is called the evolutionary game theory. In this game, players are not aware of all information of the game, and the decisions of players depend on the interactions of players. In every round of the game, a player learns others' strategies, and adopts them. Although the players have bounded rationality, the repeated interactions can produce cooperation (Axelrod, 1987, 1981; Easley and Kleinberg, 2010).

In the real world, our decision-making occurs in the given social context, and we repeatedly play the similar games. In addition, an agent cannot exploit all information of the games in the society. Thus, a proper approach for the games in the real society can be the evolutionary game in a network. The network provides the players with the structured interaction environments. A player's strategy is affected by interactions with other nodes in a network. Then the player's strategy is adapted by changes in the structure of the network. It is considered as an evolution process in the game (Lazer and Friedman, 2006; Fu et al., 2007; Kim et al., 2002; Abramson and Kuperman, 2001; Szolnoki et al., 2008). Our model is based on the evolutionary PD game in the network.

6.3 Evolutionary Prisoner's Dilemma Game in a Network

Initially, each agent has two neighbors and two links in the model. In every round, an agent plays the PD games with the neighbors, connected by links. An agent has two strategies, which are cooperation (C) and defection (D).

Table 6.2. Basic payoff matrix

	C	D
C	R,R	S,T
D	T,S	P,P

T=1, R=0.9, P=0.3, S=0 (Alexander, 2007)

In the first round, an agent randomly chooses one of the strategies, and obtains a payoff. In the second round, the agent compares the neighbors' strategies, and imitates the best strategy of its neighbors. If the agent's payoff is the highest one, he keeps his strategy in the next round.

Table 6.2 shows the basic payoffs for this PD game. The basic payoff follows the typical two-person PD game payoff condition, which is T > R > P > S[1]. For our prisoner's dilemma game model, we add one more payoff structure of Alexander (2007) to the initial one.

$$\text{Cooperator's payoff}: \; mp + c_i$$

$$\text{Defector's payoff}: \; mp + d_i$$

These payoffs are for a multiplayer game. Each player plays two-person PD games and multiplayer games, because a player is a member of a group in a network. Here, m means

[1] T, R, P, and S stand for Temptation, Reward, Punishment, and Sucker, respectively.

the increase rate of payoffs as the proportion of cooperators in the group increases. p denotes the proportion of cooperators in the group. Also, c_i is the payoff limit of cooperators in the case of that the proportion of cooperators in the group is zero. As for the defector's payoff, d_i means the payoff limit of defectors in the case of the proportion of cooperators in the group approaches zero. Under this payoff structure, the minimal condition of cooperation is $d_i \leq m + c_i$. It means that when all players cooperate, the payoffs of cooperators should be greater than or equal to the payoff limit of defectors (Alexander, 2007).

In addition, an agent does not always imitate the best strategy. With 5 percent probability, he can choose his own strategy. In this case, his random choice follows the Poisson distribution, like the initial round of the game.

Table 6.3. Parameters for ABM PD game model

Parameter	value	Description
num-nodes	80	Number of players
mutation	5	% for random strategy
lim_co	0	c_i
lim_de	0.25	d_i
rate_coop	0.5	m
p	varies	p
weight	$\frac{1}{2.5} \cdot e$	Weight for economies of scale

Table 6.3 shows the initial parameter values. Basically, they are calibrated by Alexander(2007)'s model. In the model, we consider economies of scale for cooperators. Thus, the payoffs of cooperators nonlinearly increase. The weighted cooperator's payoff is as follows : $\frac{1}{2.5} \cdot e^{mp} + c_i$.

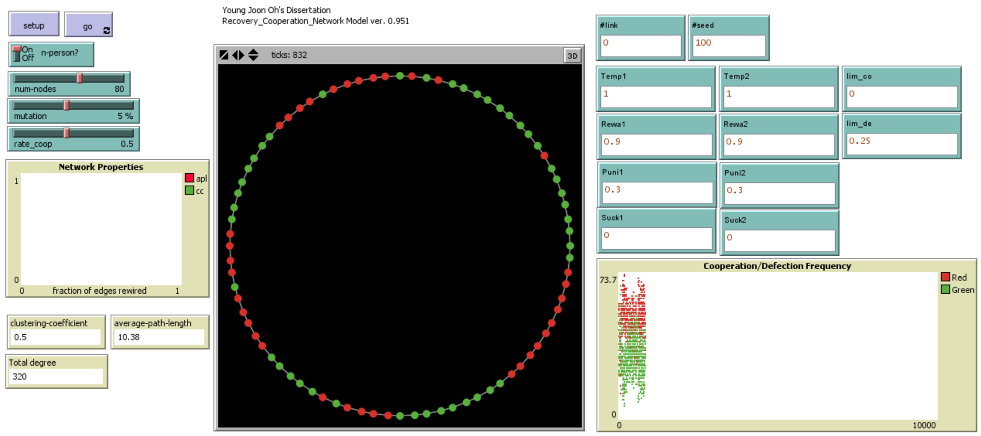

Figure 6.1. Agent-Based Network PD Game Model

Figure 6.1 illustrates our PD game model [2]. Initially, the network is a regular network. It has a circular shape, and each node has two links from its both sides. An agent is a member in the small community which consists of the agent and two neighbors. His strategy and payoffs heavily rely on other nodes' strategies of the network. In every round, a player plays three games, which consist of two two-person PD games and one multiplayer PD game. Thus, the player plays a two-person PD game with each neighbor, and then he plays a multiplayer PD game with the neighbors. If an agent and his neighbors choose cooperation strategies, the agent's payoff will be $0.9 + 0.9 + 0.66 = 2.46$. If two neighbors choose cooperation and the agent chooses defection, his payoff will be $1 + 1 + 0.81 = 2.81$. However, strictly speaking, an agent plays three different multiplayer games in every round, because the neighbors' strategies are the outcomes of their own multiplayer PD games.

To investigate the results of the PD games with different network structures, we rewire ten links in each experiment. It means the nodes are reconnected to other nodes which are randomly chosen. This is the algorithm to create a small-world network. As explained

[2]Watch video clips for the model : `https://www.youtube.com/channel/UC8aCUQu3pE3x96QN2HjosHA`

before, as randomness increases, a regular network is transformed to a small-world network and then a random network with this simple algorithm (See Figure 3.2). But, it is trickier to change the random network to the small-world network with a simple algorithm. The small-world network resembles the real world. In fact, we live in a small world due to innovations in technology, economy, and finance. We do not need distant linkages to use services and knowledge. In particular, the financial innovations make the economic world even smaller. Therefore, the small-world network can reflect the development and efficiency of the real economic system. The small-world network has the typical properties which are a large clustering coefficient (CC) and a small average path length (APL). Since the two properties have different scales, it is hard to make a direct comparison between them. In our model, the standardized CC and APL are used, and they will have a value between 0 and 1.

Table 6.4. Standardized APL and CC

Rewire	0	10	20	30	40	50	60	70	80	90	150
APL	1	0.506	0.421	0.382	0.360	0.347	0.337	0.330	0.325	0.322	0.317
CC	1	0.836	0.702	0.574	0.469	0.375	0.305	0.237	0.189	0.148	0.084

We run the model 100 times with each scenario. In Table 6.4, we can find the small-world properties when the rewired links are between 10 and 50. As mentioned earlier, the initial network is the regular network. A random network tends to have high CC and APL. We can check them in the first column of the Table 6.4. If all links are rewired, the network becomes a random network. A random network tends to have small CC and APL. The last column of Table 6.4 shows the typical properties of a random network, because considerably many number of links are rewired.

Figure 6.2 and Figure 6.3 present the results of our model. The green lines are the fitted curves for cooperator frequency, and the red lines are the curves for defector frequency (See

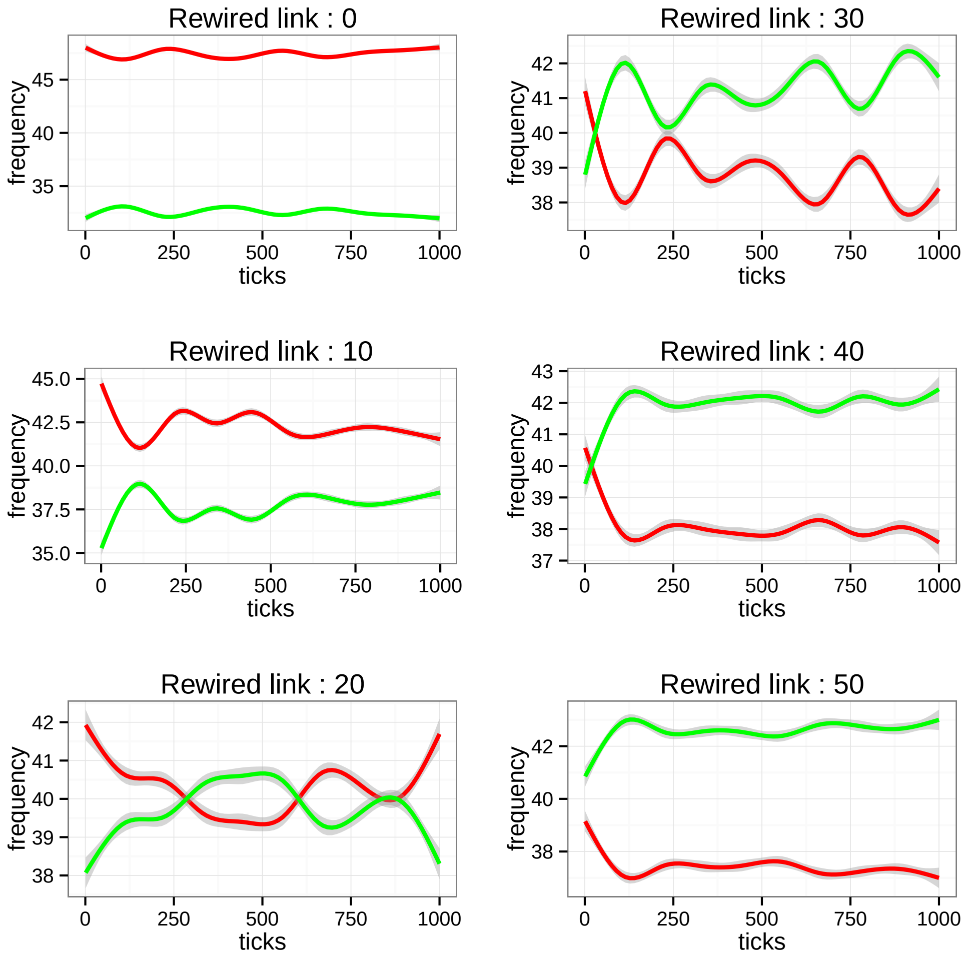

Figure 6.2. Model Results (Rewired links 0-50)

Appendix D to check the original time series data). As for the regular network model which is rewired links = 0, it shows the typical PD game result. The red line is higher than the green line, which implies that the frequency of defectors is greater than that of cooperators. Like the two-person PD game, defection is the dominant strategy. However, as the number of rewired links increases, and the networks show the properties of the small-world network, the frequency of cooperators increases. From the rewired links 30, cooperation becomes the dominant strategy in the games. However, when the number of rewired links is 90, the number of defectors is greater than that of cooperators. Therefore, our model shows

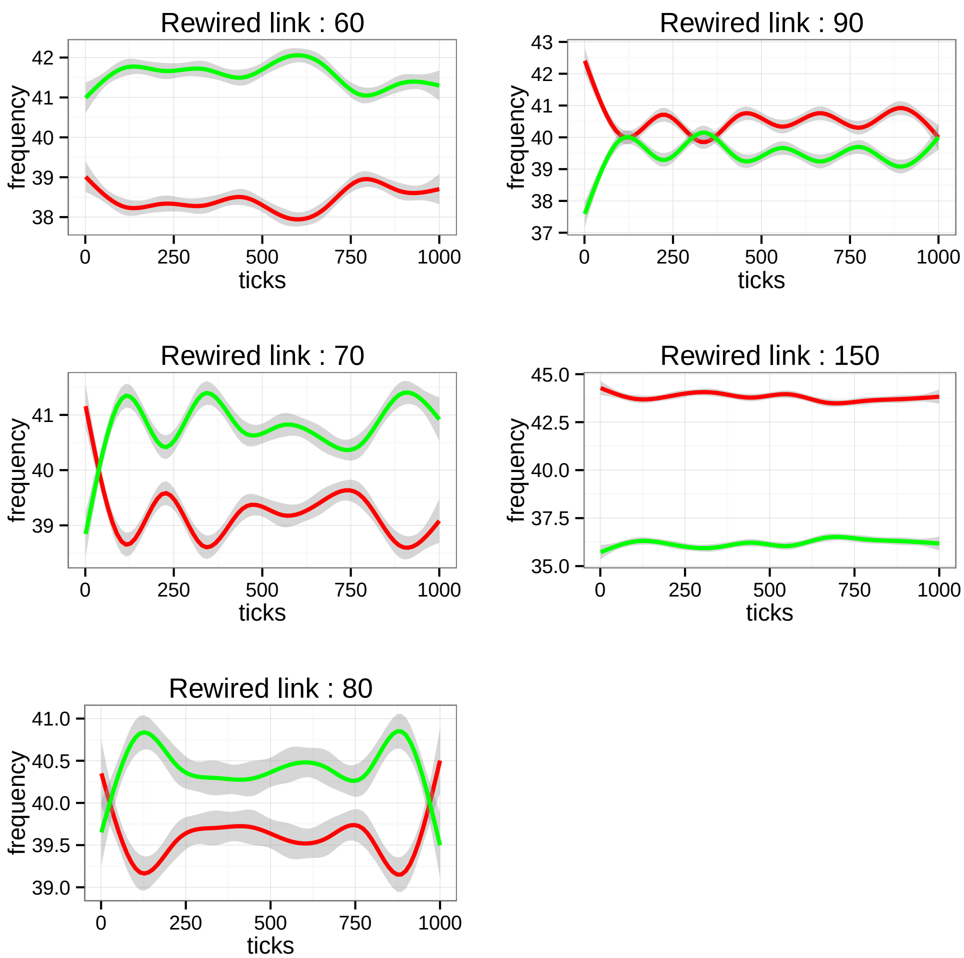

Figure 6.3. Model Results (Rewired links 60-150)

that there are two transition points: rewired links 30 and 90. Finally, the network, having 150 rewired links shows the pattern which is very similar to that of the regular network. Now, the frequency of defectors are greater than that of cooperators. To analyze these results, we need to understand the games in the network. As noted before, a payoff of an agent in the multiplayer game depends on the proportion of neighbors's strategies. The neighbors' decisions directly influence the agent's strategy and payoffs, and neighbors of the neighbors also affect an agent's decision, and so forth. This kind of game is called a graphical game (Jackson et al., 2008). Basically, our PD game model is based on the graphical game.

Although a player's payoff is affected by the other players' decisions, the player does not have to care about others' decisions. The player needs to care only about his neighbors in the game. Now, suppose three agents of a network group in our model. The middle agent needs to consider the direct neighbors' decisions. If the middle agent and the left side neighbor choose cooperation and the right side neighbor chooses defection, the payoff of the middle agent will be $0.9 + 0 + 0.56 = 1.46$. After rewiring, if the middle agent has one more degree from a cooperator, the new payoff is $0.9 + 0 + 0.9 + 0.58 = 2.38$. The right side neighbor who chooses defection can obtain two possible payoffs. When another neighbor of the agent is a defector, the payoff will be $1 + 0.3 + 0.72 = 2.02$. If the neighbor is a cooperator, the right side neighbor's payoff will be $1 + 1 + 0.81 = 2.81$. Thus, the right side neighbor agent can obtain the maximum payoff when he is the only defector. But if he is not the only defector, he will imitate the strategy of the middle agent who has one more link from the cooperator. In the next round, the right side neighbor will be a cooperator. This is the very simple example. In fact, in our model, rewiring links can change the agents' decisions in much more complicated ways.

Consequently, as our results show, the network structure which has some rewired links transmits cooperation to other parts of the network, and cooperation can survive well in the small-world network. However, when the small-world network becomes the random network, the effect of the rewired links disappears. Since almost all links are rewired, there is no node to play the role of transmitter. In the random network, all nodes have the same degree, and they are randomly connected. Thus, we can conclude that as randomness increases, the frequency of cooperation decreases.

6.4 Implications

Randomly connected nodes can imply uncertainty in the real world. If social relations depend on randomness, we cannot expect any social capital in the society. On the other hand, the small-world network can refer to an efficient diffusion system. In fact, the small-world network means the network has shortcuts to reach another part of the network. This network resembles the real economic system. Economic agents are efficiently connected. Furthermore, a financial innovation plays a role as a shortcut in the system. For example, the securitization puts certain types of assets into a pool, and repackages them. Thus, many financial institutions are involved with the repackaged securities. Now, banks, companies,and hedge funds are closely connected each other. In the real world, although defection can guarantee the maximum payoff, cooperation, social capital and trust are equilibria in the system, because the efficient system can produce stable profits. Our model also shows the frequent cooperation in the small-world network. However, as our models shows, high randomness or uncertainty seriously impedes the spread of cooperation. In the small-world network, some nodes are cooperation transmitters, and cooperation spreads to another part of the network. But, they cannot play that role in the random network. Therefore, the frequency of cooperation decreases. In the real world, high uncertainty interferes with investments, because agents can obtain more payoffs from choosing defection, such as hoarding money. As a result, cooperation cannot be the dominant strategy under high uncertainty, and the governmental policies for the recovery can be exploited by the defectors. Therefore, the recovery is delayed.

In addition, our model proposes a possible answer to the question why it is hard to restore the destroyed trust. An increase of randomness of the network can be regarded as rising entropy. According to the second law of thermodynamics, once entropy increases, it is hard to decrease it (Mitchell, 2009). In fact, a small-world network can be transformed to a random network with the simple algorithm, but it is more difficult to transform the random network to the small-world network or the regular network.

CHAPTER 7

CONCLUSION

The 2008 financial crisis was a highly unpredictable event. The conventional theories show their limitations to predict and diagnose the crisis. Thus we propose the agent-based modeling as an alternative approach. Since the ABM is based on more realistic and flexible assumptions, it can capture the underlying dynamics of the crisis.

Our questions for the 2008 financial crisis are as follows: What made the 2008 financial crisis more unpredictable? and why was the recovery so slow?

For the first question, we make the agent-based network model for the 2008 financial crisis. We find two phase transitions from our BA network model. In the first phase, the BA networks show the "robust and fragile" property. In the second phase, the BA network systems are very safe, but they can face very-rare-but-extremely-dangerous events, which is called "Dragon kings". Although they are very rare, we cannot ignore them, because these events have been observed in the real world, such as the Great Depression, the 1997 financial crisis, the 2008 financial crisis, and South Korea MERS. Because of limited data and the features of the Dragon kings, it is difficult to predict or diagnose these events with previous data and studies. Even if policy makers create a very resilient system, it can be vulnerable to these events. Paradoxically, the Dragon kings can be born only in safe systems. The safer systems are, the more likely they can face the very-rare-but-extremely dangerous events. Thus, we need to make more effort to understand the Dragon kings. We believe that it is time to bring these events to the main stage of social sciences.

Even though a network system cannot avoid the Dragon king, if the network system has higher transitivity and centrality, the network tends to be resilient on average.

Finally, once multiple networks are exposed to risks, the Dragon king can be realized, because the high complexity of the multiple networks makes the system more vulnerable. Our model shows that risks can move around the interdependent networks. We may not notice risks in our network, but the risks are hidden in another network and then can attack nodes of our network. As the complexity of the system increases, it is more difficult to predict and diagnose the risk spread patterns. The hidden spread of risks produces the pop-corn effect which is observed in the real world. In fact, the pop-corn effect represents the high level of unpredictability of the crisis. It is hard to know which kernel will pop next.

For the second question, we create the evolutionary PD game model. As many studies suggest, uncertainty and crisis have a close relationship. Our model also shows this relationship. Our model generates three types of networks. The first one is a regular network. In this network, defection is the dominant strategy, like two-person PD game. However, as the number of rewired links increases and the properties of a small-world network emerges, cooperation becomes new dominant strategy. A node, having more degrees plays a role as the cooperation transmitter in the small-world network. In terms of diffusion, the small-world network is very efficient system. Information in a node can be easily transmitted to any node in the network. Cooperation also spreads widely in the small-world network. As the number of rewired links increases more, the properties of the small-world network disappear and the network becomes a random network. In the random network, defection defeats cooperation. Thus, our model has two phase transitions. Since the connections of nodes depends on randomness, the level of uncertainty is high in the network. This situation resembles the economic system after the crisis. While cooperation is a key to restoring norms and trust which are destroyed by the crisis, economic agents play their roles as players of two-person PD game under uncertainty. Therefore, fiscal stimulus packages, monetary policies, and investments of other agents can be exploited by defectors, and the recovery is delayed. Furthermore, our model shows that once randomness or uncertainty increases, it is difficult to back to the normal status, because of the second law of thermodynamics.

Our models have some limitations. First, the size of simulation is relatively small. Due to hardware limitations, we use these small-sized simulation models. In the future research, we plan to run models with a large number of agents. Second, we exclude the role of the government for our simple models. In fact, interventions of the government can be important factors. Thus, we need to put the government as an agent in our developed model.

APPENDIX A

DESCRIPTIVE STATISTICS TABLES

Table A.1. ER Network - *outlink* : 1

Statistic	N	Mean	St. Dev.	Min	Max
maxlink	10	4.300	0.483	4	5
avglink	10	1.385	0.027	1.348	1.432
slope	10	−3.106	0.317	−3.471	−2.591
C.C.	10	0.000	0.000	0	0
path_length	10	0.000	0.000	0	0
hub	10	0.000	0.000	0	0
eigenvector	10	0.000	0.000	0	0
kurtosis	10	5.847	0.891	4.701	7.795

Table A.2. ER Network - *outlink* : 2

Statistic	N	Mean	St. Dev.	Min	Max
maxlink	10	5.900	0.738	5	7
avglink	10	2.052	0.039	1.984	2.112
slope	10	−2.379	0.395	−2.822	−1.662
C.C.	10	0.001	0.003	0.000	0.009
path_length	10	0.000	0.000	0	0
hub	10	0.000	0.000	0	0
eigenvector	10	0.000	0.000	0	0
kurtosis	10	4.396	0.809	3.242	5.597

Table A.3. ER Network - *outlink* : 3

Statistic	N	Mean	St. Dev.	Min	Max
maxlink	10	7.200	0.789	6	9
avglink	10	2.742	0.060	2.644	2.856
slope	10	−1.680	0.283	−2.222	−1.218
C.C.	10	0.003	0.002	0.000	0.008
path_length	10	0.000	0.000	0	0
hub	10	0.000	0.000	0	0
eigenvector	10	0.000	0.000	0	0
kurtosis	10	3.587	0.523	3.011	4.615

Table A.4. ER Network - *outlink* : 4

Statistic	N	Mean	St. Dev.	Min	Max
maxlink	10	8.900	0.738	8	10
avglink	10	3.386	0.049	3.328	3.472
slope	10	−1.533	0.195	−1.891	−1.243
C.C.	10	0.006	0.003	0.003	0.011
path_length	10	3.293	2.835	0.000	5.565
hub	10	0.000	0.000	0	0
eigenvector	10	0.000	0.000	0	0
kurtosis	10	3.400	0.460	2.835	4.076

Table A.5. ER Network - *outlink* : 5

Statistic	N	Mean	St. Dev.	Min	Max
maxlink	10	9.800	0.919	9	11
avglink	10	4.038	0.095	3.904	4.200
slope	10	−1.082	0.290	−1.519	−0.605
C.C.	10	0.008	0.003	0.003	0.012
path_length	10	4.220	1.485	0.000	4.817
hub	10	0.000	0.000	0	0
eigenvector	10	0.000	0.000	0	0
kurtosis	10	2.979	0.443	2.515	3.556

Table A.6. ER Network - *outlink* : 6

Statistic	N	Mean	St. Dev.	Min	Max
maxlink	10	11.700	1.418	10	15
avglink	10	4.718	0.134	4.576	5.000
slope	10	−0.924	0.226	−1.242	−0.565
C.C.	10	0.009	0.002	0.006	0.011
path_length	10	4.215	0.072	4.065	4.302
hub	10	0.000	0.000	0	0
eigenvector	10	0.000	0.000	0	0
kurtosis	10	2.814	0.348	2.428	3.586

Table A.7. ER Network - *outlink* : 7

Statistic	N	Mean	St. Dev.	Min	Max
maxlink	10	12.800	1.476	11	15
avglink	10	5.393	0.077	5.260	5.504
slope	10	−0.704	0.346	−1.155	−0.026
C.C.	10	0.010	0.003	0.008	0.016
path_length	10	3.881	0.032	3.830	3.939
hub	10	0.000	0.000	0	0
eigenvector	10	0.000	0.000	0	0
kurtosis	10	2.796	0.263	2.530	3.374

Table A.8. ER Network - *outlink* : 8

Statistic	N	Mean	St. Dev.	Min	Max
maxlink	10	14.100	0.876	13	16
avglink	10	6.034	0.150	5.824	6.372
slope	10	−0.570	0.132	−0.781	−0.362
C.C.	10	0.012	0.001	0.010	0.014
path_length	10	3.659	0.046	3.562	3.718
hub	10	0.000	0.000	0	0
eigenvector	10	0.000	0.000	0	0
kurtosis	10	2.612	0.187	2.404	2.905

Table A.9. ER Network - *outlink* : 9

Statistic	N	Mean	St. Dev.	Min	Max
maxlink	10	15.700	0.483	15	16
avglink	10	6.739	0.127	6.524	6.892
slope	10	−0.438	0.194	−0.680	0.045
C.C.	10	0.013	0.002	0.010	0.018
path_length	10	3.462	0.032	3.419	3.517
hub	10	0.000	0.000	0	0
eigenvector	10	0.000	0.000	0	0
kurtosis	10	2.620	0.203	2.364	3.025

Table A.10. ER Network - *outlink* : 10

Statistic	N	Mean	St. Dev.	Min	Max
maxlink	10	16.900	1.853	15	21
avglink	10	7.402	0.142	7.192	7.608
slope	10	−0.188	0.185	−0.403	0.259
C.C.	10	0.017	0.002	0.013	0.019
path_length	10	3.322	0.027	3.281	3.365
hub	10	0.000	0.000	0	0
eigenvector	10	0.000	0.000	0	0
kurtosis	10	2.614	0.253	2.342	3.018

Table A.11. BA Network - *outlink* : 1

Statistic	N	Mean	St. Dev.	Min	Max
maxlink	100	44.090	15.377	17	89
avglink	100	1.996	0.000	1.996	1.996
slope	100	−1.716	0.123	−1.994	−1.464
C.C.	100	0.000	0.000	0	0
path_length	100	6.362	0.566	4.881	8.052
hub	100	5.170	1.491	2	9
eigenvector	100	0.381	0.123	0.147	0.783
kurtosis	100	105.504	68.187	18.689	314.648

Table A.12. BA Network - *outlink* : 2

Statistic	N	Mean	St. Dev.	Min	Max
maxlink	100	49.130	11.497	29	79
avglink	100	2.986	0.048	2.880	3.080
slope	100	−1.665	0.075	−1.873	−1.501
C.C.	100	0.012	0.003	0.007	0.020
path_length	100	4.378	0.125	4.065	4.653
hub	100	4.830	1.223	2	7
eigenvector	100	0.568	0.113	0.333	0.928
kurtosis	100	59.924	28.033	22.718	152.857

Table A.13. BA Network - *outlink* : 3

Statistic	N	Mean	St. Dev.	Min	Max
maxlink	100	57.660	11.969	35	85
avglink	100	3.980	0.080	3.812	4.152
slope	100	−1.589	0.058	−1.725	−1.445
C.C.	100	0.023	0.003	0.016	0.031
path_length	100	3.787	0.067	3.617	3.953
hub	100	4.850	1.395	2	9
eigenvector	100	0.679	0.120	0.353	0.997
kurtosis	100	47.487	18.946	19.360	99.744

Table A.14. BA Network - *outlink* : 4

Statistic	N	Mean	St. Dev.	Min	Max
maxlink	100	63.950	11.520	38	99
avglink	100	4.966	0.102	4.684	5.212
slope	100	−1.527	0.047	−1.645	−1.431
C.C.	100	0.033	0.003	0.027	0.040
path_length	100	3.491	0.055	3.372	3.621
hub	100	4.360	1.227	2	8
eigenvector	100	0.747	0.104	0.513	0.950
kurtosis	100	38.388	13.434	14.998	86.059

Table A.15. BA Network - *outlink* : 5

Statistic	N	Mean	St. Dev.	Min	Max
maxlink	100	70.390	13.300	49	104
avglink	100	5.954	0.139	5.592	6.260
slope	100	−1.470	0.040	−1.594	−1.374
C.C.	100	0.040	0.004	0.031	0.053
path_length	100	3.286	0.044	3.176	3.387
hub	100	3.760	1.173	1	7
eigenvector	100	0.796	0.101	0.570	1.000
kurtosis	100	32.873	12.092	17.103	74.675

Table A.16. BA Network - *outlink* : 6

Statistic	N	Mean	St. Dev.	Min	Max
maxlink	100	77.340	12.982	54	109
avglink	100	6.913	0.139	6.628	7.256
slope	100	−1.418	0.034	−1.523	−1.329
C.C.	100	0.048	0.003	0.039	0.061
path_length	100	3.137	0.032	3.069	3.205
hub	100	3.510	1.159	1	6
eigenvector	100	0.834	0.093	0.565	1.000
kurtosis	100	29.361	9.693	13.747	60.928

Table A.17. BA Network - *outlink* : 7

Statistic	N	Mean	St. Dev.	Min	Max
maxlink	100	82.470	13.230	55	127
avglink	100	7.926	0.175	7.536	8.404
slope	100	−1.364	0.036	−1.452	−1.267
C.C.	100	0.055	0.004	0.046	0.062
path_length	100	3.016	0.029	2.946	3.095
hub	100	3.040	1.302	0	7
eigenvector	100	0.855	0.147	0.000	1.000
kurtosis	100	25.742	8.161	12.534	66.514

Table A.18. BA Network - *outlink* : 8

Statistic	N	Mean	St. Dev.	Min	Max
maxlink	100	88.240	11.150	61	120
avglink	100	8.880	0.223	8.236	9.372
slope	100	−1.322	0.032	−1.397	−1.234
C.C.	100	0.062	0.004	0.052	0.069
path_length	100	2.927	0.030	2.853	2.996
hub	100	2.630	1.002	0	5
eigenvector	100	0.882	0.115	0.000	1.000
kurtosis	100	22.976	5.333	13.722	41.146

Table A.19. BA Network - *outlink* : 9

Statistic	N	Mean	St. Dev.	Min	Max
maxlink	100	94.010	11.917	64	129
avglink	100	9.849	0.234	9.236	10.428
slope	100	−1.269	0.035	−1.357	−1.152
C.C.	100	0.067	0.004	0.055	0.078
path_length	100	2.851	0.023	2.799	2.908
hub	100	2.330	1.016	0	5
eigenvector	100	0.917	0.108	0.000	1.000
kurtosis	100	21.615	5.319	11.722	39.511

Table A.20. BA Network - *outlink* : 10

Statistic	N	Mean	St. Dev.	Min	Max
maxlink	100	97.030	13.426	71	142
avglink	100	10.825	0.273	10.080	11.504
slope	100	−1.234	0.036	−1.307	−1.149
C.C.	100	0.074	0.004	0.064	0.084
path_length	100	2.786	0.026	2.725	2.877
hub	100	2.220	0.927	0	5
eigenvector	100	0.907	0.142	0.000	1.000
kurtosis	100	19.292	4.682	11.837	37.926

APPENDIX B

BA NETWORK STATISTICS TABLES

Table B.1. BA Network Statistics : $outlink = 1$

Case	maxlink	avglink	slope	C.C.	path_length	hub	eigenvector	kurtosis
1	34	2	-1.73	0.0000	6.9081	2	0.78	57.29
2	59	2	-1.60	0.0000	5.8178	6	0.26	172.08
3	27	2	-1.80	0.0000	6.0421	7	0.42	34.79
4	55	2	-1.56	0.0000	6.0880	4	0.31	128.07
5	24	2	-1.92	0.0000	6.8493	7	0.44	33.09
6	70	2	-1.57	0.0000	5.9484	4	0.34	233.48
7	66	2	-1.66	0.0000	6.0999	5	0.24	225.93
8	50	2	-1.54	0.0000	5.7391	6	0.29	111.79
9	45	2	-1.67	0.0000	5.9872	4	0.46	94.06
10	54	2	-1.69	0.0000	6.3201	7	0.21	134.69
11	44	2	-1.71	0.0000	6.3147	8	0.20	91.24
12	34	2	-1.86	0.0000	6.6281	3	0.34	64.81
13	43	2	-1.65	0.0000	5.9937	5	0.36	95.62
14	46	2	-1.79	0.0000	6.8181	4	0.25	119.15
15	77	2	-1.61	0.0000	5.9073	4	0.30	275.49
16	42	2	-1.79	0.0000	7.4788	4	0.38	93.59
17	53	2	-1.72	0.0000	5.9178	5	0.32	146.35
18	74	2	-1.54	0.0000	5.9292	3	0.43	287.12
19	31	2	-1.78	0.0000	6.3589	6	0.42	46.95
20	42	2	-1.79	0.0000	7.3608	3	0.43	101.25
21	28	2	-1.77	0.0000	6.4847	7	0.41	38.16
22	50	2	-1.70	0.0000	6.1340	7	0.26	116.87
23	24	2	-1.89	0.0000	6.4573	5	0.54	34.21
24	49	2	-1.70	0.0000	6.0899	3	0.49	122.97
25	73	2	-1.58	0.0000	5.9240	5	0.29	261.21
26	37	2	-1.84	0.0000	7.1813	6	0.20	72.48
27	20	2	-1.87	0.0000	7.3109	8	0.57	25.97
28	27	2	-1.81	0.0000	6.6935	6	0.46	41.12
29	20	2	-1.99	0.0000	7.0428	5	0.54	24.45
30	49	2	-1.74	0.0000	7.0363	6	0.24	118.25
31	25	2	-1.93	0.0000	7.0615	6	0.41	31.97
32	45	2	-1.74	0.0000	6.6935	5	0.26	112.69
33	50	2	-1.61	0.0000	7.0055	5	0.26	113.48
34	32	2	-1.85	0.0000	6.4570	7	0.32	43.91
35	34	2	-1.75	0.0000	5.8596	5	0.55	73.89
36	29	2	-1.68	0.0000	6.4216	5	0.58	52.33
37	34	2	-1.85	0.0000	6.2184	4	0.46	59.03
38	37	2	-1.73	0.0000	6.4090	5	0.39	70.00
39	38	2	-1.69	0.0000	6.5241	4	0.39	70.83
40	41	2	-1.63	0.0000	5.8976	4	0.38	76.01
41	32	2	-1.90	0.0000	7.8833	7	0.15	45.61
42	34	2	-1.75	0.0000	6.5376	5	0.39	55.43
43	22	2	-1.95	0.0000	6.7331	8	0.38	29.62
44	52	2	-1.73	0.0000	7.0158	5	0.30	136.91
45	43	2	-1.65	0.0000	6.2646	8	0.25	76.05
46	58	2	-1.61	0.0000	6.2018	5	0.28	157.00
47	32	2	-1.88	0.0000	6.8436	5	0.41	52.69
48	31	2	-1.77	0.0000	6.4570	4	0.46	53.71
49	36	2	-1.77	0.0000	6.2214	6	0.37	66.10
50	33	2	-1.88	0.0000	7.2180	6	0.32	53.15

Table B.1 continued

Case	maxlink	avglink	slope	C.C.	path_length	hub	eigenvector	kurtosis
51	43	2	-1.70	0.0000	6.3389	6	0.27	83.60
52	62	2	-1.50	0.0000	6.1702	7	0.19	153.40
53	27	2	-1.83	0.0000	6.3972	7	0.48	38.92
54	31	2	-1.86	0.0000	6.5687	6	0.37	51.51
55	39	2	-1.69	0.0000	6.1181	6	0.29	68.43
56	89	2	-1.51	0.0000	4.8808	3	0.42	314.65
57	41	2	-1.72	0.0000	6.4812	5	0.28	82.06
58	47	2	-1.67	0.0000	6.0406	5	0.37	96.40
59	25	2	-1.83	0.0000	6.5635	7	0.52	36.87
60	71	2	-1.55	0.0000	5.5522	4	0.33	237.84
61	39	2	-1.69	0.0000	6.3632	5	0.34	71.21
62	40	2	-1.68	0.0000	6.4395	9	0.19	66.22
63	68	2	-1.51	0.0000	6.1845	2	0.59	241.63
64	60	2	-1.62	0.0000	5.9459	4	0.30	193.54
65	17	2	-1.92	0.0000	8.0524	7	0.62	18.69
66	53	2	-1.60	0.0000	5.5830	6	0.25	132.30
67	26	2	-1.82	0.0000	6.6919	6	0.48	37.30
68	30	2	-1.78	0.0000	6.3508	6	0.47	50.88
69	51	2	-1.75	0.0000	6.0475	4	0.34	141.95
70	44	2	-1.57	0.0000	5.8549	6	0.40	95.00
71	45	2	-1.75	0.0000	6.0515	3	0.44	113.25
72	43	2	-1.75	0.0000	6.7480	6	0.30	96.46
73	51	2	-1.67	0.0000	6.7211	4	0.27	133.43
74	72	2	-1.54	0.0000	5.8030	3	0.38	240.37
75	28	2	-1.82	0.0000	6.2494	6	0.46	46.53
76	44	2	-1.78	0.0000	7.6796	5	0.26	108.19
77	52	2	-1.68	0.0000	6.0235	6	0.28	125.28
78	58	2	-1.65	0.0000	6.2005	4	0.39	178.53
79	48	2	-1.63	0.0000	5.8340	5	0.34	111.52
80	36	2	-1.86	0.0000	6.6716	5	0.40	66.02
81	73	2	-1.50	0.0000	5.4995	3	0.35	258.04
82	29	2	-1.88	0.0000	6.9154	5	0.40	40.50
83	32	2	-1.74	0.0000	6.1635	7	0.41	57.73
84	41	2	-1.73	0.0000	6.1543	7	0.29	68.01
85	31	2	-1.84	0.0000	7.0980	3	0.57	62.80
86	30	2	-1.73	0.0000	6.6266	5	0.75	52.87
87	42	2	-1.62	0.0000	6.0881	6	0.37	83.76
88	39	2	-1.71	0.0000	5.8201	6	0.36	68.70
89	27	2	-1.88	0.0000	7.0754	5	0.49	43.01
90	78	2	-1.50	0.0000	5.0325	5	0.28	230.96
91	47	2	-1.46	0.0000	5.4702	3	0.69	108.02
92	53	2	-1.54	0.0000	5.9257	3	0.46	136.43
93	54	2	-1.63	0.0000	6.2198	4	0.34	137.05
94	61	2	-1.53	0.0000	5.6146	6	0.27	144.47
95	25	2	-1.82	0.0000	6.9102	6	0.56	38.49
96	67	2	-1.54	0.0000	5.5974	2	0.61	212.92
97	62	2	-1.49	0.0000	5.3945	3	0.52	146.63
98	35	2	-1.86	0.0000	6.2837	5	0.35	57.79
99	66	2	-1.63	0.0000	6.1279	7	0.20	193.33
100	52	2	-1.71	0.0000	6.8235	4	0.35	143.98

Table B.2. BA Network Statistics : $outlink = 2$

Case	maxlink	avglink	slope	C.C.	path_length	hub	eigenvector	kurtosis
1	64	3	-1.54	0.0125	4.3610	2	0.69	95.87
2	57	3	-1.60	0.0125	4.2941	7	0.44	70.50
3	69	3	-1.53	0.0153	4.3015	4	0.53	102.39
4	52	3	-1.62	0.0202	4.2754	4	0.72	68.35
5	38	3	-1.73	0.0154	4.4065	5	0.72	39.05
6	48	3	-1.67	0.0146	4.2744	5	0.54	64.73
7	34	3	-1.73	0.0167	4.4859	6	0.48	25.31
8	51	3	-1.70	0.0084	4.3956	4	0.53	62.19
9	44	3	-1.67	0.0121	4.3118	6	0.53	43.69
10	47	3	-1.77	0.0142	4.5056	4	0.50	54.05
11	79	3	-1.51	0.0112	4.2176	3	0.51	152.86
12	38	3	-1.74	0.0069	4.5018	5	0.67	33.54
13	35	3	-1.62	0.0110	4.3803	5	0.59	26.96
14	45	3	-1.66	0.0165	4.2905	7	0.57	52.18
15	69	3	-1.70	0.0090	4.3125	4	0.35	123.69
16	39	3	-1.76	0.0094	4.5714	6	0.49	41.21
17	42	3	-1.61	0.0131	4.2624	4	0.82	47.45
18	38	3	-1.75	0.0085	4.4104	5	0.61	34.71
19	58	3	-1.62	0.0099	4.3708	5	0.45	77.08
20	61	3	-1.67	0.0088	4.5396	2	0.55	105.38
21	39	3	-1.62	0.0129	4.2880	6	0.56	37.72
22	51	3	-1.67	0.0146	4.3021	4	0.57	54.99
23	57	3	-1.75	0.0095	4.4246	5	0.35	76.72
24	43	3	-1.68	0.0103	4.4511	5	0.48	39.84
25	60	3	-1.60	0.0141	4.2964	4	0.55	83.31
26	53	3	-1.64	0.0136	4.3806	6	0.46	66.17
27	53	3	-1.51	0.0136	4.2695	3	0.93	81.15
28	33	3	-1.77	0.0072	4.4352	6	0.72	30.01
29	33	3	-1.77	0.0103	4.5665	5	0.69	29.77
30	34	3	-1.79	0.0083	4.5313	7	0.56	26.88
31	49	3	-1.62	0.0102	4.1820	6	0.49	50.36
32	69	3	-1.63	0.0178	4.3478	2	0.68	127.62
33	44	3	-1.72	0.0142	4.5379	6	0.53	47.50
34	49	3	-1.59	0.0137	4.2905	6	0.55	50.78
35	52	3	-1.57	0.0109	4.3033	5	0.62	62.83
36	47	3	-1.71	0.0136	4.5512	4	0.44	53.44
37	30	3	-1.81	0.0121	4.6242	5	0.70	25.68
38	72	3	-1.56	0.0107	4.2219	3	0.55	116.70
39	37	3	-1.71	0.0077	4.6408	5	0.59	38.21
40	57	3	-1.58	0.0186	4.4079	3	0.74	86.61
41	38	3	-1.71	0.0087	4.4335	6	0.52	32.73
42	45	3	-1.70	0.0103	4.4147	6	0.42	44.21
43	46	3	-1.71	0.0158	4.4845	5	0.50	48.49
44	63	3	-1.56	0.0124	4.1067	4	0.49	84.84
45	56	3	-1.55	0.0116	4.1512	7	0.54	68.71
46	63	3	-1.59	0.0148	4.2227	4	0.53	87.95
47	55	3	-1.61	0.0130	4.3302	3	0.60	63.75
48	71	3	-1.57	0.0119	4.0647	6	0.41	98.32
49	73	3	-1.54	0.0113	4.1881	3	0.53	116.60
50	53	3	-1.60	0.0136	4.3419	5	0.50	64.70

Table B.2 continued

Case	maxlink	avglink	slope	C.C.	path_length	hub	eigenvector	kurtosis
51	55	3	-1.65	0.0143	4.2233	5	0.63	70.31
52	79	3	-1.62	0.0128	4.2031	5	0.42	146.18
53	42	3	-1.69	0.0124	4.5764	4	0.51	41.44
54	34	3	-1.80	0.0149	4.5984	4	0.61	25.90
55	49	3	-1.57	0.0154	4.2766	6	0.55	57.93
56	52	3	-1.72	0.0142	4.3512	4	0.60	60.14
57	41	3	-1.67	0.0129	4.3478	6	0.62	40.81
58	44	3	-1.60	0.0145	4.3961	5	0.76	49.38
59	43	3	-1.78	0.0092	4.6533	3	0.56	44.03
60	66	3	-1.62	0.0115	4.4399	3	0.47	112.64
61	49	3	-1.58	0.0127	4.3248	6	0.56	52.75
62	42	3	-1.74	0.0146	4.4765	3	0.64	40.46
63	64	3	-1.67	0.0155	4.3397	4	0.48	100.04
64	30	3	-1.81	0.0131	4.5510	5	0.68	25.38
65	41	3	-1.65	0.0134	4.3177	7	0.54	38.95
66	45	3	-1.65	0.0153	4.4334	4	0.73	56.89
67	39	3	-1.68	0.0085	4.4847	6	0.61	36.67
68	51	3	-1.61	0.0146	4.3287	4	0.52	52.00
69	49	3	-1.68	0.0078	4.3942	5	0.44	56.28
70	48	3	-1.65	0.0157	4.4426	4	0.55	55.44
71	55	3	-1.63	0.0153	4.3517	4	0.51	71.54
72	36	3	-1.69	0.0094	4.4751	7	0.54	31.83
73	51	3	-1.71	0.0138	4.4123	4	0.53	62.63
74	46	3	-1.67	0.0100	4.3092	6	0.59	56.38
75	56	3	-1.66	0.0118	4.3208	5	0.48	66.36
76	70	3	-1.64	0.0151	4.3288	4	0.46	117.52
77	68	3	-1.50	0.0110	4.1119	5	0.52	97.26
78	49	3	-1.70	0.0135	4.3553	5	0.52	53.18
79	44	3	-1.64	0.0156	4.3735	4	0.85	49.47
80	40	3	-1.64	0.0121	4.3781	7	0.64	38.48
81	52	3	-1.67	0.0102	4.4377	5	0.33	63.02
82	35	3	-1.72	0.0098	4.6076	5	0.51	25.66
83	43	3	-1.66	0.0127	4.3799	5	0.70	47.77
84	39	3	-1.65	0.0108	4.3804	5	0.69	37.70
85	29	3	-1.87	0.0095	4.5787	6	0.77	22.72
86	54	3	-1.61	0.0106	4.3147	7	0.36	62.40
87	51	3	-1.72	0.0136	4.4442	5	0.45	57.70
88	41	3	-1.77	0.0123	4.5229	7	0.75	40.13
89	38	3	-1.76	0.0068	4.4485	4	0.69	43.18
90	46	3	-1.65	0.0119	4.4147	3	0.72	53.21
91	45	3	-1.70	0.0142	4.3043	5	0.64	43.61
92	44	3	-1.68	0.0125	4.2529	6	0.50	37.34
93	61	3	-1.62	0.0149	4.2525	5	0.51	74.78
94	53	3	-1.73	0.0108	4.3878	5	0.42	59.99
95	55	3	-1.65	0.0123	4.2160	6	0.49	70.71
96	35	3	-1.83	0.0137	4.6344	3	0.73	33.24
97	40	3	-1.67	0.0094	4.4367	4	0.63	33.94
98	34	3	-1.72	0.0073	4.3559	5	0.65	27.67
99	44	3	-1.65	0.0130	4.3611	5	0.58	46.07
100	63	3	-1.57	0.0170	4.2195	5	0.48	85.45

Table B.3. BA Network Statistics : $outlink = 3$

Case	maxlink	avglink	slope	C.C.	path_length	hub	eigenvector	kurtosis
1	56	4	-1.64	0.0194	3.8027	5	0.82	43.19
2	85	4	-1.55	0.0263	3.7318	8	0.35	92.51
3	72	4	-1.51	0.0227	3.7743	3	0.61	74.81
4	59	4	-1.51	0.0226	3.7029	6	0.71	43.19
5	48	4	-1.57	0.0216	3.8218	4	0.80	38.63
6	68	4	-1.61	0.0229	3.7726	3	0.67	60.51
7	58	4	-1.66	0.0235	3.7539	5	0.57	40.94
8	38	4	-1.64	0.0159	3.8948	2	1.00	19.69
9	69	4	-1.56	0.0238	3.7693	7	0.55	62.43
10	85	4	-1.54	0.0207	3.6892	6	0.43	99.74
11	70	4	-1.60	0.0253	3.8059	5	0.55	63.24
12	79	4	-1.59	0.0232	3.7219	6	0.45	80.09
13	48	4	-1.60	0.0206	3.8303	5	0.77	37.38
14	69	4	-1.45	0.0224	3.7323	6	0.53	62.35
15	58	4	-1.53	0.0231	3.7550	4	0.70	48.92
16	63	4	-1.54	0.0302	3.6784	5	0.73	55.12
17	62	4	-1.58	0.0252	3.7353	8	0.48	41.57
18	65	4	-1.59	0.0261	3.8193	4	0.62	61.07
19	52	4	-1.58	0.0271	3.7575	6	0.62	34.64
20	57	4	-1.64	0.0214	3.8131	4	0.69	49.80
21	45	4	-1.64	0.0259	3.7714	5	0.84	32.62
22	57	4	-1.59	0.0182	3.7729	4	0.68	37.93
23	43	4	-1.64	0.0166	3.8117	6	0.76	25.73
24	40	4	-1.66	0.0271	3.8519	5	0.78	22.74
25	79	4	-1.50	0.0247	3.7097	3	0.65	77.91
26	48	4	-1.54	0.0257	3.8114	6	0.73	38.99
27	55	4	-1.61	0.0306	3.6939	8	0.57	33.40
28	54	4	-1.58	0.0240	3.7473	3	0.71	32.99
29	41	4	-1.69	0.0214	3.8901	5	0.81	22.72
30	44	4	-1.62	0.0245	3.7666	6	0.88	27.61
31	53	4	-1.65	0.0240	3.8196	3	0.68	37.75
32	68	4	-1.59	0.0204	3.7466	4	0.67	65.66
33	62	4	-1.60	0.0205	3.8280	6	0.53	48.18
34	56	4	-1.58	0.0259	3.7709	5	0.74	44.37
35	82	4	-1.54	0.0258	3.7011	3	0.66	88.16
36	49	4	-1.57	0.0239	3.7970	6	0.61	31.25
37	49	4	-1.62	0.0189	3.9160	3	0.87	45.27
38	64	4	-1.49	0.0263	3.7428	2	0.93	60.04
39	69	4	-1.59	0.0245	3.8501	4	0.60	69.99
40	68	4	-1.59	0.0264	3.8138	4	0.54	60.41
41	54	4	-1.60	0.0244	3.8527	4	0.61	37.93
42	41	4	-1.57	0.0215	3.8137	6	0.80	26.34
43	70	4	-1.62	0.0251	3.7255	5	0.54	57.88
44	47	4	-1.64	0.0237	3.8454	5	0.72	30.62
45	61	4	-1.53	0.0249	3.8091	4	0.76	63.86
46	70	4	-1.51	0.0238	3.7663	4	0.65	68.02
47	49	4	-1.58	0.0237	3.8543	4	0.88	34.41
48	44	4	-1.65	0.0238	3.8147	5	0.74	27.42
49	44	4	-1.66	0.0221	3.8854	5	0.71	30.31
50	61	4	-1.54	0.0213	3.6650	5	0.64	45.13

Table B.3 continued

Case	maxlink	avglink	slope	C.C.	path_length	hub	eigenvector	kurtosis
51	43	4	-1.70	0.0223	3.8945	6	0.67	29.43
52	59	4	-1.63	0.0238	3.9283	4	0.57	45.24
53	59	4	-1.55	0.0286	3.8010	4	0.83	47.68
54	35	4	-1.67	0.0264	3.8085	7	0.72	19.36
55	50	4	-1.62	0.0210	3.7915	6	0.63	31.79
56	76	4	-1.46	0.0256	3.6354	4	0.76	82.66
57	64	4	-1.55	0.0255	3.7753	4	0.62	54.26
58	53	4	-1.58	0.0193	3.8176	3	0.87	42.37
59	74	4	-1.52	0.0244	3.7318	3	0.69	79.75
60	45	4	-1.67	0.0231	3.7816	6	0.74	28.11
61	58	4	-1.44	0.0237	3.6913	5	0.73	53.95
62	66	4	-1.52	0.0281	3.6772	7	0.54	48.88
63	78	4	-1.49	0.0272	3.6418	9	0.41	66.38
64	60	4	-1.57	0.0195	3.7681	4	0.63	48.85
65	56	4	-1.57	0.0210	3.8390	6	0.68	45.82
66	57	4	-1.58	0.0261	3.7454	7	0.71	37.93
67	53	4	-1.60	0.0220	3.7292	7	0.61	39.45
68	53	4	-1.61	0.0232	3.8042	6	0.53	34.82
69	47	4	-1.60	0.0211	3.8374	4	0.80	29.79
70	67	4	-1.55	0.0249	3.7258	5	0.55	62.40
71	39	4	-1.69	0.0236	3.8806	5	0.69	22.35
72	56	4	-1.54	0.0275	3.6788	6	0.77	41.81
73	52	4	-1.56	0.0282	3.7491	6	0.70	38.60
74	59	4	-1.59	0.0255	3.8210	4	0.62	42.14
75	55	4	-1.60	0.0227	3.7991	4	0.69	36.84
76	44	4	-1.59	0.0181	3.8440	5	0.80	28.27
77	79	4	-1.61	0.0262	3.8014	3	0.62	98.19
78	43	4	-1.64	0.0269	3.7913	4	0.88	28.27
79	40	4	-1.72	0.0250	3.9530	5	0.80	25.00
80	44	4	-1.70	0.0200	3.8679	5	0.68	29.12
81	66	4	-1.54	0.0210	3.8124	4	0.66	71.24
82	75	4	-1.48	0.0220	3.6170	3	0.73	76.92
83	56	4	-1.61	0.0201	3.8011	7	0.66	41.42
84	45	4	-1.68	0.0201	3.8950	4	0.69	27.68
85	63	4	-1.61	0.0271	3.8065	3	0.70	53.21
86	38	4	-1.64	0.0236	3.8995	5	0.74	21.33
87	61	4	-1.53	0.0257	3.7883	5	0.74	52.20
88	61	4	-1.53	0.0202	3.8071	6	0.47	44.47
89	56	4	-1.58	0.0235	3.8081	6	0.54	42.29
90	73	4	-1.57	0.0245	3.7520	3	0.78	68.07
91	55	4	-1.66	0.0250	3.8351	6	0.66	35.96
92	46	4	-1.63	0.0222	3.8657	3	0.87	38.63
93	39	4	-1.69	0.0181	3.8931	4	0.74	25.33
94	58	4	-1.55	0.0183	3.7219	6	0.59	45.55
95	59	4	-1.58	0.0234	3.7569	4	0.78	48.02
96	51	4	-1.62	0.0294	3.7342	6	0.67	31.99
97	82	4	-1.59	0.0215	3.7146	4	0.54	87.43
98	68	4	-1.54	0.0238	3.8049	5	0.56	65.92
99	52	4	-1.55	0.0216	3.7893	3	0.87	41.14
100	70	4	-1.68	0.0238	3.8274	4	0.52	74.96

Table B.4. BA Network Statistics : $outlink = 4$

Case	maxlink	avglink	slope	C.C.	path_length	hub	eigenvector	kurtosis
1	66	5	-1.56	0.0306	3.4601	3	0.72	36.01
2	63	5	-1.58	0.0271	3.5081	3	0.80	30.74
3	69	5	-1.49	0.0400	3.4581	5	0.74	40.41
4	63	5	-1.51	0.0296	3.4866	5	0.68	34.59
5	49	5	-1.52	0.0339	3.5031	7	0.82	28.86
6	64	5	-1.44	0.0383	3.4388	5	0.85	43.64
7	70	5	-1.49	0.0332	3.4746	4	0.78	48.88
8	72	5	-1.60	0.0379	3.5083	3	0.69	45.18
9	71	5	-1.49	0.0363	3.4812	4	0.94	46.34
10	69	5	-1.52	0.0325	3.4594	4	0.72	40.01
11	63	5	-1.51	0.0307	3.4868	2	0.92	36.62
12	70	5	-1.51	0.0312	3.5243	3	0.70	44.15
13	58	5	-1.56	0.0324	3.4786	6	0.73	32.19
14	53	5	-1.52	0.0330	3.5002	5	0.80	30.89
15	66	5	-1.51	0.0315	3.4294	4	0.79	43.21
16	54	5	-1.53	0.0307	3.5965	3	0.81	30.05
17	58	5	-1.56	0.0292	3.4931	4	0.70	28.63
18	59	5	-1.58	0.0340	3.5794	2	0.95	30.46
19	56	5	-1.50	0.0340	3.4917	5	0.77	31.15
20	72	5	-1.47	0.0306	3.3997	5	0.70	48.08
21	56	5	-1.59	0.0296	3.4380	5	0.79	29.02
22	38	5	-1.61	0.0291	3.5630	2	0.92	15.00
23	89	5	-1.47	0.0337	3.3962	4	0.67	63.67
24	62	5	-1.60	0.0265	3.5891	2	0.84	36.05
25	70	5	-1.49	0.0276	3.5112	4	0.64	42.74
26	64	5	-1.57	0.0318	3.5710	4	0.70	38.68
27	85	5	-1.51	0.0326	3.5115	3	0.62	69.28
28	69	5	-1.49	0.0337	3.4650	4	0.69	38.25
29	63	5	-1.43	0.0311	3.5406	5	0.66	41.54
30	41	5	-1.65	0.0294	3.5280	5	0.90	20.12
31	54	5	-1.49	0.0276	3.4778	6	0.80	28.94
32	59	5	-1.55	0.0314	3.4852	6	0.65	31.54
33	77	5	-1.54	0.0377	3.5450	3	0.60	53.11
34	99	5	-1.47	0.0337	3.3971	4	0.56	86.06
35	60	5	-1.54	0.0341	3.4389	4	0.94	31.76
36	71	5	-1.45	0.0362	3.4200	5	0.68	47.08
37	70	5	-1.49	0.0285	3.4872	3	0.84	48.04
38	90	5	-1.59	0.0378	3.4974	2	0.71	82.59
39	77	5	-1.52	0.0328	3.4793	5	0.57	51.50
40	72	5	-1.54	0.0317	3.5399	3	0.74	46.03
41	71	5	-1.47	0.0345	3.4006	3	0.88	49.80
42	68	5	-1.45	0.0339	3.4309	4	0.84	41.70
43	61	5	-1.50	0.0298	3.4741	5	0.78	30.46
44	58	5	-1.53	0.0294	3.4870	5	0.74	30.37
45	46	5	-1.59	0.0350	3.5363	4	0.88	20.83
46	63	5	-1.53	0.0363	3.5044	7	0.74	36.70
47	86	5	-1.43	0.0296	3.4188	5	0.60	59.04
48	49	5	-1.53	0.0299	3.5087	6	0.86	21.94
49	68	5	-1.55	0.0332	3.4723	4	0.72	38.01
50	62	5	-1.51	0.0316	3.4210	4	0.84	35.68

Table B.4 continued

Case	maxlink	avglink	slope	C.C.	path_length	hub	eigenvector	kurtosis
51	80	5	-1.48	0.0333	3.4057	4	0.60	49.37
52	67	5	-1.53	0.0344	3.4508	4	0.64	38.14
53	52	5	-1.62	0.0348	3.6004	3	0.84	27.20
54	58	5	-1.55	0.0335	3.5242	3	0.84	30.98
55	41	5	-1.57	0.0312	3.5695	4	0.79	18.08
56	73	5	-1.46	0.0326	3.4794	8	0.51	44.33
57	51	5	-1.51	0.0297	3.4769	4	0.88	28.97
58	57	5	-1.59	0.0307	3.5426	4	0.76	29.83
59	75	5	-1.55	0.0345	3.5346	2	0.82	49.19
60	59	5	-1.55	0.0362	3.5172	3	0.90	29.86
61	56	5	-1.58	0.0296	3.5451	4	0.71	29.37
62	72	5	-1.51	0.0333	3.4946	5	0.60	43.95
63	67	5	-1.45	0.0341	3.3892	5	0.77	42.01
64	47	5	-1.52	0.0340	3.4814	7	0.77	20.90
65	58	5	-1.61	0.0403	3.5478	4	0.86	29.79
66	90	5	-1.43	0.0404	3.3998	2	0.92	83.76
67	59	5	-1.55	0.0329	3.5710	5	0.68	33.28
68	51	5	-1.52	0.0370	3.5253	5	0.78	23.17
69	52	5	-1.55	0.0336	3.5325	5	0.79	30.64
70	71	5	-1.52	0.0314	3.4680	4	0.57	37.65
71	67	5	-1.57	0.0294	3.5277	4	0.61	36.65
72	64	5	-1.56	0.0311	3.5302	4	0.61	34.12
73	54	5	-1.56	0.0349	3.5461	4	0.80	29.93
74	56	5	-1.51	0.0300	3.5661	4	0.68	26.44
75	58	5	-1.49	0.0336	3.5066	5	0.79	32.73
76	73	5	-1.50	0.0318	3.4263	5	0.68	46.10
77	50	5	-1.60	0.0322	3.6015	5	0.84	23.26
78	59	5	-1.53	0.0330	3.5358	3	0.86	35.40
79	70	5	-1.52	0.0368	3.5459	6	0.59	43.11
80	58	5	-1.52	0.0321	3.5142	5	0.72	30.40
81	68	5	-1.46	0.0296	3.4861	4	0.84	46.10
82	84	5	-1.57	0.0347	3.5111	4	0.56	65.73
83	80	5	-1.49	0.0391	3.4651	5	0.63	56.25
84	69	5	-1.48	0.0271	3.4682	5	0.66	43.93
85	49	5	-1.60	0.0275	3.6205	4	0.80	27.68
86	58	5	-1.53	0.0347	3.4507	7	0.64	26.07
87	63	5	-1.47	0.0294	3.4220	6	0.85	35.11
88	50	5	-1.55	0.0298	3.4795	6	0.80	22.67
89	48	5	-1.56	0.0352	3.5934	5	0.75	22.34
90	78	5	-1.52	0.0289	3.4357	3	0.70	51.03
91	65	5	-1.50	0.0339	3.3957	5	0.78	38.89
92	53	5	-1.56	0.0327	3.4661	4	0.91	24.78
93	77	5	-1.47	0.0343	3.3716	5	0.64	48.34
94	49	5	-1.54	0.0356	3.4513	6	0.83	26.99
95	60	5	-1.57	0.0308	3.5116	6	0.66	33.68
96	64	5	-1.49	0.0341	3.4006	5	0.80	37.27
97	62	5	-1.56	0.0321	3.4832	5	0.71	29.94
98	60	5	-1.55	0.0310	3.5069	4	0.67	28.86
99	85	5	-1.47	0.0339	3.4710	4	0.55	64.25
100	65	5	-1.54	0.0324	3.4652	5	0.69	34.64

Table B.5. BA Network Statistics : $outlink = 5$

Case	maxlink	avglink	slope	C.C.	path_length	hub	eigenvector	kurtosis
1	74	6	-1.44	0.0378	3.2543	5	0.74	34.05
2	80	6	-1.50	0.0412	3.3141	2	0.80	36.92
3	93	6	-1.40	0.0400	3.2605	4	0.66	53.03
4	69	6	-1.55	0.0383	3.3117	3	0.94	32.13
5	53	6	-1.48	0.0340	3.3367	3	0.96	18.80
6	61	6	-1.50	0.0395	3.2844	4	0.80	26.55
7	64	6	-1.52	0.0441	3.3035	3	0.68	21.97
8	73	6	-1.53	0.0403	3.2751	4	0.67	29.26
9	59	6	-1.51	0.0371	3.3040	4	0.72	23.56
10	57	6	-1.49	0.0428	3.2817	5	0.85	23.59
11	79	6	-1.46	0.0429	3.2341	4	0.80	37.54
12	71	6	-1.46	0.0426	3.2947	4	0.77	32.40
13	71	6	-1.43	0.0462	3.2509	6	0.80	29.34
14	53	6	-1.59	0.0351	3.3818	3	0.84	19.08
15	70	6	-1.37	0.0453	3.2150	5	0.81	31.22
16	66	6	-1.41	0.0375	3.2632	4	0.95	31.77
17	63	6	-1.51	0.0444	3.3526	4	0.81	30.40
18	79	6	-1.47	0.0466	3.2931	3	0.80	40.15
19	104	6	-1.44	0.0436	3.1922	4	0.59	59.40
20	74	6	-1.39	0.0430	3.2388	3	0.87	35.66
21	76	6	-1.49	0.0371	3.2651	4	0.68	32.81
22	53	6	-1.50	0.0394	3.3217	4	0.86	20.92
23	89	6	-1.47	0.0425	3.2715	3	0.77	51.12
24	91	6	-1.47	0.0527	3.2346	3	0.78	51.12
25	74	6	-1.42	0.0410	3.2554	4	0.90	40.33
26	94	6	-1.46	0.0430	3.2145	4	0.62	54.06
27	66	6	-1.42	0.0411	3.2735	6	0.74	30.98
28	62	6	-1.47	0.0424	3.2252	3	0.97	24.13
29	79	6	-1.47	0.0423	3.2648	3	0.80	38.63
30	98	6	-1.43	0.0430	3.2983	3	0.62	62.69
31	65	6	-1.45	0.0390	3.3359	2	0.94	29.04
32	75	6	-1.41	0.0391	3.3118	4	0.71	35.54
33	65	6	-1.50	0.0402	3.2594	4	0.91	28.50
34	68	6	-1.45	0.0369	3.2576	3	0.85	26.41
35	69	6	-1.46	0.0387	3.2439	3	0.98	36.38
36	86	6	-1.40	0.0395	3.2622	5	0.67	49.53
37	92	6	-1.51	0.0439	3.3036	2	0.77	51.35
38	95	6	-1.44	0.0377	3.2502	1	1.00	56.30
39	63	6	-1.50	0.0403	3.3123	3	0.88	26.04
40	49	6	-1.50	0.0429	3.3869	5	0.87	18.37
41	55	6	-1.53	0.0387	3.2797	4	0.85	20.78
42	70	6	-1.46	0.0383	3.2914	1	1.00	25.56
43	66	6	-1.44	0.0417	3.3521	3	0.85	31.05
44	86	6	-1.50	0.0413	3.2566	5	0.61	44.44
45	88	6	-1.44	0.0424	3.2197	5	0.70	47.86
46	100	6	-1.47	0.0385	3.2523	3	0.61	66.63
47	56	6	-1.52	0.0381	3.2928	4	0.83	20.41
48	74	6	-1.45	0.0407	3.2895	5	0.75	39.25
49	64	6	-1.52	0.0354	3.3244	3	0.90	28.79
50	68	6	-1.46	0.0429	3.3169	5	0.71	29.18

Table B.5 continued

Case	maxlink	avglink	slope	C.C.	path_length	hub	eigenvector	kurtosis
51	61	6	-1.57	0.0309	3.3631	3	0.76	22.79
52	68	6	-1.46	0.0353	3.2630	5	0.75	34.20
53	67	6	-1.47	0.0350	3.2940	4	0.76	26.47
54	61	6	-1.41	0.0393	3.2677	6	0.79	25.45
55	60	6	-1.46	0.0334	3.3329	4	0.77	25.68
56	79	6	-1.44	0.0371	3.3096	2	0.83	40.06
57	55	6	-1.48	0.0350	3.2876	3	0.90	17.89
58	68	6	-1.45	0.0448	3.3511	2	0.86	28.25
59	75	6	-1.49	0.0420	3.2399	5	0.79	34.58
60	56	6	-1.53	0.0365	3.3750	2	0.95	18.56
61	54	6	-1.51	0.0376	3.2705	4	0.87	20.26
62	78	6	-1.43	0.0397	3.2549	5	0.65	37.15
63	79	6	-1.45	0.0472	3.1758	4	0.68	31.43
64	68	6	-1.46	0.0387	3.2854	4	0.73	28.03
65	58	6	-1.49	0.0403	3.2673	6	0.78	25.38
66	56	6	-1.46	0.0409	3.2724	7	0.83	23.91
67	74	6	-1.47	0.0450	3.2637	4	0.69	32.26
68	66	6	-1.46	0.0343	3.3023	2	0.78	24.41
69	86	6	-1.46	0.0447	3.2594	4	0.65	44.35
70	65	6	-1.44	0.0406	3.2566	4	0.84	30.09
71	62	6	-1.50	0.0372	3.3129	4	0.74	24.58
72	64	6	-1.46	0.0405	3.2531	3	0.98	23.08
73	104	6	-1.39	0.0419	3.2149	3	0.73	74.68
74	52	6	-1.49	0.0450	3.3608	5	0.85	19.32
75	85	6	-1.46	0.0463	3.2475	4	0.76	42.53
76	72	6	-1.47	0.0369	3.3371	3	0.70	32.18
77	65	6	-1.56	0.0353	3.3732	3	0.76	30.11
78	60	6	-1.52	0.0376	3.3344	1	1.00	19.76
79	72	6	-1.48	0.0429	3.3364	3	0.84	37.94
80	52	6	-1.51	0.0371	3.2844	4	0.83	18.55
81	54	6	-1.48	0.0391	3.2851	6	0.89	22.04
82	74	6	-1.47	0.0376	3.2889	4	0.74	35.27
83	82	6	-1.45	0.0443	3.2528	4	0.76	36.78
84	73	6	-1.42	0.0409	3.2458	3	0.95	37.57
85	88	6	-1.42	0.0405	3.3214	2	0.83	55.36
86	50	6	-1.47	0.0324	3.3171	3	0.79	17.10
87	71	6	-1.47	0.0384	3.2617	4	0.69	29.29
88	60	6	-1.48	0.0430	3.3070	5	0.83	24.13
89	67	6	-1.40	0.0383	3.2494	3	0.95	31.37
90	52	6	-1.46	0.0393	3.3700	3	0.93	21.50
91	69	6	-1.54	0.0395	3.3631	3	0.79	32.00
92	55	6	-1.50	0.0397	3.3165	4	0.78	21.40
93	65	6	-1.47	0.0383	3.2706	4	0.64	24.81
94	67	6	-1.50	0.0422	3.2755	3	0.80	28.36
95	103	6	-1.41	0.0448	3.1883	6	0.57	58.25
96	60	6	-1.50	0.0328	3.3227	4	0.77	21.87
97	59	6	-1.45	0.0393	3.2654	5	0.81	24.45
98	93	6	-1.46	0.0415	3.2938	3	0.71	55.97
99	61	6	-1.46	0.0411	3.2793	4	0.79	24.16
100	65	6	-1.49	0.0443	3.3257	6	0.74	26.70

Table B.6. BA Network Statistics : $outlink = 6$

Case	maxlink	avglink	slope	C.C.	path_length	hub	eigenvector	kurtosis
1	90	7	-1.37	0.0519	3.1185	3	0.79	34.19
2	72	7	-1.39	0.0512	3.1238	5	0.76	26.54
3	72	7	-1.44	0.0471	3.1733	4	0.88	24.77
4	69	7	-1.45	0.0442	3.1709	3	0.84	22.77
5	74	7	-1.43	0.0503	3.1681	4	0.87	28.65
6	84	7	-1.44	0.0473	3.1587	4	0.81	33.80
7	109	7	-1.39	0.0451	3.1074	2	0.73	60.03
8	68	7	-1.41	0.0497	3.1409	4	0.87	23.09
9	64	7	-1.41	0.0487	3.1308	4	0.88	21.41
10	102	7	-1.41	0.0472	3.0827	4	0.68	45.69
11	106	7	-1.39	0.0495	3.0917	2	0.86	51.41
12	76	7	-1.38	0.0497	3.1336	3	0.88	32.29
13	66	7	-1.40	0.0472	3.1147	5	0.86	21.85
14	74	7	-1.41	0.0464	3.1455	4	0.80	26.86
15	86	7	-1.37	0.0527	3.1270	4	0.78	36.12
16	97	7	-1.40	0.0503	3.1499	4	0.67	43.93
17	91	7	-1.41	0.0497	3.0928	2	0.74	30.83
18	67	7	-1.42	0.0429	3.1741	3	0.84	21.28
19	66	7	-1.42	0.0523	3.1525	3	0.96	22.58
20	89	7	-1.39	0.0478	3.1659	4	0.68	38.53
21	71	7	-1.45	0.0476	3.1532	3	0.93	25.17
22	94	7	-1.39	0.0538	3.0763	5	0.79	39.87
23	60	7	-1.48	0.0473	3.1959	1	1.00	17.02
24	73	7	-1.43	0.0440	3.1056	3	0.95	24.32
25	62	7	-1.41	0.0512	3.1567	5	0.88	19.42
26	77	7	-1.42	0.0495	3.1656	3	0.78	25.27
27	80	7	-1.43	0.0435	3.1693	3	0.76	30.57
28	72	7	-1.37	0.0445	3.1052	2	0.99	26.15
29	77	7	-1.40	0.0509	3.1223	2	0.83	22.71
30	94	7	-1.40	0.0510	3.0880	5	0.73	38.15
31	73	7	-1.46	0.0506	3.1465	1	1.00	20.50
32	93	7	-1.46	0.0527	3.1615	3	0.73	42.77
33	63	7	-1.41	0.0430	3.1971	5	0.87	22.23
34	83	7	-1.43	0.0491	3.1620	3	0.82	36.46
35	102	7	-1.38	0.0443	3.1127	3	0.72	48.63
36	87	7	-1.41	0.0488	3.1405	4	0.74	36.23
37	70	7	-1.40	0.0468	3.1046	3	0.88	22.92
38	68	7	-1.44	0.0496	3.1545	4	0.88	23.56
39	62	7	-1.44	0.0462	3.1158	4	0.91	20.71
40	83	7	-1.38	0.0451	3.1319	2	0.99	39.21
41	62	7	-1.38	0.0469	3.1695	5	0.84	22.39
42	63	7	-1.43	0.0487	3.1211	3	0.95	20.66
43	70	7	-1.41	0.0454	3.1223	5	0.78	25.15
44	73	7	-1.38	0.0465	3.1377	6	0.82	28.26
45	107	7	-1.43	0.0429	3.1611	3	0.63	60.93
46	64	7	-1.43	0.0456	3.1513	3	0.90	18.74
47	60	7	-1.43	0.0471	3.1215	4	0.89	18.12
48	56	7	-1.44	0.0516	3.1562	3	0.96	15.50
49	68	7	-1.46	0.0469	3.1299	3	0.88	21.31
50	70	7	-1.47	0.0495	3.1945	4	0.78	22.34

Table B.6 continued

Case	maxlink	avglink	slope	C.C.	path_length	hub	eigenvector	kurtosis
51	64	7	-1.40	0.0522	3.1305	3	0.96	22.35
52	82	7	-1.41	0.0481	3.1047	4	0.88	33.61
53	105	7	-1.35	0.0486	3.1102	3	0.71	49.41
54	74	7	-1.43	0.0512	3.1283	3	0.88	26.67
55	67	7	-1.47	0.0438	3.1665	3	0.85	20.60
56	83	7	-1.40	0.0613	3.1044	3	0.96	28.78
57	98	7	-1.37	0.0507	3.1600	2	0.91	51.59
58	69	7	-1.42	0.0392	3.1852	4	0.80	26.73
59	100	7	-1.40	0.0479	3.1260	5	0.56	44.94
60	75	7	-1.48	0.0475	3.1585	3	0.82	23.80
61	77	7	-1.44	0.0484	3.0955	4	0.80	26.75
62	64	7	-1.40	0.0470	3.1109	4	0.87	21.26
63	90	7	-1.39	0.0505	3.1419	4	0.73	38.29
64	83	7	-1.42	0.0505	3.1293	6	0.81	32.57
65	87	7	-1.42	0.0462	3.0985	5	0.74	32.76
66	90	7	-1.45	0.0503	3.0896	4	0.68	32.33
67	72	7	-1.42	0.0457	3.1783	3	0.85	24.56
68	60	7	-1.40	0.0430	3.1731	2	0.99	16.93
69	73	7	-1.44	0.0482	3.1693	3	0.84	28.74
70	81	7	-1.45	0.0465	3.1172	2	0.87	28.83
71	91	7	-1.43	0.0515	3.1003	5	0.68	36.92
72	89	7	-1.43	0.0510	3.1897	3	0.72	36.49
73	87	7	-1.33	0.0500	3.1104	3	0.91	37.59
74	62	7	-1.43	0.0433	3.1802	1	1.00	15.62
75	73	7	-1.52	0.0413	3.1919	3	0.80	26.09
76	65	7	-1.41	0.0498	3.0867	5	0.93	22.54
77	81	7	-1.39	0.0486	3.1670	5	0.70	29.46
78	54	7	-1.47	0.0440	3.1856	1	1.00	13.75
79	62	7	-1.42	0.0462	3.1286	4	0.94	20.31
80	78	7	-1.37	0.0499	3.1573	6	0.77	29.69
81	59	7	-1.50	0.0512	3.2052	2	1.00	16.14
82	64	7	-1.42	0.0433	3.1165	3	0.91	21.89
83	83	7	-1.40	0.0539	3.1095	5	0.78	33.16
84	96	7	-1.36	0.0451	3.1532	3	0.79	47.55
85	73	7	-1.49	0.0458	3.2048	2	0.90	26.76
86	96	7	-1.44	0.0484	3.0691	2	0.77	36.60
87	76	7	-1.46	0.0467	3.1168	4	0.89	25.40
88	80	7	-1.40	0.0458	3.1220	3	0.84	30.34
89	96	7	-1.39	0.0532	3.0762	4	0.71	36.94
90	74	7	-1.48	0.0487	3.1369	4	0.76	24.28
91	66	7	-1.45	0.0427	3.1362	3	0.84	20.84
92	68	7	-1.36	0.0488	3.1413	4	0.81	25.15
93	75	7	-1.45	0.0517	3.1408	4	0.80	25.50
94	95	7	-1.41	0.0413	3.1473	2	0.79	41.00
95	84	7	-1.38	0.0497	3.1162	4	0.83	36.58
96	71	7	-1.44	0.0517	3.1325	5	0.76	24.65
97	71	7	-1.39	0.0496	3.0982	5	0.92	27.18
98	77	7	-1.40	0.0500	3.1383	4	0.76	29.53
99	66	7	-1.39	0.0503	3.1171	6	0.86	24.37
100	69	7	-1.45	0.0466	3.1209	2	0.91	20.35

Table B.7. BA Network Statistics : $outlink = 7$

Case	maxlink	avglink	slope	C.C.	path_length	hub	eigenvector	kurtosis
1	94	8	-1.35	0.0563	3.0140	3	0.89	34.15
2	75	8	-1.36	0.0567	3.0166	2	0.93	20.39
3	59	8	-1.45	0.0512	3.0716	2	0.96	14.61
4	97	8	-1.34	0.0601	3.0555	2	0.94	37.49
5	85	8	-1.35	0.0529	3.0253	4	0.83	30.28
6	87	8	-1.40	0.0594	3.0176	3	0.86	27.65
7	67	8	-1.38	0.0457	3.0768	3	0.83	18.51
8	74	8	-1.40	0.0625	3.0095	3	0.96	20.19
9	82	8	-1.34	0.0530	3.0093	4	0.85	23.63
10	100	8	-1.32	0.0552	2.9869	2	0.94	39.32
11	85	8	-1.37	0.0610	2.9659	5	0.76	25.52
12	74	8	-1.41	0.0516	3.0109	6	0.82	22.42
13	70	8	-1.40	0.0491	3.0171	2	0.86	17.63
14	69	8	-1.35	0.0583	3.0747	4	0.87	17.90
15	77	8	-1.39	0.0518	3.0416	1	1.00	19.49
16	68	8	-1.39	0.0515	2.9927	2	0.94	17.22
17	55	8	-1.43	0.0539	3.0477	0	0.00	14.55
18	100	8	-1.37	0.0599	2.9993	3	0.79	32.53
19	67	8	-1.35	0.0549	3.0333	2	0.94	18.10
20	81	8	-1.39	0.0523	3.0492	4	0.92	28.17
21	75	8	-1.35	0.0559	2.9929	3	0.88	21.36
22	89	8	-1.31	0.0537	2.9945	2	0.97	29.33
23	104	8	-1.34	0.0530	3.0290	2	0.81	37.91
24	79	8	-1.41	0.0549	2.9915	4	0.79	22.88
25	76	8	-1.41	0.0572	3.0401	1	1.00	17.33
26	78	8	-1.36	0.0551	3.0112	3	0.87	19.90
27	78	8	-1.39	0.0552	3.0114	2	0.99	22.83
28	90	8	-1.40	0.0593	3.0638	3	0.72	28.39
29	89	8	-1.34	0.0521	3.0456	1	1.00	24.59
30	109	8	-1.38	0.0547	3.0110	4	0.65	40.50
31	79	8	-1.31	0.0581	3.0107	3	0.94	21.25
32	73	8	-1.36	0.0531	3.0495	1	1.00	16.11
33	89	8	-1.37	0.0533	3.0155	2	0.86	27.02
34	74	8	-1.37	0.0588	2.9738	5	0.91	23.91
35	83	8	-1.36	0.0571	2.9920	4	0.83	24.70
36	67	8	-1.39	0.0561	2.9988	5	0.81	19.70
37	92	8	-1.34	0.0611	2.9460	5	0.78	29.11
38	84	8	-1.33	0.0512	3.0043	3	0.87	26.39
39	81	8	-1.37	0.0541	2.9977	3	0.86	24.97
40	80	8	-1.39	0.0569	3.0093	2	0.99	24.99
41	89	8	-1.36	0.0594	3.0075	2	0.86	27.14
42	76	8	-1.39	0.0580	2.9895	3	0.94	19.62
43	73	8	-1.37	0.0521	3.0352	3	0.93	22.36
44	69	8	-1.34	0.0590	2.9771	4	0.93	20.06
45	74	8	-1.36	0.0499	3.0382	3	0.88	21.27
46	108	8	-1.35	0.0584	2.9469	3	0.79	36.60
47	84	8	-1.38	0.0581	3.0245	4	0.89	25.02
48	110	8	-1.36	0.0546	2.9904	3	0.72	46.24
49	86	8	-1.36	0.0611	3.0292	4	0.87	29.53
50	60	8	-1.35	0.0518	3.0048	4	0.86	14.85

Table B.7 continued

Case	maxlink	avglink	slope	C.C.	path_length	hub	eigenvector	kurtosis
51	72	8	-1.28	0.0592	3.0067	7	0.86	25.68
52	94	8	-1.30	0.0485	3.0218	3	0.82	37.53
53	100	8	-1.32	0.0543	3.0350	2	0.78	33.54
54	66	8	-1.37	0.0541	3.0034	4	0.93	17.93
55	59	8	-1.37	0.0482	3.0589	1	1.00	12.53
56	85	8	-1.40	0.0507	3.0777	2	0.84	26.40
57	82	8	-1.30	0.0567	3.0488	5	0.83	27.08
58	81	8	-1.40	0.0597	3.0023	3	0.89	23.96
59	112	8	-1.30	0.0618	2.9856	3	0.80	51.27
60	127	8	-1.36	0.0542	3.0008	2	0.71	66.51
61	90	8	-1.32	0.0609	3.0294	2	0.95	26.81
62	89	8	-1.34	0.0596	3.0076	3	0.83	25.30
63	67	8	-1.34	0.0540	3.0273	4	0.92	18.38
64	85	8	-1.38	0.0575	2.9694	4	0.87	26.40
65	84	8	-1.34	0.0557	3.0194	3	0.86	27.08
66	78	8	-1.41	0.0480	3.0716	2	0.88	21.27
67	87	8	-1.37	0.0612	3.0079	3	0.92	26.42
68	82	8	-1.27	0.0603	3.0038	6	0.82	30.23
69	83	8	-1.28	0.0517	3.0288	3	0.80	25.23
70	60	8	-1.40	0.0510	3.0952	4	0.95	17.32
71	75	8	-1.39	0.0549	3.0463	2	0.93	18.93
72	87	8	-1.35	0.0528	3.0237	4	0.77	27.68
73	99	8	-1.28	0.0602	2.9916	5	0.69	36.00
74	84	8	-1.35	0.0508	3.0339	4	0.86	29.00
75	74	8	-1.36	0.0496	3.0687	3	0.95	23.73
76	92	8	-1.37	0.0606	3.0131	5	0.78	29.34
77	86	8	-1.41	0.0473	3.0376	2	0.97	31.78
78	88	8	-1.30	0.0584	2.9695	4	0.84	27.77
79	66	8	-1.34	0.0470	3.0215	3	0.91	18.29
80	83	8	-1.35	0.0530	2.9624	3	0.85	22.10
81	81	8	-1.38	0.0572	3.0061	4	0.82	23.28
82	108	8	-1.31	0.0610	2.9739	4	0.71	36.98
83	55	8	-1.42	0.0560	3.0446	0	0.00	14.27
84	64	8	-1.38	0.0552	3.0176	5	0.87	18.39
85	74	8	-1.35	0.0554	2.9944	4	0.95	22.35
86	91	8	-1.38	0.0552	3.0182	2	0.85	25.72
87	80	8	-1.40	0.0563	3.0390	3	0.80	21.76
88	91	8	-1.36	0.0612	2.9862	3	0.88	27.17
89	105	8	-1.35	0.0576	3.0042	1	1.00	36.59
90	80	8	-1.30	0.0605	2.9825	3	0.93	25.88
91	65	8	-1.41	0.0555	3.0271	2	0.93	14.94
92	98	8	-1.42	0.0494	3.0529	1	1.00	34.09
93	85	8	-1.42	0.0564	3.0320	5	0.74	27.98
94	89	8	-1.36	0.0599	2.9807	1	1.00	21.17
95	79	8	-1.38	0.0528	3.0072	2	0.85	20.68
96	74	8	-1.36	0.0492	3.0234	4	0.96	22.76
97	95	8	-1.37	0.0571	2.9883	4	0.72	31.34
98	76	8	-1.40	0.0505	2.9982	3	0.90	22.87
99	91	8	-1.40	0.0592	3.0166	2	0.78	26.46
100	85	8	-1.39	0.0540	3.0391	2	0.89	22.43

Table B.8. BA Network Statistics : *outlink* = 8

Case	maxlink	avglink	slope	C.C.	path_length	hub	eigenvector	kurtosis
1	97	9	-1.28	0.0652	2.9000	3	0.82	22.35
2	96	9	-1.32	0.0627	2.9301	3	0.91	29.66
3	82	9	-1.27	0.0594	2.9260	3	0.88	21.09
4	94	9	-1.29	0.0567	2.9147	2	0.87	24.37
5	119	9	-1.34	0.0641	2.9025	2	0.76	38.92
6	97	9	-1.28	0.0668	2.9053	3	0.92	32.76
7	103	9	-1.31	0.0597	2.8865	3	0.84	35.76
8	76	9	-1.37	0.0603	2.9373	2	0.96	17.22
9	85	9	-1.32	0.0686	2.8991	4	0.88	23.84
10	67	9	-1.34	0.0671	2.9358	2	0.93	14.33
11	73	9	-1.32	0.0675	2.9262	4	0.89	17.50
12	111	9	-1.30	0.0658	2.8955	3	0.72	30.70
13	92	9	-1.36	0.0597	2.9505	2	0.85	24.69
14	91	9	-1.34	0.0643	2.9319	3	0.82	21.15
15	81	9	-1.32	0.0574	2.9676	3	0.93	20.61
16	86	9	-1.31	0.0622	2.9356	3	0.91	23.88
17	101	9	-1.28	0.0649	2.9060	3	0.85	32.06
18	94	9	-1.33	0.0640	2.9091	5	0.81	25.21
19	67	8	-1.37	0.0602	2.9826	2	0.97	15.52
20	78	9	-1.35	0.0592	2.9380	2	0.89	18.17
21	108	9	-1.31	0.0604	2.8783	2	0.82	29.30
22	96	9	-1.27	0.0604	2.9406	1	1.00	24.29
23	82	9	-1.37	0.0524	2.9549	1	1.00	17.28
24	76	9	-1.35	0.0617	2.9111	3	0.95	17.82
25	93	9	-1.33	0.0617	2.9457	4	0.83	25.76
26	98	9	-1.35	0.0621	2.9749	3	0.77	27.60
27	106	9	-1.36	0.0644	2.9070	2	0.82	27.96
28	92	9	-1.32	0.0666	2.9065	4	0.86	27.86
29	95	9	-1.30	0.0593	2.9378	4	0.75	26.34
30	83	9	-1.30	0.0577	2.9398	2	0.90	17.87
31	87	9	-1.32	0.0614	2.9231	3	0.92	22.36
32	94	9	-1.28	0.0651	2.8902	3	0.86	24.47
33	66	9	-1.33	0.0641	2.9480	2	0.97	13.80
34	88	8	-1.33	0.0597	2.9539	2	0.98	25.53
35	85	9	-1.30	0.0555	2.9055	3	0.89	21.26
36	80	9	-1.34	0.0643	2.9434	3	0.92	19.36
37	74	9	-1.34	0.0641	2.9604	2	0.93	17.48
38	76	9	-1.30	0.0664	2.9439	3	0.98	17.30
39	90	9	-1.32	0.0607	2.8955	3	0.89	25.18
40	96	9	-1.34	0.0638	2.8884	2	0.94	23.42
41	89	9	-1.33	0.0549	2.9548	2	0.83	20.86
42	92	9	-1.31	0.0545	2.9657	1	1.00	24.56
43	88	9	-1.28	0.0616	2.9669	2	0.95	22.34
44	87	9	-1.29	0.0652	2.9152	4	0.89	26.20
45	88	9	-1.35	0.0557	2.9323	3	0.81	22.09
46	78	9	-1.34	0.0584	2.9059	2	0.94	17.10
47	99	9	-1.29	0.0604	2.9494	2	0.90	26.63
48	78	9	-1.37	0.0638	2.9696	4	0.87	21.05
49	83	9	-1.37	0.0624	2.9563	3	0.90	20.39
50	65	9	-1.35	0.0607	2.9373	2	0.94	17.03

Table B.8 continued

Case	maxlink	avglink	slope	C.C.	path_length	hub	eigenvector	kurtosis
51	94	9	-1.30	0.0583	2.9301	1	1.00	22.95
52	92	9	-1.25	0.0612	2.9365	4	0.89	33.12
53	77	9	-1.32	0.0658	2.9234	3	0.88	17.55
54	61	9	-1.37	0.0540	2.9663	0	0.00	13.72
55	86	9	-1.31	0.0598	2.9219	2	0.98	22.19
56	88	9	-1.35	0.0564	2.9131	1	1.00	18.69
57	84	8	-1.32	0.0610	2.9773	3	0.76	18.72
58	96	8	-1.32	0.0611	2.9775	4	0.73	27.35
59	83	9	-1.33	0.0542	2.9677	1	1.00	19.05
60	89	9	-1.33	0.0627	2.8704	3	0.79	20.88
61	92	8	-1.37	0.0641	2.9837	3	0.87	26.23
62	75	9	-1.35	0.0587	2.9662	4	0.89	20.76
63	84	9	-1.35	0.0590	2.9006	3	0.90	21.71
64	78	9	-1.33	0.0613	2.9312	1	1.00	16.78
65	92	9	-1.29	0.0664	2.8625	3	0.91	22.44
66	99	9	-1.32	0.0613	2.9097	3	0.88	30.59
67	96	9	-1.23	0.0615	2.8846	3	0.84	24.01
68	86	9	-1.32	0.0581	2.9530	1	1.00	17.75
69	120	9	-1.32	0.0601	2.9144	1	1.00	41.15
70	94	9	-1.31	0.0611	2.8949	4	0.82	25.30
71	85	9	-1.34	0.0596	2.9058	1	1.00	17.27
72	110	9	-1.32	0.0642	2.9184	3	0.81	32.28
73	82	9	-1.34	0.0665	2.9359	3	0.97	21.75
74	78	9	-1.38	0.0529	2.9764	1	1.00	16.61
75	71	9	-1.34	0.0580	2.9088	2	0.92	16.13
76	88	9	-1.32	0.0628	2.9348	2	0.92	21.81
77	89	9	-1.36	0.0600	2.9069	3	0.84	21.23
78	76	8	-1.35	0.0632	2.9960	3	0.82	17.45
79	95	9	-1.36	0.0624	2.9523	2	0.77	25.07
80	99	9	-1.31	0.0672	2.9054	3	0.91	27.68
81	90	9	-1.27	0.0646	2.9039	3	0.80	23.79
82	91	9	-1.27	0.0656	2.9222	4	0.83	25.00
83	94	9	-1.28	0.0637	2.9440	4	0.87	26.25
84	84	9	-1.32	0.0693	2.9328	3	0.89	19.36
85	96	9	-1.24	0.0672	2.8528	4	0.82	24.57
86	85	9	-1.30	0.0677	2.8772	4	0.92	24.37
87	70	9	-1.35	0.0596	2.9285	2	0.91	16.63
88	80	9	-1.31	0.0671	2.8909	4	0.91	19.04
89	98	9	-1.40	0.0599	2.9706	1	1.00	25.86
90	101	9	-1.27	0.0647	2.8918	2	0.95	31.50
91	100	9	-1.35	0.0627	2.9280	2	0.75	24.96
92	74	9	-1.33	0.0571	2.9195	3	0.88	17.36
93	82	9	-1.31	0.0620	2.9592	2	0.89	18.35
94	107	9	-1.28	0.0666	2.8782	4	0.79	28.66
95	78	9	-1.36	0.0536	2.9616	1	1.00	17.19
96	94	9	-1.31	0.0589	2.8947	4	0.85	26.10
97	88	9	-1.28	0.0668	2.9091	3	0.93	21.14
98	97	9	-1.33	0.0635	2.8991	2	0.98	26.26
99	84	9	-1.35	0.0590	2.9382	2	0.90	19.53
100	90	9	-1.31	0.0611	2.8927	4	0.85	23.23

Table B.9. BA Network Statistics : $outlink = 9$

Case	maxlink	avglink	slope	C.C.	path_length	hub	eigenvector	kurtosis
1	98	10	-1.31	0.0634	2.8339	2	0.89	19.54
2	105	10	-1.21	0.0727	2.8290	2	0.95	27.17
3	93	10	-1.15	0.0648	2.8068	3	0.95	23.47
4	103	10	-1.23	0.0703	2.8441	1	1.00	22.40
5	105	10	-1.28	0.0689	2.8637	4	0.82	25.09
6	82	10	-1.28	0.0658	2.8925	2	0.95	16.19
7	98	10	-1.27	0.0756	2.8055	3	0.98	24.53
8	79	10	-1.21	0.0681	2.8611	2	0.98	16.02
9	89	9	-1.30	0.0655	2.8765	2	0.90	19.96
10	101	10	-1.28	0.0700	2.8367	3	0.90	23.18
11	72	10	-1.28	0.0687	2.8435	5	0.94	15.84
12	80	10	-1.27	0.0656	2.8627	2	0.99	15.21
13	91	10	-1.30	0.0628	2.8457	2	0.88	20.05
14	111	10	-1.23	0.0666	2.8692	3	0.81	31.22
15	105	10	-1.26	0.0669	2.8028	2	0.99	27.02
16	95	10	-1.27	0.0684	2.8929	2	1.00	23.64
17	91	10	-1.29	0.0686	2.8595	5	0.86	22.82
18	102	10	-1.24	0.0680	2.8226	1	1.00	20.68
19	80	10	-1.31	0.0621	2.8832	2	0.95	16.52
20	80	10	-1.27	0.0707	2.8225	1	1.00	14.79
21	84	10	-1.32	0.0642	2.8560	3	0.94	17.24
22	86	10	-1.21	0.0692	2.8344	3	0.93	21.12
23	93	10	-1.27	0.0684	2.8227	2	0.88	19.19
24	77	10	-1.32	0.0652	2.8821	1	0.95	15.03
25	104	10	-1.27	0.0779	2.8173	3	0.85	22.93
26	79	10	-1.22	0.0623	2.8553	1	1.00	14.32
27	86	10	-1.26	0.0635	2.8649	2	0.95	19.81
28	64	10	-1.36	0.0615	2.8750	0	0.00	11.72
29	103	10	-1.26	0.0735	2.8270	2	0.90	21.13
30	128	10	-1.25	0.0654	2.8338	1	1.00	37.73
31	87	10	-1.30	0.0649	2.8433	3	0.91	21.83
32	97	10	-1.29	0.0662	2.8710	2	0.91	22.00
33	113	9	-1.32	0.0761	2.8806	1	1.00	28.07
34	91	10	-1.30	0.0667	2.8350	2	0.94	22.12
35	81	10	-1.29	0.0732	2.8811	2	0.96	15.83
36	107	9	-1.32	0.0681	2.8790	2	0.79	24.06
37	78	10	-1.25	0.0718	2.8596	4	0.91	15.84
38	84	10	-1.21	0.0661	2.8192	4	0.97	21.38
39	99	9	-1.35	0.0699	2.9084	3	0.83	24.73
40	95	10	-1.23	0.0645	2.8660	3	0.97	25.60
41	100	10	-1.26	0.0632	2.8654	2	0.87	25.16
42	87	10	-1.22	0.0714	2.8403	1	1.00	16.89
43	96	10	-1.30	0.0641	2.8741	3	0.92	24.72
44	86	10	-1.26	0.0649	2.8972	2	0.89	17.25
45	97	10	-1.28	0.0681	2.8613	2	0.92	19.14
46	108	10	-1.29	0.0657	2.8634	1	1.00	25.81
47	97	10	-1.26	0.0554	2.8737	1	1.00	21.42
48	85	10	-1.30	0.0738	2.8451	4	0.94	19.74
49	83	10	-1.30	0.0699	2.8540	2	0.93	16.95
50	88	10	-1.28	0.0654	2.8551	3	0.90	18.53

Table B.9 continued

Case	maxlink	avglink	slope	C.C.	path_length	hub	eigenvector	kurtosis
51	95	10	-1.28	0.0690	2.8711	3	0.88	22.00
52	99	10	-1.27	0.0690	2.8698	2	0.99	26.65
53	93	10	-1.27	0.0684	2.8436	2	0.97	20.03
54	89	10	-1.26	0.0678	2.8515	2	0.93	18.09
55	79	10	-1.24	0.0634	2.8616	2	0.94	17.06
56	111	10	-1.23	0.0655	2.8504	1	1.00	24.93
57	92	10	-1.29	0.0701	2.8260	2	0.87	17.64
58	84	10	-1.27	0.0639	2.8390	3	0.90	16.97
59	92	10	-1.24	0.0750	2.8338	2	0.99	18.97
60	108	10	-1.27	0.0612	2.8368	2	0.86	26.39
61	91	10	-1.25	0.0725	2.8581	4	0.84	22.40
62	97	10	-1.21	0.0697	2.8225	4	0.79	21.04
63	93	10	-1.27	0.0685	2.8387	4	0.96	24.01
64	99	10	-1.23	0.0672	2.8171	2	0.87	18.50
65	75	10	-1.25	0.0680	2.8609	2	0.91	13.49
66	86	10	-1.33	0.0674	2.8663	4	0.87	20.23
67	96	10	-1.27	0.0711	2.8266	2	0.99	21.97
68	110	10	-1.26	0.0640	2.8558	1	1.00	26.18
69	88	10	-1.25	0.0733	2.8377	1	1.00	15.78
70	89	10	-1.27	0.0684	2.8437	3	0.97	23.41
71	89	10	-1.24	0.0711	2.8335	3	0.94	21.09
72	85	10	-1.24	0.0677	2.8500	4	0.87	19.86
73	106	10	-1.28	0.0698	2.8482	4	0.86	25.56
74	96	10	-1.30	0.0647	2.8572	2	0.86	18.63
75	91	10	-1.26	0.0691	2.8269	2	0.96	19.49
76	88	10	-1.27	0.0687	2.7986	4	0.95	17.19
77	122	10	-1.20	0.0649	2.8310	2	0.89	38.91
78	102	9	-1.30	0.0635	2.8774	2	0.92	28.99
79	93	10	-1.25	0.0750	2.8482	3	0.85	21.97
80	98	10	-1.27	0.0703	2.8630	2	0.90	19.90
81	84	10	-1.21	0.0615	2.8883	1	1.00	15.82
82	94	10	-1.31	0.0660	2.8656	1	1.00	20.03
83	126	10	-1.24	0.0638	2.8159	2	0.88	39.51
84	129	10	-1.25	0.0667	2.8405	1	1.00	36.69
85	113	10	-1.34	0.0685	2.8698	2	0.83	28.35
86	100	10	-1.26	0.0635	2.8384	2	0.92	22.77
87	86	10	-1.27	0.0621	2.8367	1	1.00	16.10
88	105	10	-1.21	0.0755	2.8328	3	0.91	28.62
89	84	10	-1.28	0.0647	2.8529	3	0.92	19.14
90	92	10	-1.25	0.0669	2.8515	2	0.88	19.82
91	97	10	-1.30	0.0720	2.8439	3	0.91	21.69
92	71	10	-1.31	0.0591	2.8607	2	0.94	14.40
93	94	10	-1.33	0.0630	2.8869	1	1.00	19.52
94	103	10	-1.24	0.0699	2.8504	4	0.79	27.07
95	86	10	-1.27	0.0662	2.8755	2	0.95	18.38
96	81	10	-1.28	0.0609	2.8649	3	0.91	17.23
97	103	10	-1.26	0.0689	2.8129	4	0.88	28.96
98	94	10	-1.28	0.0680	2.8334	2	0.90	19.41
99	93	10	-1.30	0.0670	2.8567	2	0.87	18.75
100	107	10	-1.26	0.0651	2.8633	2	0.93	29.24

Table B.10. BA Network Statistics : $outlink = 10$

Case	maxlink	avglink	slope	C.C.	path_length	hub	eigenvector	kurtosis
1	113	11	-1.29	0.0737	2.7678	2	0.94	23.24
2	109	11	-1.25	0.0706	2.7851	2	0.87	20.89
3	107	11	-1.24	0.0797	2.7665	2	0.93	20.91
4	93	11	-1.27	0.0778	2.8269	2	0.93	16.80
5	98	11	-1.20	0.0776	2.8015	3	0.92	18.39
6	128	11	-1.15	0.0699	2.7365	2	0.85	30.53
7	88	11	-1.25	0.0760	2.7854	2	0.90	15.29
8	97	11	-1.21	0.0740	2.7905	5	0.90	22.56
9	98	11	-1.25	0.0821	2.7389	5	0.89	21.16
10	99	11	-1.25	0.0810	2.7630	4	0.87	20.15
11	100	11	-1.23	0.0764	2.8214	2	0.88	18.50
12	89	12	-1.21	0.0721	2.7252	2	0.99	15.28
13	85	11	-1.23	0.0763	2.7694	1	1.00	13.04
14	86	11	-1.29	0.0773	2.8125	2	0.89	14.87
15	100	11	-1.28	0.0763	2.7883	4	0.80	20.47
16	93	11	-1.27	0.0792	2.7931	3	0.89	17.73
17	113	11	-1.23	0.0796	2.7963	2	0.92	24.75
18	97	11	-1.24	0.0730	2.7781	1	1.00	16.66
19	98	10	-1.23	0.0726	2.8284	2	0.86	17.32
20	83	11	-1.25	0.0718	2.8158	2	0.90	14.03
21	86	11	-1.23	0.0729	2.7528	1	1.00	13.28
22	105	11	-1.22	0.0776	2.8205	2	0.89	20.57
23	86	11	-1.22	0.0690	2.7986	2	0.96	16.15
24	90	11	-1.23	0.0653	2.8272	2	0.94	17.22
25	100	11	-1.20	0.0732	2.7657	3	0.89	21.02
26	83	10	-1.28	0.0711	2.8136	3	0.97	15.14
27	88	10	-1.28	0.0771	2.8077	3	0.91	16.19
28	95	11	-1.24	0.0685	2.7747	2	0.92	17.15
29	88	11	-1.19	0.0760	2.7890	1	1.00	15.85
30	103	11	-1.20	0.0739	2.7945	1	1.00	17.90
31	71	11	-1.26	0.0659	2.7723	0	0.00	11.84
32	94	11	-1.15	0.0642	2.7820	3	0.87	20.24
33	114	11	-1.19	0.0647	2.7837	2	0.82	25.24
34	99	11	-1.19	0.0707	2.7713	2	0.94	18.59
35	93	11	-1.19	0.0747	2.8147	2	0.98	18.56
36	142	11	-1.22	0.0744	2.7370	2	0.79	37.93
37	101	11	-1.25	0.0721	2.7993	2	0.88	20.54
38	89	11	-1.19	0.0761	2.7407	1	1.00	15.80
39	101	10	-1.28	0.0733	2.8086	1	1.00	19.30
40	101	11	-1.19	0.0747	2.7738	2	0.94	17.67
41	107	11	-1.22	0.0761	2.7389	4	0.81	22.14
42	89	11	-1.28	0.0687	2.8165	2	0.95	16.92
43	81	11	-1.25	0.0674	2.7540	1	1.00	12.51
44	92	10	-1.21	0.0719	2.8262	3	0.93	18.48
45	92	11	-1.28	0.0750	2.8249	3	0.93	17.15
46	85	11	-1.18	0.0749	2.7844	2	0.97	16.81
47	83	10	-1.27	0.0710	2.8198	2	0.86	14.60
48	105	10	-1.24	0.0759	2.7964	3	0.85	24.26
49	118	11	-1.23	0.0843	2.7905	3	0.85	25.85
50	91	11	-1.21	0.0667	2.8131	2	0.98	19.42

Table B.10 continued

Case	maxlink	avglink	slope	C.C.	path_length	hub	eigenvector	kurtosis
51	102	11	-1.25	0.0740	2.7631	3	0.86	19.63
52	78	11	-1.27	0.0682	2.7902	1	1.00	12.83
53	85	11	-1.28	0.0692	2.7758	2	0.96	16.56
54	95	11	-1.24	0.0698	2.8054	3	0.89	21.30
55	103	11	-1.21	0.0799	2.8013	3	0.87	22.86
56	101	11	-1.26	0.0736	2.7868	2	0.99	20.82
57	118	11	-1.25	0.0791	2.7756	1	1.00	22.58
58	91	11	-1.25	0.0762	2.7786	3	0.91	17.99
59	122	11	-1.23	0.0778	2.7805	3	0.84	30.51
60	89	11	-1.22	0.0756	2.7801	4	0.84	18.62
61	111	11	-1.22	0.0759	2.7992	2	0.89	23.00
62	93	11	-1.21	0.0749	2.7675	2	0.94	18.18
63	107	11	-1.24	0.0720	2.7739	2	0.87	21.17
64	126	11	-1.16	0.0708	2.7536	2	0.84	29.05
65	95	11	-1.23	0.0738	2.7488	2	0.97	16.90
66	91	11	-1.15	0.0680	2.7524	2	0.96	18.48
67	95	11	-1.18	0.0794	2.7883	1	1.00	18.09
68	93	11	-1.27	0.0798	2.7877	3	0.94	17.22
69	96	11	-1.21	0.0811	2.7445	4	0.97	21.73
70	84	10	-1.27	0.0756	2.7956	3	0.94	17.38
71	92	10	-1.30	0.0763	2.8304	2	0.95	17.18
72	76	11	-1.20	0.0750	2.7645	0	0.00	13.84
73	115	11	-1.18	0.0759	2.7760	2	0.93	27.70
74	77	10	-1.24	0.0731	2.8197	3	0.94	14.94
75	77	11	-1.27	0.0665	2.7566	1	1.00	13.64
76	87	11	-1.25	0.0734	2.7855	2	0.97	15.71
77	109	11	-1.19	0.0683	2.7829	2	0.85	22.43
78	95	11	-1.22	0.0722	2.7792	2	0.99	16.78
79	112	10	-1.23	0.0755	2.8273	2	0.94	28.20
80	80	11	-1.28	0.0715	2.7945	2	0.90	13.79
81	120	11	-1.22	0.0783	2.7871	3	0.79	27.22
82	80	11	-1.22	0.0752	2.8024	2	0.93	14.61
83	96	11	-1.27	0.0750	2.7891	2	0.94	16.87
84	96	11	-1.25	0.0730	2.7730	3	0.95	20.92
85	91	11	-1.28	0.0752	2.7879	2	0.98	16.19
86	80	11	-1.27	0.0674	2.8169	1	1.00	12.42
87	97	11	-1.29	0.0775	2.7834	2	0.96	19.96
88	99	11	-1.23	0.0712	2.7944	3	0.90	22.49
89	112	11	-1.18	0.0739	2.7684	2	0.93	23.43
90	115	11	-1.21	0.0818	2.7520	4	0.82	24.07
91	78	11	-1.20	0.0662	2.8126	1	1.00	13.89
92	104	11	-1.24	0.0760	2.7743	1	1.00	18.59
93	90	11	-1.19	0.0725	2.8134	3	1.00	18.34
94	119	11	-1.23	0.0806	2.7807	2	0.83	25.07
95	105	11	-1.24	0.0697	2.7896	2	0.94	21.49
96	86	11	-1.24	0.0794	2.7556	3	0.95	17.49
97	84	11	-1.30	0.0728	2.8036	2	0.98	14.93
98	84	10	-1.31	0.0697	2.8774	3	0.97	16.67
99	90	11	-1.24	0.0734	2.7845	2	0.91	16.15
100	136	11	-1.20	0.0808	2.7504	1	1.00	32.49

APPENDIX C

BOXPLOTS OF FAILURES

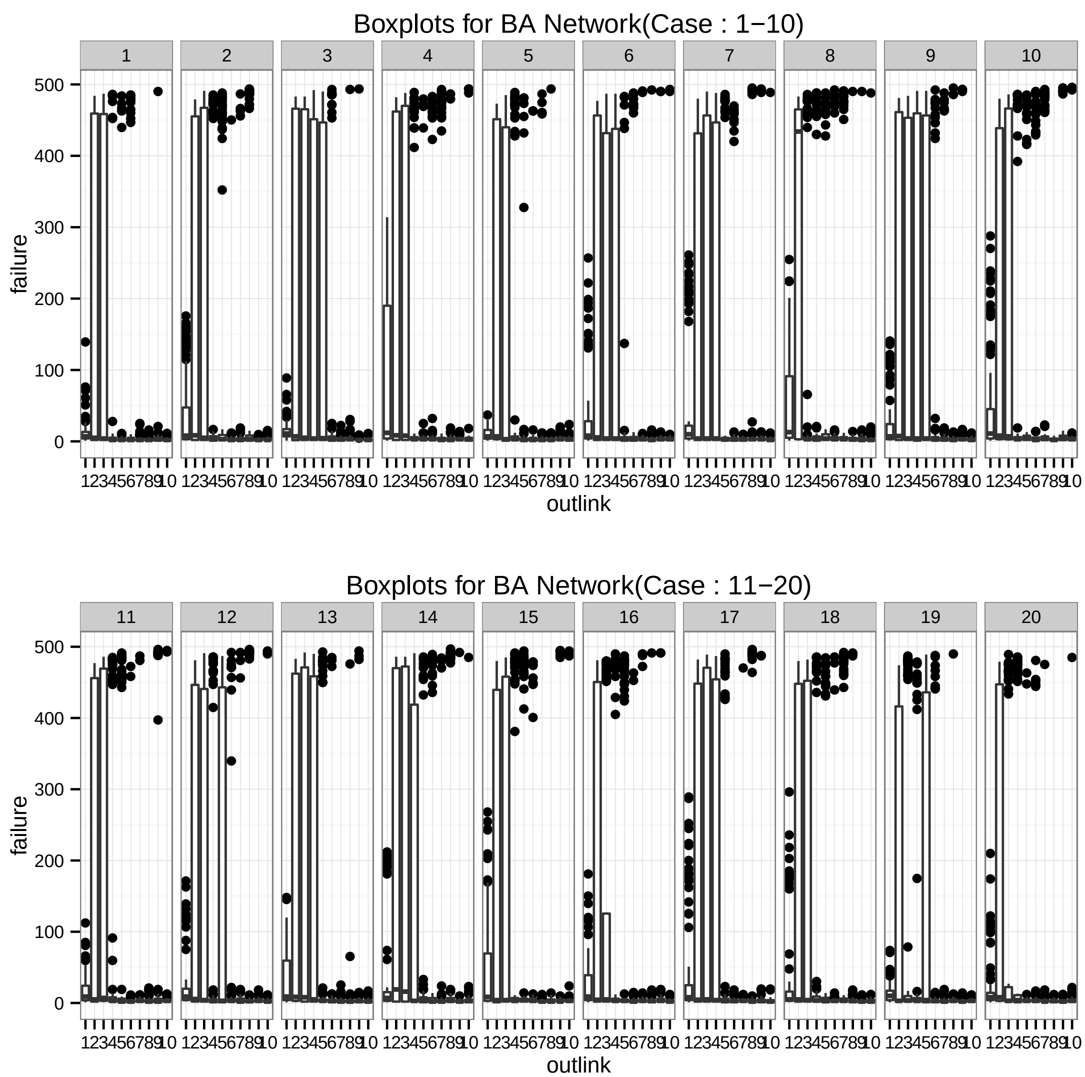

Figure C.1. Boxplots (Case: 1-20)

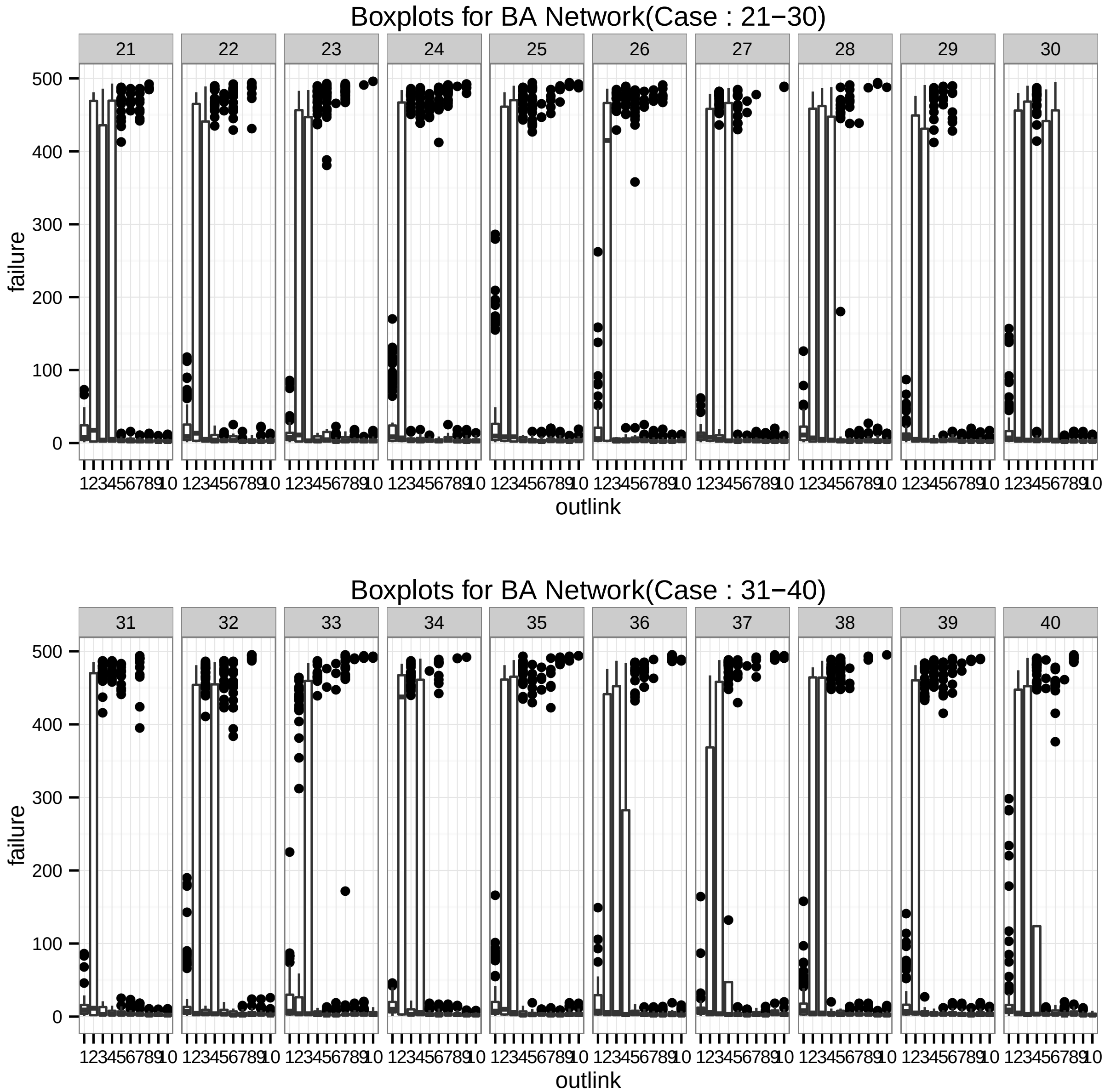

Figure C.2. Boxplots (Case: 21-40)

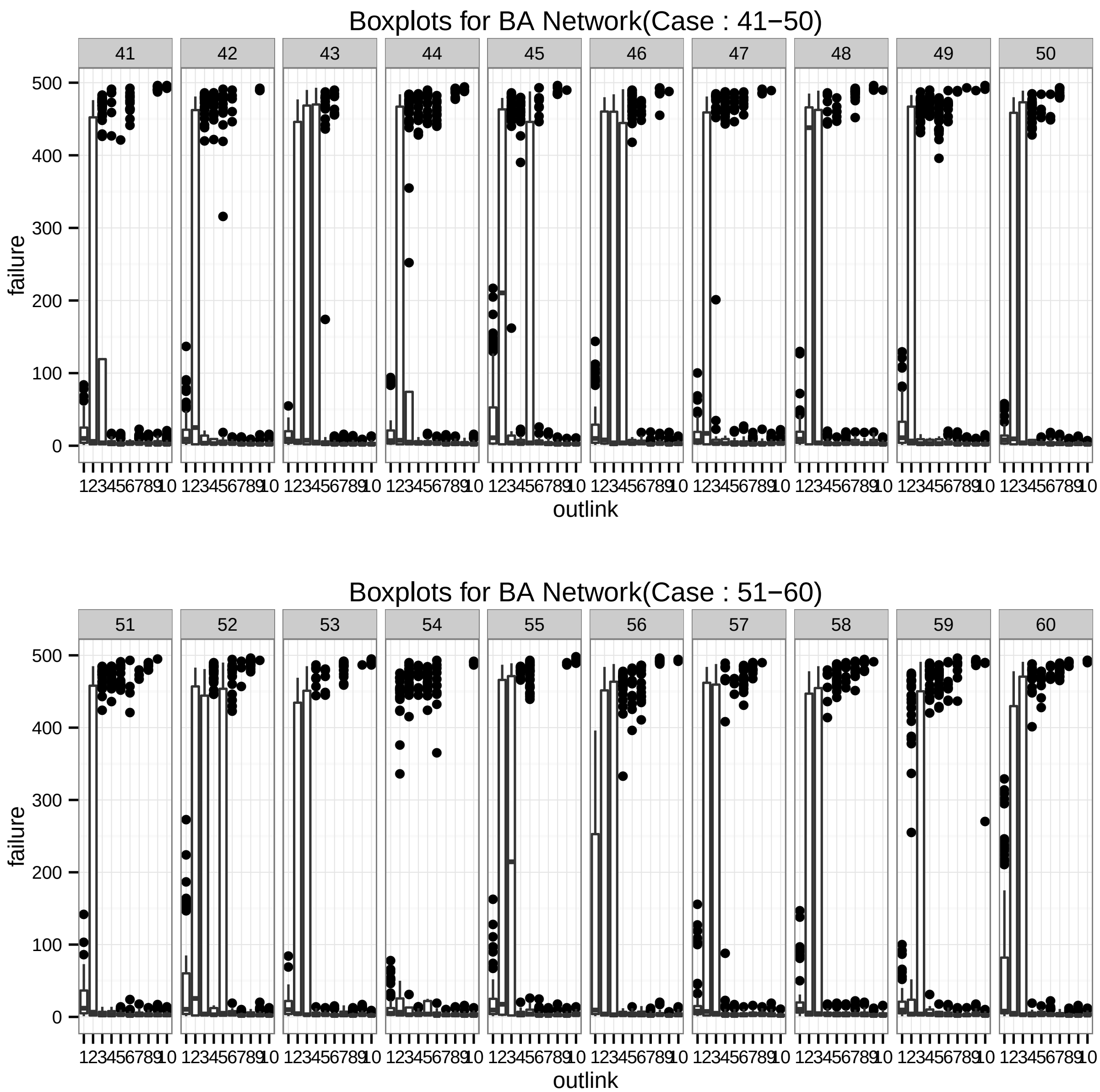

Figure C.3. Boxplots (Case: 41-60)

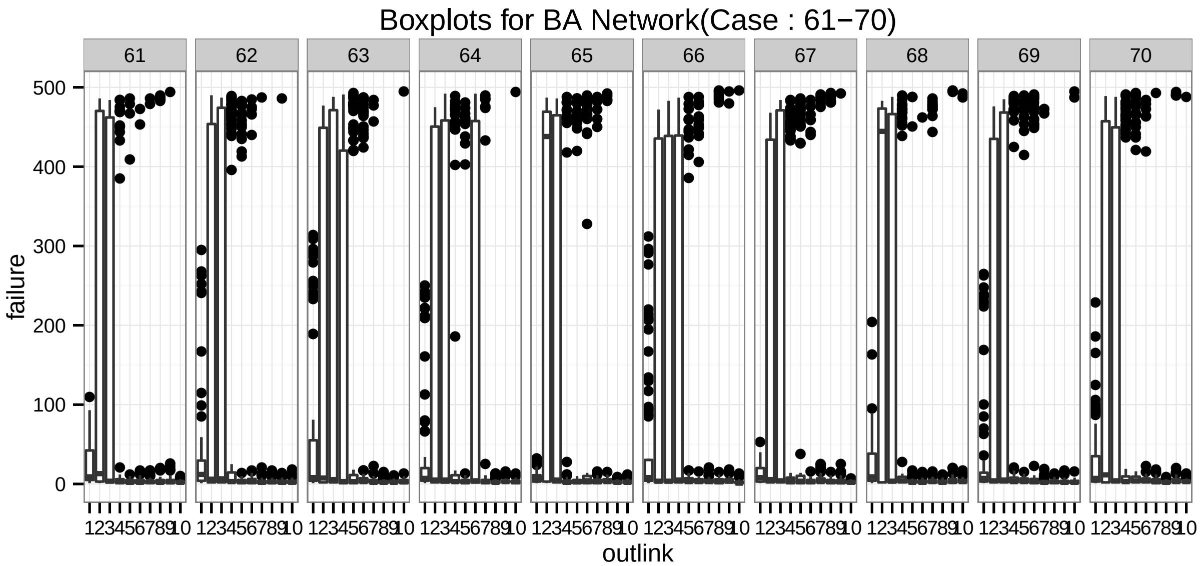

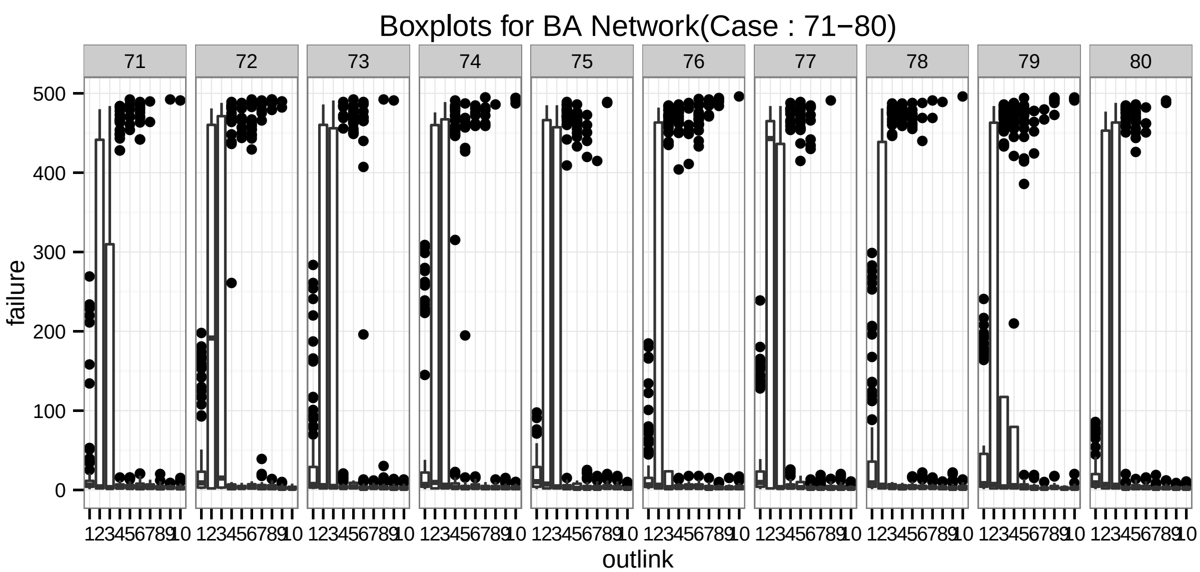

Figure C.4. Boxplots (Case: 61-80)

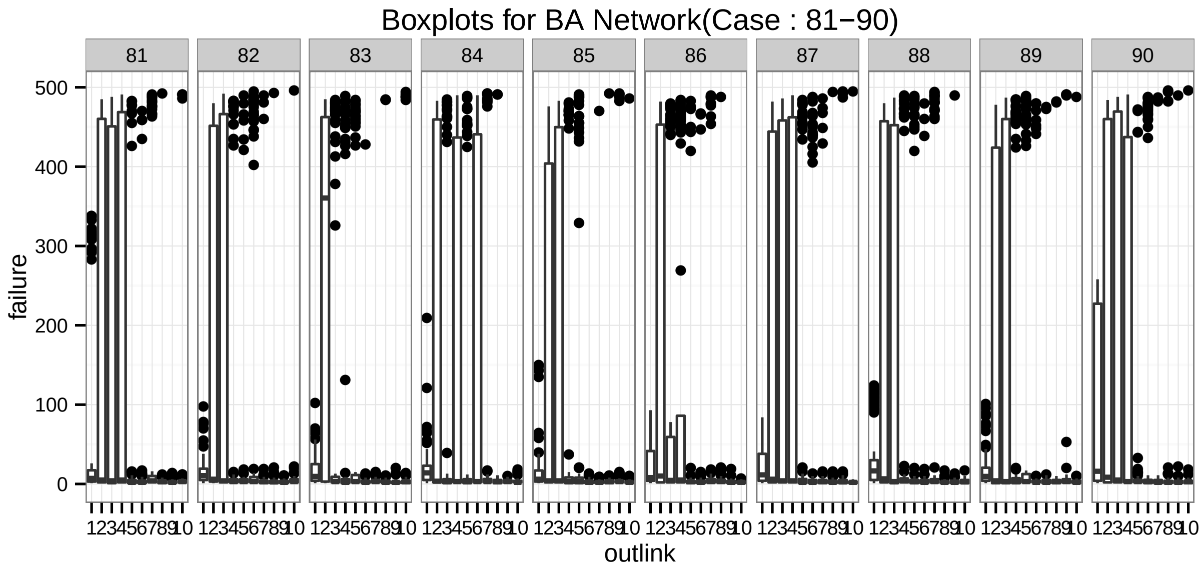

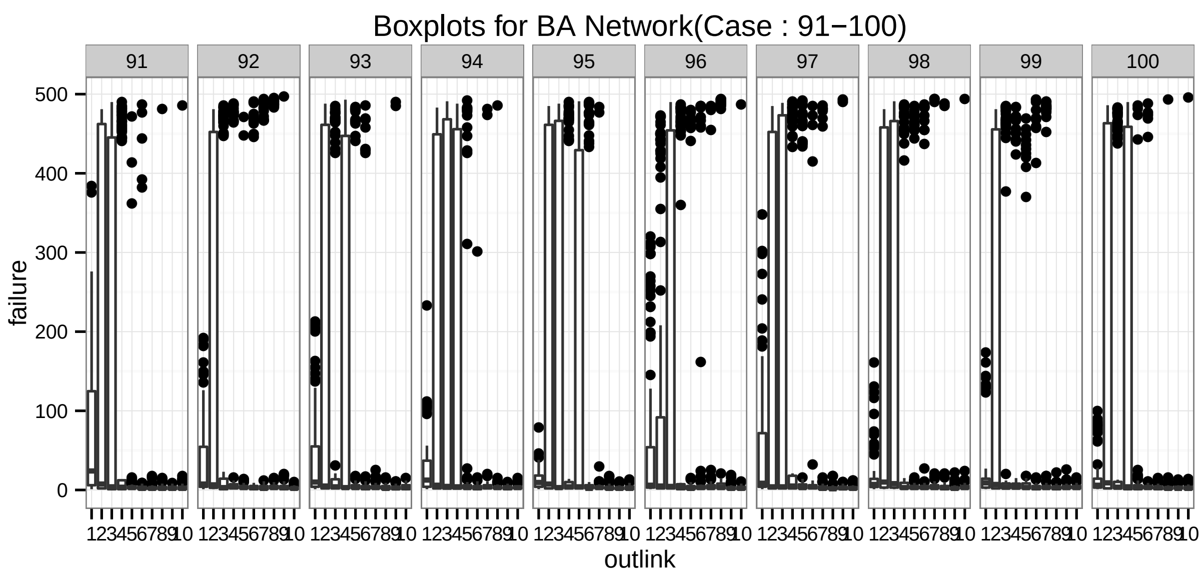

Figure C.5. Boxplots (Case: 81-100)

APPENDIX D

SUPPLEMENTARY FIGURES FOR PD GAMES

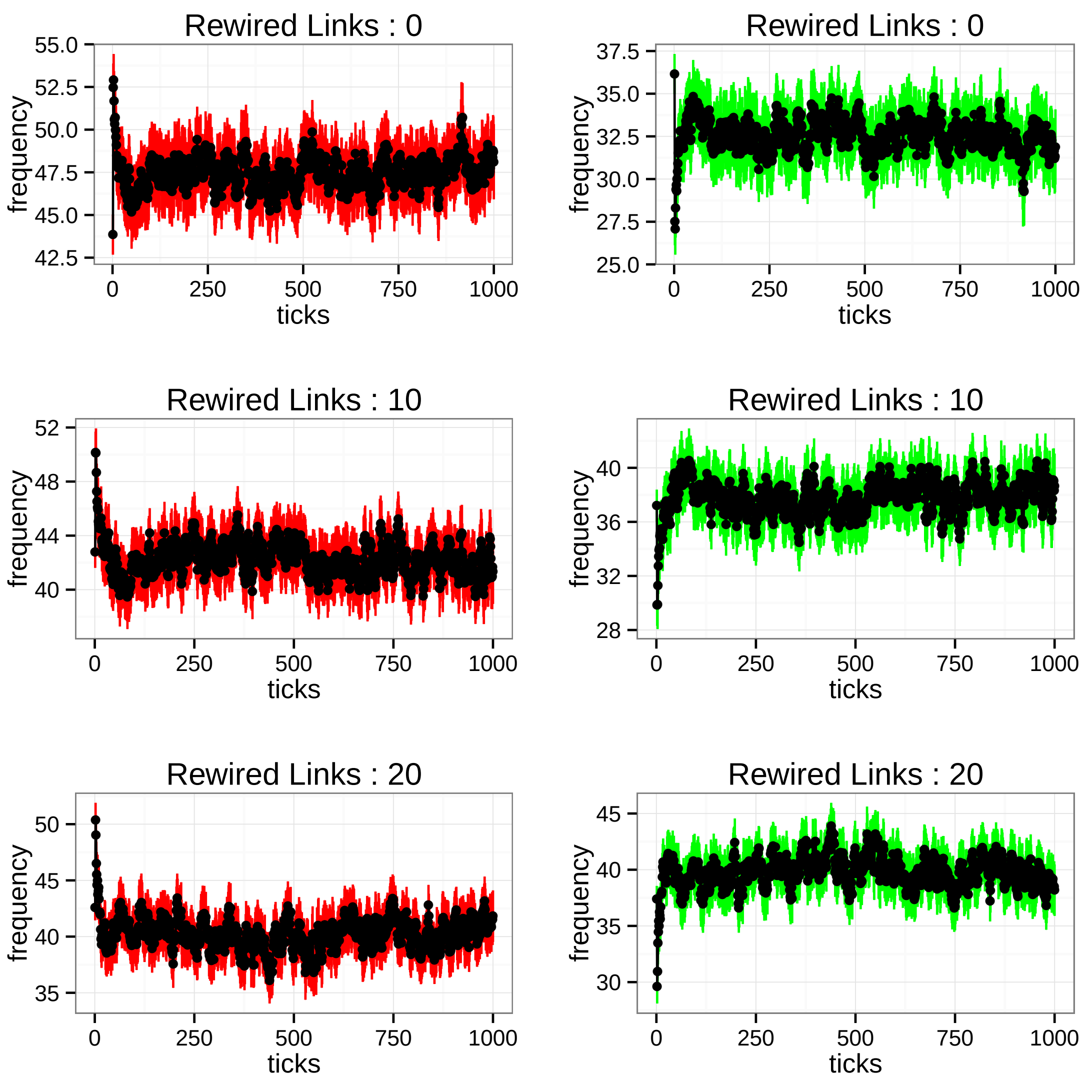

Figure D.1. Defection vs. Cooperation (Rewired links 0 - 20)

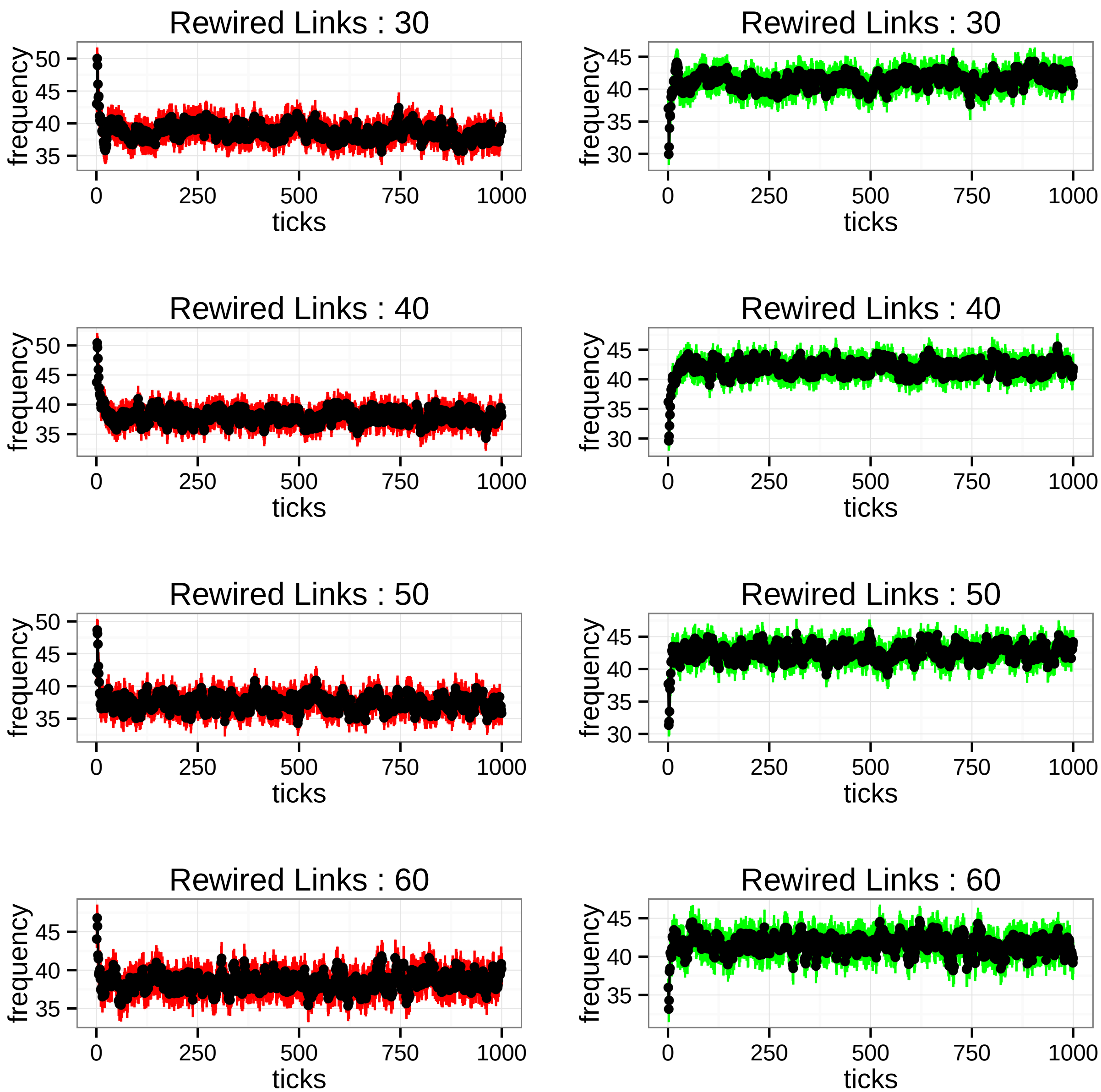

Figure D.2. Defection vs. Cooperation (Rewired links 30 - 60)

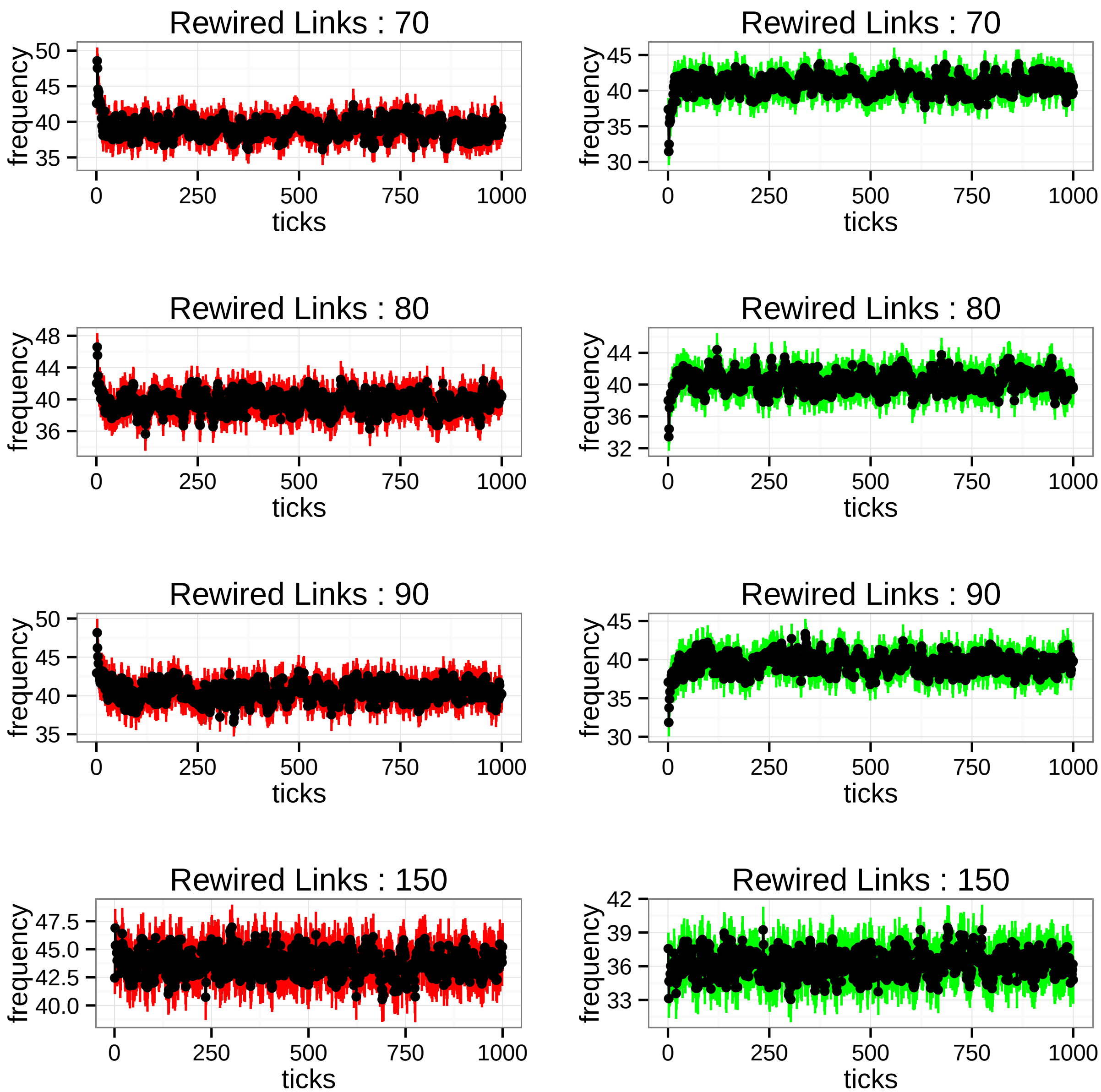

Figure D.3. Defection vs. Cooperation (Rewired links 70 - 150)

REFERENCES

Abramson, G. and M. Kuperman (2001). Social games in a social network. *Physical Review E 63*(3), 030901.

Albert, R., H. Jeong, and A.-L. Barabási (1999). Internet: Diameter of the world-wide web. *Nature 401*(6749), 130–131.

Albert, R., H. Jeong, and A.-L. Barabási (2000). Error and attack tolerance of complex networks. *Nature 406*(6794), 378–382.

Alexander, J. M. (2007). *The structural evolution of morality.* Cambridge University Press Cambridge.

Algan, Y. and P. Cahuc (2013). Trust, growth and well-being: New evidence and policy implications. *CEPR Discussion Paper No. DP9548*.

Allen, F., A. Babus, and E. Carletti (2012). Asset commonality, debt maturity and systemic risk. *Journal of Financial Economics 104*(3), 519–534.

Allen, F. and D. Gale (2000). Financial contagion. *Journal of political economy 108*(1), 1–33.

Ananyev, M. and S. M. Guriev (2015). Effect of income on trust: Evidence from the 2009 crisis in Russia. *CEPR Discussion Paper No. DP10354*.

Anderson, R. M. and R. M. May (1991). *Infectious diseases of humans*, Volume 1. Oxford university press Oxford.

Arrow, K. J. and G. Debreu (1954). Existence of an equilibrium for a competitive economy. *Econometrica: Journal of the Econometric Society*, 265–290.

Ashraf, Q., B. Gershman, and P. Howitt (2011). Banks, market organization, and macroeconomic performance: an agent-based computational analysis. Technical report, National Bureau of Economic Research.

Axelrod, R. (1981). The emergence of cooperation among egoists. *American Political Science Review 75*(02), 306–318.

Axelrod, R. (1987). The evolution of strategies in the iterated Prisoner's dilemma. In *The dynamics of norms*, pp. 1–16.

Axelrod, R. and W. D. Hamilton (1981). The evolution of cooperation. *Science 211*(4489), 1390–1396.

Axelrod, R. M. (1997). *The complexity of cooperation: Agent-based models of competition and collaboration.* Princeton University Press.

Axtell, R. L., J. M. Epstein, J. S. Dean, G. J. Gumerman, A. C. Swedlund, J. Harburger, S. Chakravarty, R. Hammond, J. Parker, and M. Parker (2002). Population growth and collapse in a multiagent model of the kayenta anasazi in long house valley. *Proceedings of the National Academy of Sciences 99*(suppl 3), 7275–7279.

Backstrom, L., P. Boldi, M. Rosa, J. Ugander, and S. Vigna (2012). Four degrees of separation. In *Proceedings of the 4th Annual ACM Web Science Conference*, pp. 33–42. ACM.

Baker, S. R., N. Bloom, and S. J. Davis (2012). Has economic policy uncertainty hampered the recovery? *Chicago Booth Research Paper* (12-06).

Barabasi, A.-L. (2015). *Network Science.* Cambridge University Press.

Barabási, A.-L. and R. Albert (1999). Emergence of scaling in random networks. *Science 286*(5439), 509–512.

Baxter, G., S. Dorogovtsev, A. Goltsev, and J. Mendes (2014). Avalanches in multiplex and interdependent networks. In *Networks of Networks: The Last Frontier of Complexity*, pp. 37–52. Springer.

Beale, N., D. G. Rand, H. Battey, K. Croxson, R. M. May, and M. A. Nowak (2011). Individual versus systemic risk and the regulator's dilemma. *Proceedings of the National Academy of Sciences 108*(31), 12647–12652.

Beaufils, B., J.-P. Delahaye, and P. Mathieu (1998). Complete classes of strategies for the classical iterated prisoner's dilemma. In *Evolutionary Programming VII*, pp. 33–41. Springer.

Bekaert, G. and G. Wu (2000). Asymmetric volatility and risk in equity markets. *Review of Financial Studies 13*(1), 1–42.

Bjørnskov, C. (2012). How does social trust affect economic growth? *Southern Economic Journal 78*(4), 1346–1368.

Blanchard, O. (Jan., 2009). Nothing to fear but fear itself. *The Economist*.

Blinder, A. S. (2013). *After the Music Stopped: The Financial Crisis, the Response, and the Work Ahead.* Penguin.

Bloom, N. (2009). The impact of uncertainty shocks. *econometrica 77*(3), 623–685.

Bloom, N., M. Floetotto, N. Jaimovich, I. Saporta-Eksten, and S. J. Terry (2012). Really uncertain business cycles. Technical report, National Bureau of Economic Research.

Boss, M., H. Elsinger, M. Summer, and S. Thurner 4 (2004). Network topology of the interbank market. *Quantitative Finance 4*(6), 677–684.

Bouchaud, J.-P. (2008). Economics needs a scientific revolution. *Nature 455*(7217), 1181–1181.

Brusco, S. and F. Castiglionesi (2007). Liquidity coinsurance, moral hazard, and financial contagion. *The Journal of Finance 62*(5), 2275–2302.

Caballero, R. J. and A. Simsek (2009). Complexity and financial panics. Technical report, National Bureau of Economic Research.

Cecconi, F., M. Campenni, G. Andrighetto, and R. Conte (2010). What do agent-based and equation-based modelling tell us about social conventions: the clash between abm and ebm in a congestion game framework. *Journal of Artificial Societies and Social Simulation 13*(1), 6.

Cincotti, S., M. Raberto, and A. Teglio (2010). Credit money and macroeconomic instability in the agent-based model and simulator eurace. *Economics: The Open-Access, Open-Assessment E-Journal 4*.

Cioffi-Revilla, C. (2013). *Introduction to Computational Social Science: Principles and Applications*. Springer Science & Business Media.

Cirillo, P. and M. Gallegati (2012). The empirical validation of an agent-based model. *Eastern Economic Journal 38*(4), 525–547.

Crucitti, P., V. Latora, and M. Marchiori (2004). Model for cascading failures in complex networks. *Physical Review E 69*(4), 045104.

Dawid, H., S. Gemkow, P. Harting, S. Van der Hoog, and M. Neugart (2012). The eurace@ unibi model: An agent-based macroeconomic model for economic policy analysis.

Dawid, H. and M. Neugart (2011). Agent-based models for economic policy design. *Eastern Economic Journal 37*(1), 44–50.

Dosi, G., G. Fagiolo, M. Napoletano, and A. Roventini (2013). Income distribution, credit and fiscal policies in an agent-based keynesian model. *Journal of Economic Dynamics and Control*.

Dosi, G., G. Fagiolo, and A. Roventini (2010). Schumpeter meeting keynes: A policy-friendly model of endogenous growth and business cycles. *Journal of Economic Dynamics and Control 34*(9), 1748–1767.

Dwyer, G. P. and J. R. Lothian (2011). The financial crisis and recovery: Why so slow? `https://www.frbatlanta.org/cenfis/publications/notesfromthevault/1110.aspx`.

Easley, D. and J. Kleinberg (2010). *Networks, crowds, and markets: Reasoning about a highly connected world*. Cambridge University Press.

Elsinger, H., A. Lehar, and M. Summer (2006). Risk assessment for banking systems. *Management Science 52*(9), 1301–1314.

Epstein, J. M. (2006). *Generative social science: Studies in agent-based computational modeling*. Princeton University Press.

Epstein, J. M. and R. Axtell (1996). *Growing artificial societies: social science from the bottom up*. Brookings Institution Press.

Erdős, P. and A. Rényi (1959). On random graphs. *Publicationes Mathematicae Debrecen 6*, 290–297.

Fagiolo, G., A. Roventini, et al. (2012). Macroeconomic policy in dsge and agent-based models. *Revue de l'OFCE* (5), 67–116.

Fama, E. F. (1970). Efficient capital markets: A review of theory and empirical work*. *The journal of Finance 25*(2), 383–417.

Farmer, J. D. and D. Foley (2009). The economy needs agent-based modelling. *Nature 460*(7256), 685–686.

Fehr, E. and U. Fischbacher (2004). Social norms and human cooperation. *Trends in Cognitive Sciences 8*(4), 185–190.

Freixas, X., B. M. Parigi, and J.-C. Rochet (2000). Systemic risk, interbank relations, and liquidity provision by the central bank. *Journal of Money, Credit and Banking*, 611–638.

Froot, K. A., D. S. Scharfstein, and J. C. Stein (1993). Risk management: Coordinating corporate investment and financing policies. *the Journal of Finance 48*(5), 1629–1658.

Fu, F., L.-H. Liu, and L. Wang (2007). Evolutionary prisoner's dilemma on heterogeneous newman-watts small-world network. *The European Physical Journal B 56*(4), 367–372.

Gai, P. (2013). *Systemic risk: the dynamics of modern financial systems*. Oxford University Press.

Gai, P., A. Haldane, and S. Kapadia (2011). Complexity, concentration and contagion. *Journal of Monetary Economics 58*(5), 453–470.

Gai, P. and S. Kapadia (2010). Contagion in financial networks. In *Proceedings of the Royal Society of London A: Mathematical, Physical and Engineering Sciences*, pp. rspa20090410. The Royal Society.

Geanakoplos, J., R. Axtell, J. Farmer, P. Howitt, B. Conlee, J. Goldstein, M. Hendrey, N. Palmer, and C.-Y. Yang (2012). Getting at systemic risk via an agent-based model of the housing market.

Gilbert, N. (2008). *Agent-based models*. Number 153. Sage.

Granovetter, M. (1985). Economic action and social structure: the problem of embeddedness. *American journal of sociology*, 481–510.

Guillén, M. (2009). The global economic & financial crisis: A timeline. *The Lauder Institute, University of Pennsylvania*.

Harrington, J. (2009). *Games, strategies and decision making*. Macmillan.

Hurd, T. R. and J. P. Gleeson (2011). A framework for analyzing contagion in banking networks. *Available at SSRN 1945748*.

Hurd, T. R. and J. P. Gleeson (2013). On wattsą́ cascade model with random link weights. *Journal of Complex Networks 1*(1), 25–43.

Jackson, M. O. et al. (2008). *Social and economic networks*, Volume 3. Princeton University Press Princeton.

Kim, B. J., A. Trusina, P. Holme, P. Minnhagen, J. S. Chung, and M. Choi (2002). Dynamic instabilities induced by asymmetric influence: Prisonersą́ dilemma game in small-world networks. *Physical Review E 66*(2), 021907.

Kim, H.-J., Y. Lee, B. Kahng, and I.-m. Kim (2002). Weighted scale-free network in financial correlations. *Journal of the Physical Society of Japan 71*(9), 2133–2136.

Kindleberger, C. P. and R. Z. Aliber (2011). *Manias, panics and crashes: a history of financial crises*. Palgrave Macmillan.

Kingsley, P. (2012). Financial crisis: timeline. *The Guardian*.

Kirman, A. (2010). *Complex economics: individual and collective rationality*. Routledge.

Knack, S. (2003). Groups, growth and trust: Cross-country evidence on the olson and putnam hypotheses. *Public Choice 117*(3-4), 341–355.

Krause, A. and S. Giansante (2012). Interbank lending and the spread of bank failures: A network model of systemic risk. *Journal of Economic Behavior & Organization 83*(3), 583–608.

Laver, M. and E. Sergenti (2011). *Party Competition: An Agent-Based Model: An Agent-Based Model*. Princeton University Press.

Lazer, D. and A. Friedman (2006). The dark side of the small world: how efficient information diffusion drives out diversity and lowers collective problem solving ability. *Retrieved February 7*, 2009.

Leitner, Y. (2005). Financial networks: Contagion, commitment, and private sector bailouts. *The Journal of Finance 60*(6), 2925–2953.

Lengnick, M. (2011). Agent-based macroeconomics-a baseline model. Technical report, Economics working paper/Christian-Albrechts-Universität Kiel, Department of Economics.

Lim, M. H. and C. Lim (2010). *Nowhere to hide: The great financial crisis and challenges for Asia*. Institute of Southeast Asian.

Meyers, L. (2007). Contact network epidemiology: Bond percolation applied to infectious disease prediction and control. *Bulletin of the American Mathematical Society 44*(1), 63–86.

Miller, J. H. and S. E. Page (2009). *Complex adaptive systems: an introduction to computational models of social life: an introduction to computational models of social life*. Princeton university press.

Mitchell, M. (2009). *Complexity: A guided tour*. Oxford University Press.

Nedic, D. P., I. Dobson, D. S. Kirschen, B. A. Carreras, and V. E. Lynch (2006). Criticality in a cascading failure blackout model. *International Journal of Electrical Power & Energy Systems 28*(9), 627–633.

Newman, M. (2010). *Networks: an introduction*. Oxford University Press.

Newman, M. E. (2002). Spread of epidemic disease on networks. *Physical review E 66*(1), 016128.

Osborne, M. J. (2004). *An introduction to game theory*, Volume 3. Oxford University Press New York.

Panousi, V. and D. Papanikolaou (2012). Investment, idiosyncratic risk, and ownership. *The Journal of Finance 67*(3), 1113–1148.

Parunak, H. V. D., R. Savit, and R. L. Riolo (1998). Agent-based modeling vs. equation-based modeling: A case study and usersąŕ guide. In *Multi-agent systems and agent-based simulation*, pp. 10–25. Springer.

Raberto, M., A. Teglio, and S. Cincotti (2008). Integrating real and financial markets in an agent-based economic model: an application to monetary policy design. *Computational Economics 32*(1-2), 147–162.

Raberto, M., A. Teglio, and S. Cincotti (2011). Debt deleveraging and business cycles: An agent-based perspective. *Economics Discussion Paper* (2011-31).

Railsback, S. F. and V. Grimm (2011). *Agent-based and individual-based modeling: a practical introduction*. Princeton University Press.

Reinhart, C. M. and K. Rogoff (2009). *This time is different: eight centuries of financial folly*. princeton university press.

Russo, A., M. Catalano, E. Gaffeo, M. Gallegati, and M. Napoletano (2007). Industrial dynamics, fiscal policy and r&d: Evidence from a computational experiment. *Journal of Economic Behavior & Organization 64*(3), 426–447.

Sargent, R. G. (2004). Validation and verification of simulation models. In *Simulation Conference, 2004. Proceedings of the 2004 Winter*, Volume 1. IEEE.

Schelling, T. C. (1971). Dynamic models of segregationćÓ. *Journal of mathematical sociology 1*(2), 143–186.

Schelling, T. C. (2006). *Micromotives and macrobehavior*. WW Norton & Company.

Schlesinger, S. (1979). Terminology for model credibility. *Simulation 32*(3), 103–104.

Shleifer, A. (2003). *Inefficient markets: An introduction to behavioral finance*. Oxford university press.

Shleifer, A. and R. W. Vishny (2010). Fire sales in finance and macroeconomics. Technical report, National Bureau of Economic Research.

Sornette, D. (2009). Dragon-kings, black swans and the prediction of crises. *Swiss Finance Institute Research Paper* (09-36).

Szolnoki, A., M. Perc, and Z. Danku (2008). Making new connections towards cooperation in the prisoner's dilemma game. *EPL (Europhysics Letters) 84*(5), 50007.

Thurner, S. (2011). Systemic financial risk: agent based models to understand the leverage cycle on national scales and its consequences. *Multi-disciplinary issues international futures program. Jan. 14th*.

Trichet, J.-C. (2010). Reflection on the nature of monetary policy non-standard measures and finance theory. `www.ecb.int/press/key/date/2010/html/sp101118.en.html`.

Van Nieuwerburgh, S. and L. Veldkamp (2006). Learning asymmetries in real business cycles. *Journal of Monetary Economics 53*(4), 753–772.

Van Steen, M. (2010). Graph theory and complex networks. *An Introduction*.

Veldkamp, L. L. (2005). Slow boom, sudden crash. *Journal of Economic Theory 124*(2), 230–257.

Von Neumann, J. (1951). The general and logical theory of automata. *Cerebral mechanisms in behavior*, 1–41.

Watts, D. J. (2002). A simple model of global cascades on random networks. *Proceedings of the National Academy of Sciences 99*(9), 5766–5771.

Watts, D. J. (2004). The "new" science of networks. *Annual Review of Sociology*, 243–270.

Watts, D. J. and S. H. Strogatz (1998). Collective dynamics of ąősmall-worldąŕnetworks. *Nature 393*(6684), 440–442.

Westerhoff, F. H. (2008). The use of agent-based financial market models to test the effectiveness of regulatory policies. *Jahrbücher für Nationalökonomie und Statistik*, 195–227.

Wilensky, U. (1999). Netlogo. `http://ccl.northwestern.edu/netlogo`.

Wilensky, U. and W. Rand (2015). *An Introduction to Agent-Based Modeling: Modeling Natural, Social, and Engineered Complex Systems with NetLogo.* MIT Press.

Woolcock, M. (1998). Social capital and economic development: Toward a theoretical synthesis and policy framework. *Theory and Society 27*(2), 151–208.

VITA

Young Joon Oh was born and brought up in South Korea. His major was Political Science and with Economics as minor at Chung-Ang University. He received a Master of Arts degree with a major in Political Science from Seoul National University. After graduation, He worked in the National Assembly of Korea for over 7 years in the office of Congressman Maeng, Hyung-Kyu and Park, Jong-Hee responsible for preparing bills and public hearings. Furthermore, he worked extensively in campaign teams in major elections in South Korea, including Presidential election in 2007, Seoul Mayoral election in 2006 and General election in 2004. He was employed as a teaching assistant at the University of Texas at Dallas from 2010 to 2015. His research interests are Agent-based model, Complex adaptive systems, Network theory, Crisis and Recovery, International political economy, Innovation network, Computational social science, and Quantitative analysis.